

REVIEW ARTICLE

[View Article Online](#)
[View Journal](#)

Cite this: DOI: 10.1039/c3cs60140d

A voyage into the synthesis and photophysics of homo- and heterobinuclear ensembles of phthalocyanines and porphyrins[†]

Gema de la Torre,^a Giovanni Bottari,^{ab} Michael Sekita,^c Anita Hausmann,^c Dirk M. Guldi^{*c} and Tomás Torres^{*ab}

The remarkable properties of both phthalocyanines and porphyrins as individual building blocks have motivated the synthesis and study of homo- and heterobinuclear conjugates as light-harvesting systems. These planar chromophores share important electronic features such as high molar absorption coefficients, rich redox chemistry and interesting photoinduced energy and/or electron transfer abilities. In addition, some of these properties can be tuned by the introduction of different peripheral substituents and metal centres. In this review, we present relevant synthetic strategies for the preparation of covalent and supramolecular, homo- and heterobinuclear systems based on phthalocyanine and porphyrin chromophores, leading to a variety of architectures. In such systems, the degree of electronic interaction between the components is highly dependent on the electronic features of the two macrocycles, their linkage, and the molecular topology of the ensemble. In addition, incorporation of electroactive units into these binuclear systems has been pursued, affording multicomponent, donor-acceptor conjugates. In-depth photophysical characterization of the ground- and excited-state features of many of these homo- and heterobinuclear phthalocyanine and/or porphyrin ensembles has also been presented. Particular attention has been paid to understand the fundamental dynamics of the energy transfer and charge separation processes of these systems. This review intends to offer a general overview of the preparation of this class of compounds and the study of their photophysical properties which clearly show their potentiality as model compounds of light-harvesting complexes.

Received 19th April 2013

DOI: 10.1039/c3cs60140d

www.rsc.org/csr

1. Introduction

Porphyrinoids, due to their preeminent role in nature, are the usual chromophores of choice to be employed as components of photovoltaic and artificial photosynthetic devices.^{1–9} Porphyrins (Pors) and their analogues, phthalocyanines (Pcs), hold some advantages with respect to other types of electro- and photoactive compounds which arise from their 18 π-electron aromatic structure, namely, high molar absorption coefficients and fast energy and/or electron transfer donor abilities to electron acceptor counterparts. Thus, porphyrinoids are widely used as

molecular components in artificial photosynthetic systems, both for energy-transfer and electron-transfer processes. On the other hand, the possibility of tailoring their redox potentials through peripheral functionalization represents an appealing feature for their use in the above-mentioned energy-related areas. In this connection, both Pors and Pcs have remarkable absorption in the visible region. However, whereas regular Pors do not display significant absorption at energies lower than 550 nm, Pcs show excellent light harvesting capabilities over a wide range of the solar light spectrum with a maximum at around 700 nm, where the maximum of the solar photon flux occurs.¹⁰ Therefore, the development of new porphyrinoid-based systems able to absorb a higher portion of the solar emissions is of paramount importance, the functions of these new derivatives ranging from light harvesting through most of the visible part of the solar spectrum to electron transport.

Modifications of the porphyrinoid structure for light harvesting purposes can be achieved, for example, by extending the conjugation of the π-system that causes a bathochromic

^a Departamento de Química Orgánica, Universidad Autónoma de Madrid, 28049, Madrid, Spain. E-mail: tomas.torres@uam.es

^b IMDEA-Nanociencia, c/Faraday 9, Campus de Cantoblanco, 28049 Madrid, Spain

^c Friedrich-Alexander-Universität Erlangen-Nürnberg, Department of Chemistry and Pharmacy & Interdisciplinary Center for Molecular Materials (ICMM), Egerlandstrasse 3, 91058 Erlangen, Germany.

E-mail: dirk.guldi@chemie.uni-erlangen.de

† Dedicated to Prof. Maurizio Prato on the occasion of his 60th birthday.

shift in the absorption spectrum. This is one of the reasons why the chemistry of conjugated Por oligomers has recently grown up, and synthetic strategies are continuously being developed, targeted to the preparation of multiPor arrays. Por dimers, trimers, and oligomers have a wide range of potential applications in areas such as photodynamic therapy (PDT), nonlinear optics (NLO), single molecular magnets, molecular photovoltaics and organic light-emitting diodes, among others.^{11–14} In this context, in the last few years, much effort has been devoted to the preparation and studies of binuclear Por systems which are formed by fusing, directly linking, or linking through different types of conjugated or non-conjugated bridges, the two chromophores.

Despite the great scientific and technological interest in the related Pc systems, the effort devoted to the preparation of binuclear Pcs or multiPc arrays is not comparable to that of Pors, but still interesting approaches have been reported in the search for excitonic and/or electronic interactions between macrocyclic subunits.^{15–19} Some examples in which the Pc subunits are connected through π -conjugated pathways have

been described.²⁰ For instance, Pcs endowed with acetylene functions have been used as precursors of Pc-Pc dimers.²¹ The utility of the alkynyl group arises from its physical and chemical features, namely its linear geometry, structural rigidity, extended π -electron delocalization and ability to be used in a variety of transition-metal catalyzed chemical reactions that allow the assembly of multicomponent systems. On the other hand, a variety of fused- and non-conjugated Pc-Pc dimers has also been described.^{15–19}

Pc-Por heteroarrays^{22–24} are also targets of choice in the search for multicomponent systems with improved optoelectronic properties, in the sense that the two macrocycles present intense and complementary optical absorption, which cover a large portion of the UV-vis-near infrared component of the solar spectrum. Both macrocycles can be linked in different ways, as will be detailed in this revision.

Many studies have also appeared regarding the photophysical properties of porphyrinoid-porphyrinoid ensembles. Model systems of Por dimers are very attractive for spectroscopic



Gema de la Torre

Gema de la Torre graduated in Chemistry (1992) and obtained her PhD (1998) from Universidad Autónoma de Madrid (UAM). Currently she is Associate Professor in the Organic Chemistry Department at UAM. Her current research interests are the synthesis of new phthalocyanines for their application in organic solar cells, double-decker phthalocyanines with single-molecule magnetic properties and new phthalocyanine-based multicomponent systems, including phthalocyanine–nanotube and phthalocyanine–graphene ensembles.



Giovanni Bottari

Giovanni Bottari graduated in Chemistry (1999) from the Università degli Studi di Messina (Italy) and received his PhD (2003) at the University of Edinburgh (United Kingdom). Currently, he is Assistant Professor at the Universidad Autónoma de Madrid and Associate Scientist at IMDEA Nanociencia (Spain). His current research interests include the preparation and study of multicomponent, phthalocyanine-based donor–acceptor molecular materials both in solution and on surfaces.



Michael Sekita

acceptor conjugates/hybrids as integrative materials for robust and photoactive films for an efficient solar energy conversion.



Anita Hausmann

Anita Hausmann started her studies in chemistry in 2000 and received her diploma from the Friedrich-Alexander University in Erlangen (Germany) in 2007. She obtained her PhD in December 2011 at the University of Erlangen under the supervision of Prof. Dr Dirk M. Guldi for her research on energy- and electron-transfer processes of supramolecular donor–acceptor systems. During her PhD studies, she joined Prof. Dr Erik Vauthey's group at the University of Geneva for two months. In 2012, she had a postdoc position in Prof. Dr Dirk M. Guldi's working group at the University of Erlangen (Germany).

and kinetic studies, in order to understand the photophysics of the *special pair*. In particular, mixed metal dimers offer the possibility of isolating the factors affecting the rates of energy and electron transfer between the two Por moieties.^{25,26} On the other hand, Pcs also produce efficient electron-transfer processes that can be modulated by choosing the appropriate central metal and the nature of the peripheral substitution. Typically, rapid charge-separation (CS) and slow charge recombination (CR) rates are facilitated by the small reorganization energies of electron transfer that these chromophores exhibit.²⁷ However, studies on excited-state interactions of Pc binuclear systems are scarce. In contrast, Pc–Por heterodimers have been targets of choice, aimed at rationalizing the effect of the structural and electronic features of each of the two components on the photoinduced electron/energy transfer dynamics of the ensemble.²³ It is well known that the long-wavelength absorption of Pcs overlaps quite well with the short-wavelength fluorescence of Pors, which results, upon photoexcitation, in an efficient transduction of singlet excited state energy from the Por to the Pc.^{28,29} On the other hand, the incorporation of a Por unit, as a secondary donor, into Pc–C₆₀ conjugates has been exploited in the search for long-lived charge-separated states.²³ Several electron-donating Pc–Pc, Por–Por, and Pc–Por dyads have been attached, either covalently or non-covalently, to electron-acceptor components such as C₆₀ or perilendiimides (PDIs).^{9,23,26,30}

This review will revise the synthetic methods developed for the preparation of outstanding Pc–Pc and Pc–Por derivatives and their multicomponent arrays in which a dimer is connected to one or more electro- or photoactive units. Some Pc–subphthalocyanine (SubPc) and Por–SubPc dyads will also be described in the first sections. Next, relevant examples of Por dimers presenting different connectivities will be given, as well as their self-organization in supramolecular ensembles. Particular attention will be paid to the synthesis and properties of multicomponent electroactive systems containing Por–Por units. The review will be closed with selected and representative examples of the

photophysical properties of the assemblies comprising Pc–Pc, Pc–Por and Por–Por as electron-donor units. Sandwich-type, rare earth Pc- and/or Por-based complexes are out of the scope of this review.³¹

2. Phthalocyanine–phthalocyanine binuclear systems

The preparation of covalently linked, binuclear Pc systems has been pursued by many different researchers in the search for excitonic or electronic interactions between macrocycles which can modify the electrical and optical behaviour of the binuclear systems with regard to the mononuclear parent compounds.^{15–19} These interactions can arise from:

(a) A cofacial arrangement of the Pc subunits, which can be achieved either when a (semi-) flexible and large enough bridge is connecting both macrocycles, or through axial–axial bonding.

(b) An extension of the π-conjugated system, which is achieved by either using rigid alkenyl–alkynyl bridging groups between the macrocyclic units or by the edge-to-edge fusion of two Pcs, resulting in binuclear systems sharing a common benzene (or naphthalene) ring.

(c) Supramolecular (*e.g.* donor–acceptor (D–A), metal–ligand, *etc.*) interactions between appropriately substituted Pcs.

2.1 Cofacially arranged, binuclear phthalocyanines

Binuclear Pcs covalently linked through their benzo rings with different flexible bridges were widely studied by Leznoff and coworkers in the late 1980's and early 1990's.³² In these systems, cofacial conformations allow π-overlap bringing about spectroscopic and electrochemical properties which differ significantly from the parent mononuclear compounds. More recently, some novel examples of cofacially arranged, binuclear Pcs have been published, most of them focused on the use of these systems as sensors. In particular, cofacial assembly of two



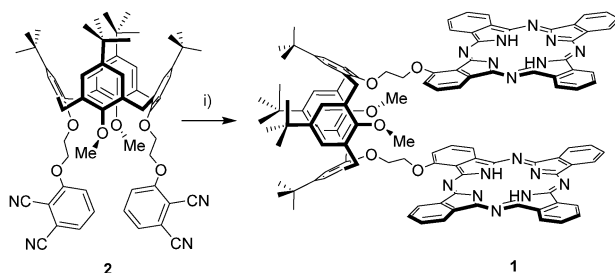
Dirk M. Guldi

Dirk M. Guldi graduated in Chemistry (1988) and received his PhD (1990) at the University of Köln. Currently, he is Chair of Physical Chemistry at the University of Erlangen-Nuremberg. He is one of the world-leading scientists in the field of charge-separation in donor–acceptor nanocarbon-based materials and construction of solar energy conversion devices. Homepage: <http://www.chemie.uni-erlangen.de/dcp/assets/pdf/DCP-Profile2010.pdf>



Tomás Torres

Tomás Torres is Full Professor of Organic Chemistry at the Autonoma University of Madrid (UAM) and Associated Senior Researcher at the IMDEA-Nanoscience. In addition to various aspects of synthetic and supramolecular chemistry his current research interests include the preparation and study of the optical properties of organic functional materials. His group, that presently consists of twenty five researchers, is currently exploring several areas of basic research and applications of phthalocyanines, porphyrins and carbon nanostructures (fullerenes, carbon nanotubes, graphene), including organic and hybrid solar cells, with a focus on nanotechnology.



Scheme 1 Synthesis of ‘Pacman’-type Pc **1**. Reagents and conditions: (i) phthalonitrile, lithium/pentanol, 110 °C, 24 h.

Pcs by means of a calixarene scaffold was reported.³³ Binuclear Pc **1** is the first example of a ‘Pacman’-type Pc, and it was conceived as a potential sensor of soft heavy metal ions such as Ag⁺ and Hg⁺. The calixarene scaffold in **1** imparts conformational flexibility, a property which is desirable in chemoreceptor applications. The bisPc architecture was built by reaction of the bis(phthalonitrile)-containing calixarene precursor **2** with an eightfold excess of phthalonitrile in Li/pentanol at 110 °C (Scheme 1). The UV-vis spectrum of **1** indicated that the dimer existed as a conformational mixture of cofacial ('clamshell') and open forms. The cation complexing ability of **1** towards Ag⁺ was evaluated, the studies indicating that the binding occurs through interaction of the Pc rings with the silver cation, since the bis(phthalonitrile)-containing calixarene precursor **1** did not possess any silver ion selectivity. Moreover, the fluorescence of **1** decreased upon the addition of silver cations demonstrating that the two Pc rings are ‘sandwiching’ the silver ion in the final complex.

Similarly, 1,1'-bi-2-naphthol (BINOL) has been used as a rigid linker to prepare cofacially coupled Pc dimers **3a,b**.³⁴ The originality of this contribution relies on the fact that enantiomerically pure BINOL was inserted, thus affording two different bisPc enantiomers **3a** and **3b**. Chiral cavity-containing dimers can be interesting as flexible-size tweezers for molecular recognition of chiral substrates and exceptional platforms for enantioselective catalytic systems. Both (*R*)-(**3a**) and (*S*)-(**3b**) enantiomers (Fig. 1) were prepared by cross-condensation of enantiomerically pure bis(phthalonitrile)-containing BINOL precursors with 18-fold excess of commercially available

4-*tert*-butyl-phthalonitrile. Exciton-coupling in these ‘clamshell’ binuclear derivatives was corroborated by electronic absorption, magnetic circular dichroism and cyclovoltammetry (CV) measurements.

A more convergent approach to prepare ‘clamshell’ bisPcs is the reaction of a preformed Pc holding a reactive moiety with an appropriately, doubly-functionalized molecule which will perform as a bridge in the target binuclear compound. An example of this approach is the nucleophilic ‘coupling’ of hydroxyPcs with 1,2-, 1,3- and 1,4-bis(bromomethyl)benzenes to give binuclear Pcs with different arrangements in excellent yields.³⁵ ‘Double-click’ chemistry was used as a tool to achieve ‘clamshell’-binuclear Pc **4** from a functionalized mononuclear Pc (Fig. 1).³⁶ The ‘double-click’ reaction between an ethynyl-containing Pc and 1,4-bis(azidomethyl)benzene, using CuI and DMSO as solvent, gave **4** in 80% yield. UV-vis and fluorescence spectra of this compound revealed that its preferred conformation is the closed ‘clamshell’ arrangement, which was also confirmed by CV measurements. This cofacial conformation could be easily opened by the addition of pyridine. On the other hand, the same authors also described a related trifluoroethoxy-coated binuclear Pc, which is the first example of a *never-closing* ‘clamshell’ Pc, the fluorophobic repulsion among lateral chains being responsible for this behaviour.³⁷

Ball-type Pcs are a new class of complexes which were firstly reported by Tomilova’s group in 2003.³⁸ These compounds have four cross linked substituents, each of them attached to both of the two face-to-face Pc molecules through their peripheral position (for example, see compound **5** in Scheme 2). Other authors have reported the synthesis and various properties of these types of Pcs with various metal centres and cross-linkages, such as calix[4]arene,^{39–41} 4,4'-isopropylidenedioxydiphenyl ligands,⁴² pentaerythritol bridges,^{43,44} and others.^{45–48} The preparation of these types of compounds is usually performed by *ipso* substitution of 4-nitrophthalonitrile with the corresponding bridging ligand having a diol functionality (see for example Scheme 2) followed by a typical cyclotetramerization reaction procedure. It has been demonstrated that the extent of the interactions is a result of the distance between the two MPcs units and, therefore, the physicochemical properties are strongly affected by the nature of the bridging ligands.

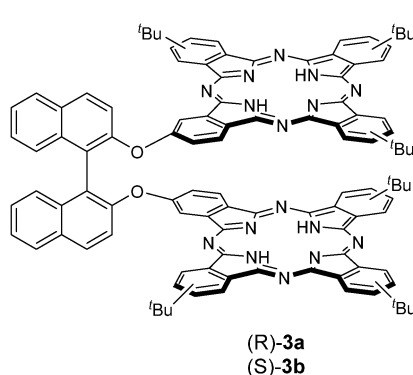
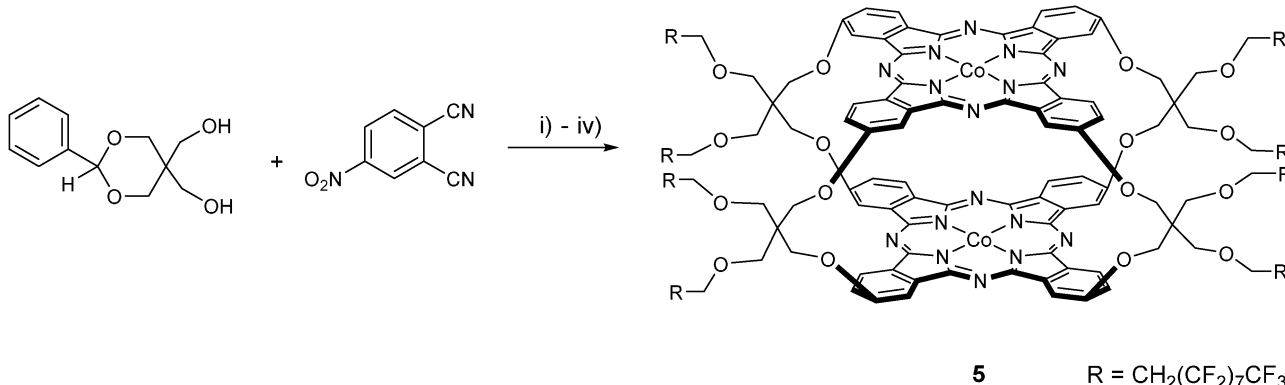


Fig. 1 Cofacially coupled bisPcs **3a,b** and **4**.



Scheme 2 Synthesis of ball-type Pc **5**. Reagents and conditions: (i) K_2CO_3 , DMF, 50°C ; (ii) $\text{Co}(\text{CH}_3\text{COO})_2 \cdot 4\text{H}_2\text{O}$, sealed tube, 300°C ; (iii) H_2 (1 atm), Pd/C (10%), DMSO, rt; (iv) NaH , heptadecafluoro-10-iododecane, DMF, 120°C .

Ball-type $\text{Co(II)}\text{Pc}$ dimers are a subject of interest in electrocatalysis for the oxygen reduction reaction at the fuel cell cathode. Recently, the synthesis and the electrochemical, electrocatalytic, electrical and gas sensing properties of a ball-type, $\text{Co(II)}\text{Pc}$ dimer **5** with eight perfluorinated chains was reported (Scheme 2).^{49,50} This complex displays high catalytic activity for oxygen reduction reaction which is attributed to the involvement of two redox-active metal centres in a rigid cofacial structure. Also, novel ball-type, binuclear MPcs ($M = \text{Co(II)}, \text{Zn(II)}, \text{Cu(II)}$) bridged by four rigid cyclopentylidisisilanoxy-polyhedral oligomeric silsesquioxanes have been prepared.⁵¹ The $\text{Co(II)}\text{Pc}_2$ derivative shows higher oxygen reduction performance in acidic medium than monomeric $\text{Co(II)}\text{Pc}$, which should be related to the presence of two redox-active, face-to-face metal centres, which promotes the interaction with O_2 molecules, probably the O–O bond breakage and thus, reduction to water. This evaluation is strongly supported by the improved electrocatalytic performance of the ball-type Pc derivative with Co(II) redox-active centres than the analogs with redox-inactive Zn(II) and Cu(II) metal centres.

Axially-bridged Pcs are an outstanding class of compounds. This type of linkage provokes relevant changes in the electronic structure of the molecule by altering the π -electronic distribution due to the dipole moment of the central metal–axial ligand bond. The most widespread axially-bridged dimeric structures are based on $\text{Fe(III)}\text{Pcs}$ linked together through oxygen (μ -oxo $\text{Fe(III)}\text{Pc}$ dimers)^{52,53} or nitrogen (μ -nitrido $\text{Fe(III)}\text{Pc}$ dimers).^{54,55} These compounds show superior catalytic properties in selective oxidation processes, and have widely been covered in previous revisions.⁵⁶

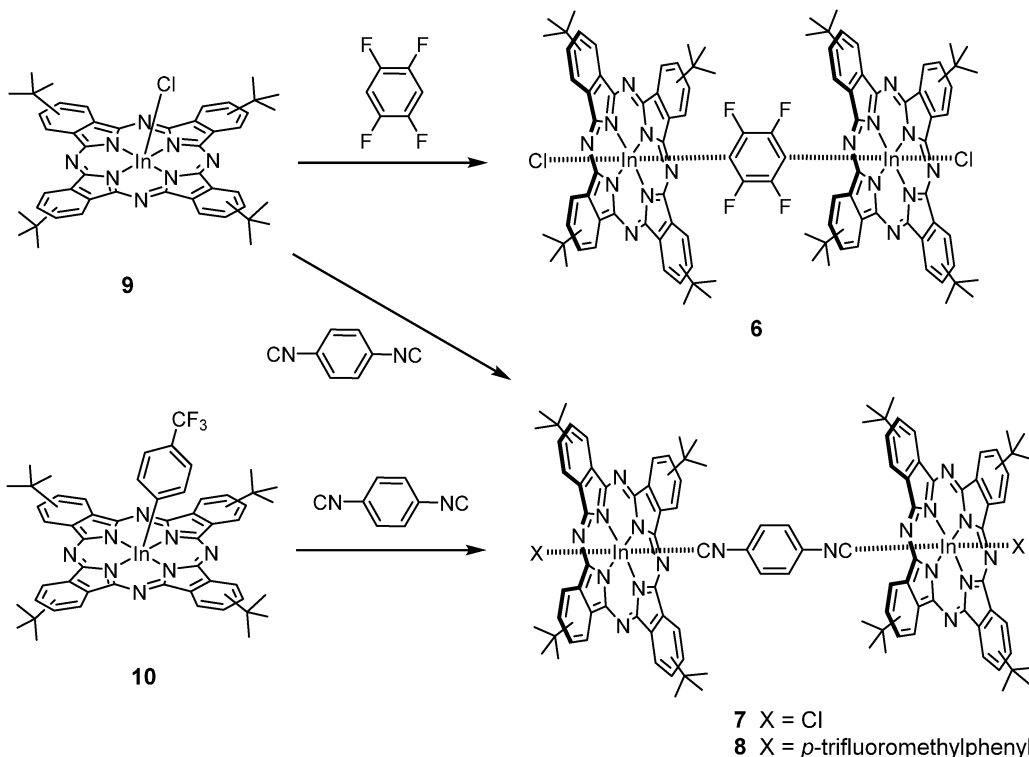
More recently, the chemical reactivity of other trivalent metallic Pcs , in particular Ga(III) and In(III) complexes, has been exploited to prepare heavy-metal containing, axially bridged bis Pcs , in the pursuit of systems with improved non-linear absorption properties for optical limiting applications. Axially bridged bis Pcs **6–8** (Scheme 3) were prepared upon dimerization of tetra-*tert*-butyl-In(III)Cl Pc (**9**) and tetra-*tert*-butyl-In(III)(*p*-trifluoromethylphenyl) Pc (**10**) through reactions with the bidentate ligands 1,4-diisocyanobenzene and 2,3,5,6-tetrafluorophenylene, respectively.⁵⁷ When compared with the parent monomers **9** and **10**, the dimers **6–8** display linear UV-vis spectra characterized by a

blue-shift of the Pc Q-band in the order of 5–10 nm. On the other hand, a $\text{Ga(III)}\text{Pc}$ -based dimer with a direct gallium–gallium bond and two coordinated dioxane molecules was also prepared.⁵⁸ This compound may exist in two different conformations: one in which the two Pcs are poorly interacting, and another in which they are very close and strongly interacting. In the latter conformer, the emission lifetime is much shorter than that of the monomer model compounds. As far as no significant difference between the absorption spectra of the monomer and dimer was observed, intramolecular interactions should exist only in the excited state.

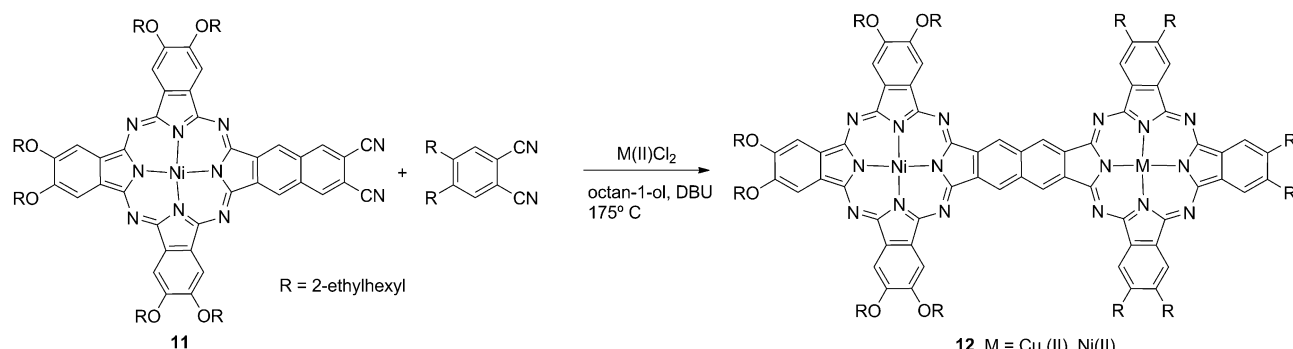
2.2 Conjugated binuclear phthalocyanines

As mentioned above, increasing the extension of the conjugated π -electronic system of Pcs brings about changes in the electronic structure and, therefore, in the optical behaviour features of the resulting systems, namely red-shift and splitting of the Q-band. Conjugated, binuclear Pc systems stand out as functional materials in molecular optoelectronics and NLO.^{59,60} Enlargement of the π -conjugation can be attained either by fusing two Pc rings in such a way that a benzene (or a naphthalene) ring is shared by the two macrocycles, or by bridging the two Pc units with short, conjugated spacers. Following are detailed several examples of these two families of outstanding derivatives.

Various alkyl- and alkoxy substituted, planar binuclear Pcs sharing either benzene^{61,62} or naphthalene rings^{63,64} are reported in the literature, as well as binuclear naphthalocyanines (Ncs).⁶⁵ For homobinuclear Pc systems, the synthesis is usually carried out by statistical condensation of alkyl/alkoxy-substituted phthalonitriles and either 1,2,4,5-tetracyanobenzene or 2,3,6,7-tetracyanonaphthalene that will be incorporated into the fused position of the final molecule. However, to synthesize fused heterobinuclear or heterodimetallic Pc systems, a multistep procedure involving the former preparation of an unsymmetrically substituted mononuclear Pc holding two cyano moieties in an *ortho* substitution pattern was formerly developed by the group of Torres (see Scheme 4).^{66,67} A more recent example of the latter approach is shown in Scheme 4.⁶⁴ The prepared dicyano-substituted intermediate **11** reacts with a selected phthalonitrile to yield binuclear compound **12**. In general, all fused, binuclear Pc compounds reported in the literature exhibit



Scheme 3 Synthesis of axially-bridged, In(III)Pcs binuclear systems **6–8**.



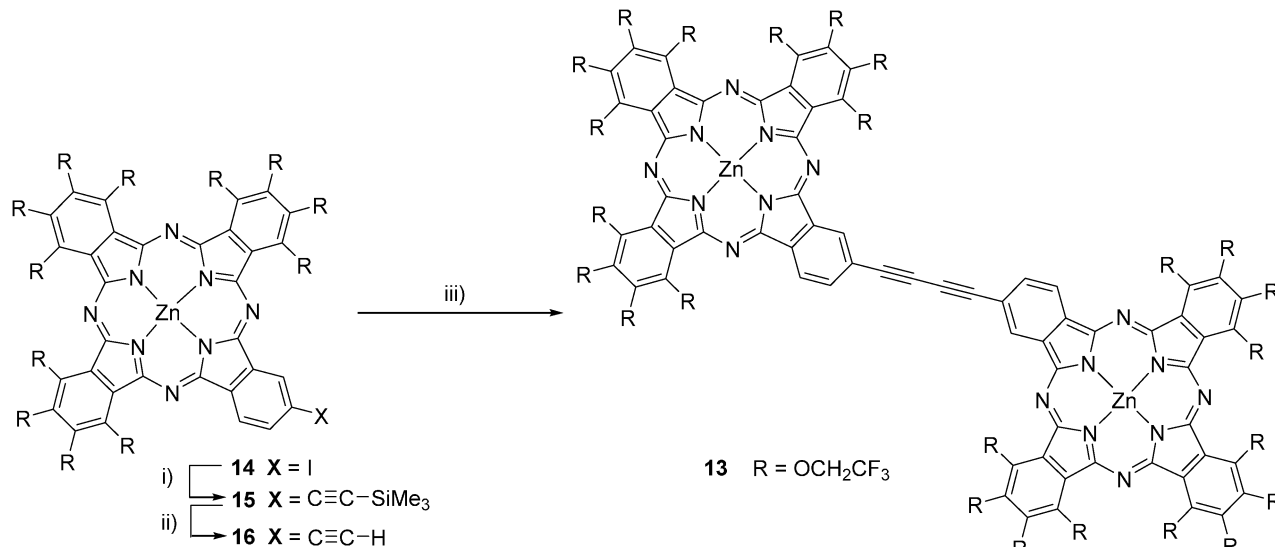
Scheme 4 Synthesis of fused, binuclear Pcs **12**.

an intense Q-band shifted to the near IR with regard to the parent mononuclear Pcs, reaching *ca.* 1000 nm in the case of planar binuclear Ncs.⁶⁵

Apart from the pursuit of systems with a delocalized π -structure, the preparation of fused, binuclear Pcs-based systems is, indeed, encouraged by the search for intramolecular interactions between components either in the ground- or excited states. An evaluation of the intramolecular interactions in the excited state of both metal-free, planar Pcs-Pcs and Pcs-pyrazinoporphyrazine dimers has been performed by means of time-resolved electron paramagnetic resonance techniques. Both types of compounds display delocalization of the excitation over the two units and a contribution of a CT configuration.⁶⁸ Steady-state and time-resolved absorption and fluorescence experiments as well as quantum mechanical density functional

theory (DFT) calculations have also been performed on binuclear metal-free and Zn(II)Pcs sharing a common benzene ring.⁶⁹ The larger fluorescence anisotropies shown by the binuclear derivatives compared to those of the monomers are consistent with the loss of symmetry and therefore the extension of the π -electron system.

Some work has been devoted to the preparation of systems having Pcs-to-Pcs conjugated linkers. For instance, ethyne bridges are proved to be ideal linkages for enabling electronic interactions between chromophores. The first synthetic approach to prepare conjugated, binuclear Pcs covalently linked by alkyne and alkene bridges was reported by Leznoff and coworkers in 1991.²⁰ Since then many other alkynyl- and alkenyl-bridged conjugated binuclear compounds have been reported. In particular, Torres' group has been involved for some years on the synthesis,



Scheme 5 Preparation of **Pc 13**. Reagents and conditions: (i) trimethylsilylacetylene, $\text{Pd}(\text{PPh}_3)_2\text{Cl}_2$, CuI , Et_3N , THF , 40°C , 24 h, 97%; (ii) K_2CO_3 , MeOH , RT, 4 h, 99%; (iii) CuCl , pyridine, RT, 3 days, 74%.

spectroscopic and electrochemical characterization of π -extended, binuclear **Pc** systems linked through one or more ethynyl and butadiynyl bridges. Palladium-catalyzed reactions are the key for preparing this type of alkynyl-linked bis**Pcs**. In particular, the Sonogashira cross-coupling reaction between **Pcs** bearing a terminal alkyne and monoiodo**Pes** has provided many different conjugated, binuclear systems. The work on this area has been compiled in some revisions.^{16–18,21} An example of the further use of these alkynyl-bridged bis**Pcs** for the construction of more complex systems is the preparation of a benzene-centered **Pc** hexamer through dicobaltoctacarbonyl-catalyzed trimerization of an ethynyl-linked bis**Pc**.⁷⁰

Cross-coupling methodology is still followed by other authors to prepare alkynyl-bridged, homodinuclear **Pc** derivatives, as shown in Scheme 5.⁷¹ Butadiynyl-bridged compound **13** was synthesized by a $\text{Pd}(\text{II})$ -catalyzed, Sonogashira cross-coupling reaction of iodo**Pc** **14** and a monoprotected ethyne (to give **15**), followed by deprotection (to give **16**) and Glaser coupling. As a

consequence of the peripheral substitution with trifluoroethoxy moieties, which causes fluorophobic repulsion, the molecule does not aggregate in solution. Even though aggregation had been minimized in previous works by the introduction of bulky substituents at the peripheral **Pc** positions, this example is one of the few reporting a fully nonaggregating binuclear **Pc** system, this feature conferring high fluorescence on the molecule.

It is worth mentioning that, in a recent work, $\text{Pt}(\text{II})$ has been inserted into the central bond of the butadiynyl bridge, this modification causing a significant decoupling of the **Pc** groups since the $\text{Pt}(\text{n})$ ion reduces or even disrupts conjugation.⁷²

In addition to alkynyl bridges, other conjugated moieties that make possible the electronic communication between **Pc** macrocycles have been exploited. An outstanding example incorporates a [2,2']paracyclophane ring as a bridge (**17**, Fig. 2).⁷³ [2,2']Paracyclophane contains two arene subunits with strong through-space, π - π coupling owing to the close proximity of the

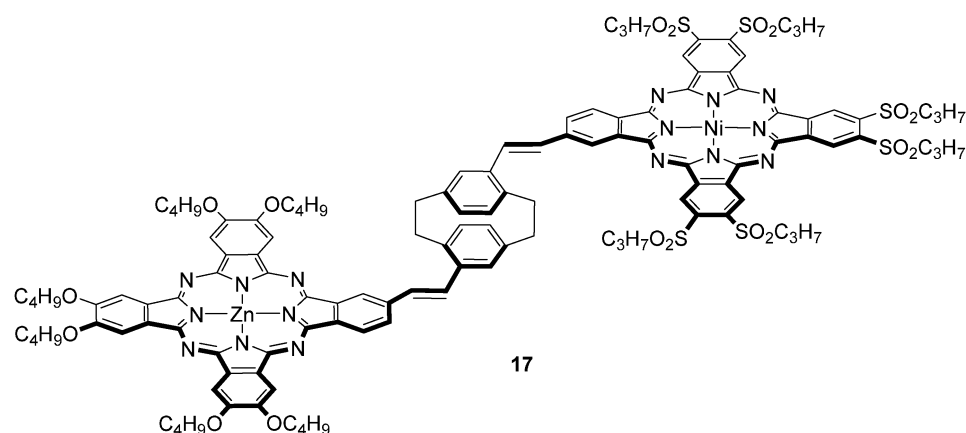


Fig. 2 Molecular structure of [2,2']paracyclophane-bridged, binuclear **Pc** **17**.

aromatic moieties. The two differently substituted Pc fragments in **17**, namely, a Pc substituted with six electron-donor alkoxy substituents and a Pc substituted with six electron-withdrawing alkylsulfonyl substituents, were connected to a pseudo-*para*-divinyl[2.2]paracyclophane derivative by two successive Heck reactions. This molecular building block, containing a π -electron-rich component and a complementary π -electron-poor counterpart, undergoes hetero-association both in solution and in the solid state by means of D-A interactions.

2.3 Supramolecular phthalocyanine dimers

Metal-ligand interactions are widely-used molecular recognition tools for the construction of well-defined supramolecular architectures.⁷⁴ Thus, it is not surprising that, over the years, some effort has been devoted to the construction of supramolecular arrays of Pcs by means of the metal coordination approach. Most of the noncovalent superstructures based on Pcs involve the coordination of Zn(II)Pcs and Ru(II)Pcs.⁷⁵

A former example of homodimer Pc-Pc formation through metal-ligand interactions reported the self-coordination of Zn(II) hexaoctylpyridino[3,4]tribenzoporphyrazine derivative **19a**, which is a Pc derivative where one of the isoindolic moieties has been replaced by a pyridine unit. This molecule showed to form alternative edge-to-face complexes through axial coordination of the pyridine moiety of one Pc to the zinc atom of another.⁷⁶ Other authors went one step further in the study of a similar Zn(II) tri-*tert*-butylpyridino[3,4]tribenzoporphyrazine **19b**. This Pc also showed a natural tendency to form homodimers such as **18** in noncoordinating solvents (Scheme 6).^{77,78} In the presence of pyridine, the dimer dissociated, giving rise to **19b**, which, in the presence of silver salts such as AgPF₆, formed a Ag(I)-coordinated homodimer **20**. On the basis of its electronic

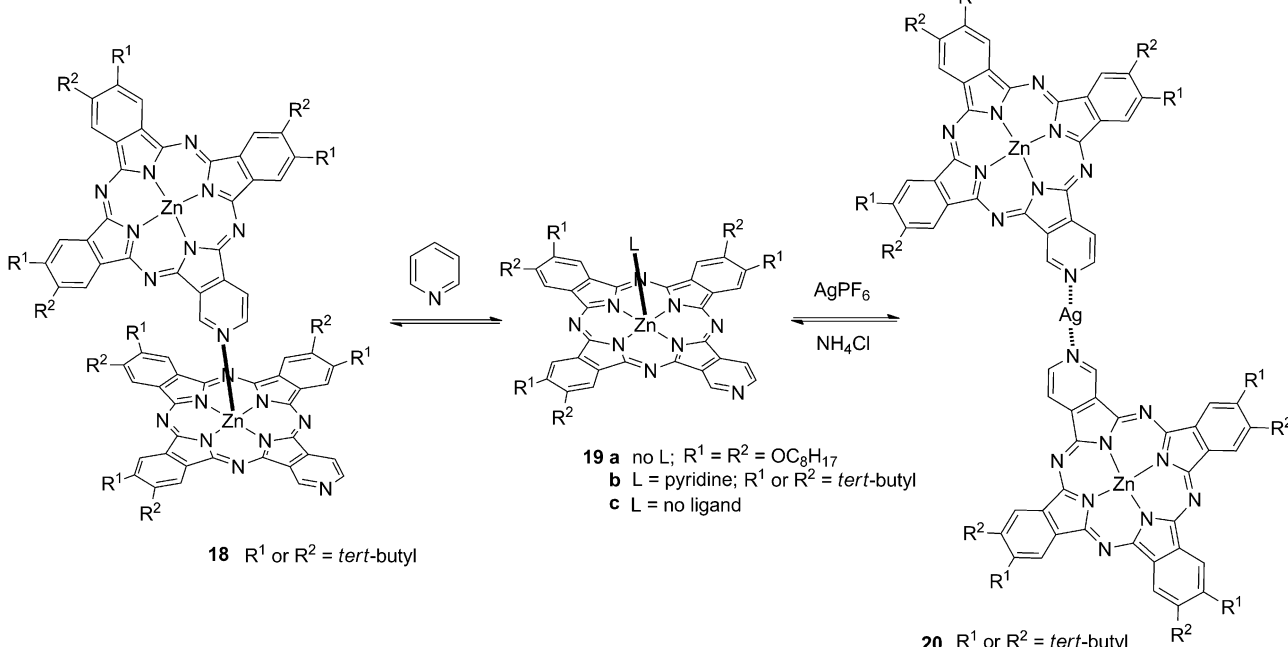
absorption and magnetic circular dichroism properties, it has been suggested that this latter dimer adopts a planar, *trans*-conformation. Addition of NH₄Cl, which can remove the silver ions as AgCl, regenerates the monomeric species **19c**. Diethylamino-substituted tetrapyrazinoPcs were also shown to self-assemble into J-dimers in noncoordinating solvents by the coordination of the free electron pair of one diethylamino group with the central metal of the adjacent molecule.⁷⁹

An outstanding example of a supramolecular Pc-Pc ensemble formed through self-coordination is shown in Fig. 3. Homodimer **21** was assembled by means of double, axial Zn(II) coordination with the imidazolyl (Im) moiety peripherally linked to the Pc macrocycle.⁸⁰ This self-coordination process was found to be extremely efficient in solution of noncoordinating solvents such as toluene, with binding constants (K_{ass}) of about $1-10 \times 10^{11} \text{ M}^{-1}$, depending on the nature of the peripheral substituents. The resulting homodimers are so stable that they can break into the monomers only in the presence of a large excess of the competing ligand *N*-methylimidazole.

2.4 Binuclear phthalocyanines connected to electroactive moieties

The enormous interest in Pcs as molecular building blocks for the construction of artificial photosynthetic systems has fostered the study of a wide range of covalent and noncovalent Pc-based, D-A systems incorporating electroactive acceptor units of a diverse nature such as fullerene, PDI and anthraquinone (AQ) units, among others. Some examples of covalent and supramolecular arrays of such a nature are illustrated below.

Among the acceptor units employed for the preparation of D-A, bisPc-based systems, C₆₀ and PDI enjoy a privileged position. Covalent Pc-Pc-PDI or Pc-Pc-fullerene assemblies have proved



Scheme 6 Zn(II) pyridino[3,4]tribenzoporphyrazine **19a,b**, and two modes of self-assembly of **19b** leading to **18** and **20**.

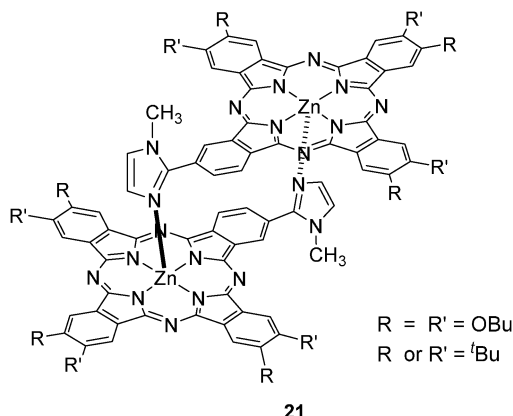


Fig. 3 Self-coordinated dimers **21** formed by axial-coordination of Im-functionalized Zn(II)Pcs.

to be efficient providing intramolecular charge separated states after photoexcitation of the chromophores. The photophysical aspects of these types of ensembles will be detailed in Section 5.

A binuclear, Pc–Pc–PDI (**22**, Fig. 4) was prepared by condensation reaction between an amino-functionalized Pc precursor and perylene dianhydride.⁸¹ The preparation of such structures can also be performed by first implementation of the phthalonitrile into the perylene structure followed by the formation of both Pc macrocycles through mixed cyclotetramerization with *tert*-butylphthalonitrile.

Pd(II)-catalyzed, cross-coupling methodology was pursued to prepare conjugated Pc–PDI–Pc derivative **23** (Fig. 4).⁸² The synthesis of this triad was thereby accomplished through two different routes. The first one involves the initial bromination of the PDI at positions 1 and 7 and subsequent Sonogashira coupling with an ethynyl-functionalized Pc. The second methodology consists of endowing the same bay positions of the PDI scaffold with two terminal triple bonds followed by the conjugation with an iodoPc derivative. A significant redistribution of charge density in the ground state, that is, from the electron-donating Zn(II)Pc to the electron-accepting PDI is deduced from the absorption spectrum of the triad.

Ethynyl-bridges are also employed to assemble Pc–Pc conjugates to C₆₀. The synthetic strategy used for the preparation of conjugate **24** consisted of an initial preparation of the diformyl-containing Pc precursor **25**, through Pd(II)-catalyzed, cross-coupling reaction of diiodo Pc **26** and 4-ethynylbenzaldehyde. Binuclear conjugate **25** was then reacted with *N*-methyl glycine and C₆₀ to afford $\text{Pc}_2(\text{C}_{60})_2$ tetrad **24** (Scheme 7).⁸³

Regarding the incorporation of alkenyl linkers for the fabrication of binuclear Pc–Pc-based multicomponent systems, Heck-type coupling proved successful to form triads **27–29** (Fig. 5), consisting of one AQ unit covalently linked to two Zn(II)Pcs.⁸⁴ The reaction of monofunctionalized tri-*tert*-butylvinyl Zn(II)Pc with 1,5-, 1,8-, and 2,6-substituted diiodoAQ yielded isomeric triads **27**, **28**, and **29**, respectively, leading to either highly interacting, packed (**28**)

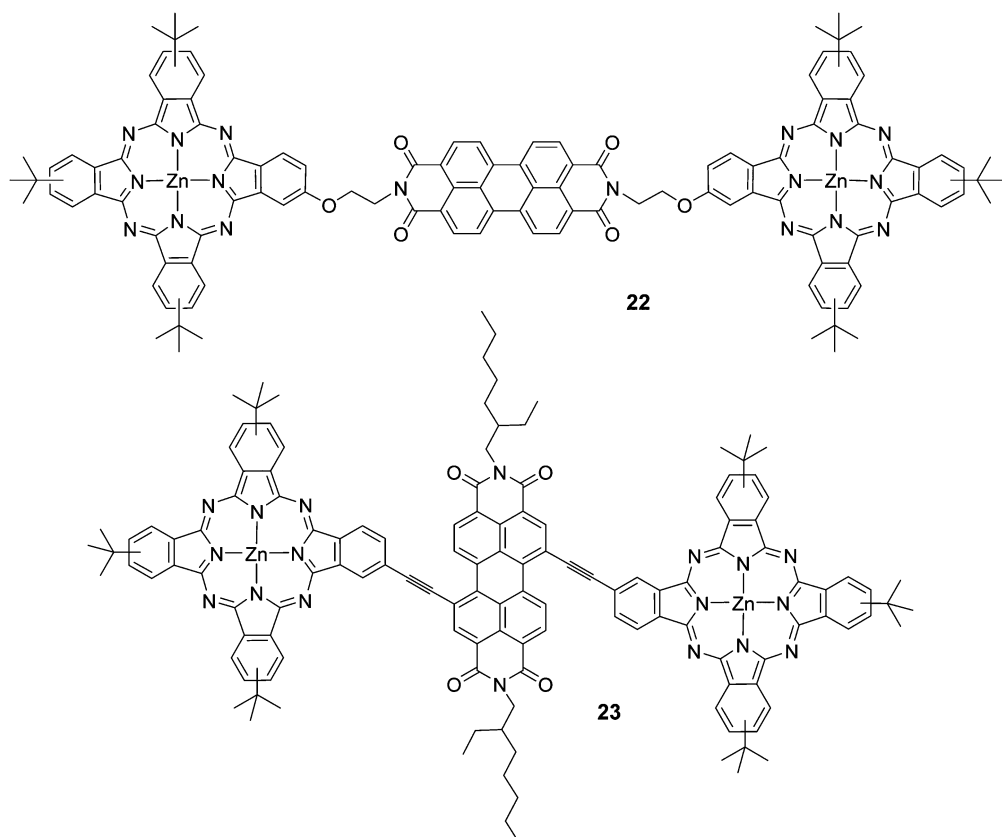
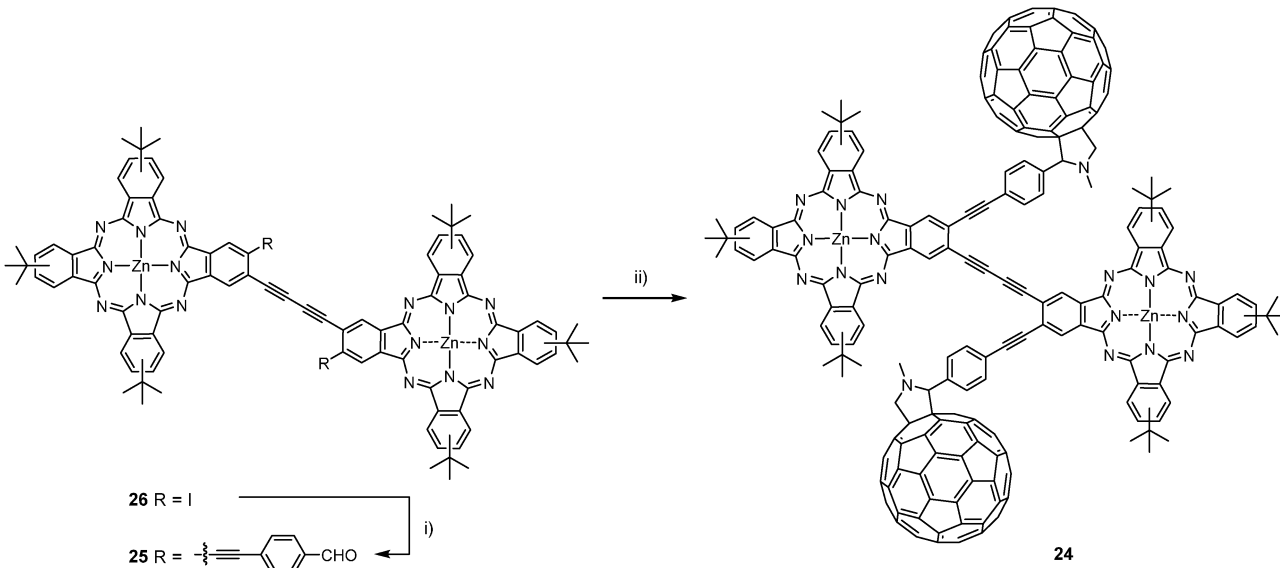


Fig. 4 Molecular structures of Pc_2 –PDI triads **22** and **23**.



Scheme 7 Synthesis of $\text{Pc}_2\text{-(C}_60\text{)}_2$ fullerene tetrad **24**. (i) 4-Ethynylbenzaldehyde, $\text{Pd}(\text{PPh}_3)_4\text{Cl}_2$, CuI , NEt_3 , THF, RT. (ii) C_60 fullerene, *N*-methylglycine, toluene, reflux.

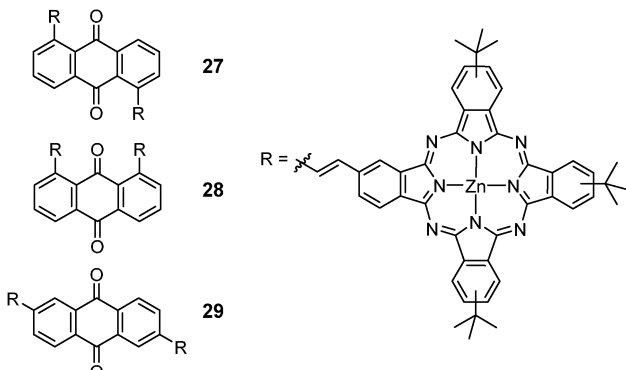


Fig. 5 Molecular structures of Zn(II)Pc₂-AQ triads **27–29**.

or extended (27 and 29) topologies. In triad 28, the Zn(II)Pc units are forced to π -stack cofacially and out of the plane of the AQ ring. Consequently, this molecule shows strong inter-Pc interactions that give rise to intramolecular excitonic coupling but a relatively small electronic communication with the AQ acceptor through the vinyl spacers. In contrast, the 1,5- or 2,6-connections of triads 27 and 29 allow for an efficient conjugation between the active units that extends over the entire planar system.

Supramolecular interactions have also been employed as a tool for the construction of Pc-Pc-based D-A systems. In particular, metal-ligand interactions are widely-used molecular recognition tools for the construction of such systems.

As mentioned above, axial Zn(II) coordination of Zn(II)Pcs with Im-containing units gives rise to rather stable supramolecular conjugates. Following this approach, a supramolecular architecture based on the assembly of two Zn(II)Pc units and a bis(Im)-substituted PDI has been recently described.⁸⁵ Supramolecular complexation studies by ¹H-NMR spectroscopy and ESI-MS, as well as UV-vis and fluorescence titration experiments, demonstrate a high coordinative K_{ass} between the two components (*ca.* 10^5 M^{-1}).

Ru(II)Pcs form strong complexes with basic sp^2 nitrogen atoms (pyridine and imidazole), either on one side or on both sides of the macrocycle depending on the mononuclear Ru(II)Pc precursor used, that is, either monocoordinated with CO or dicoordinated with benzonitrile. Cook and colleagues were the first to predict the utility of Ru(II)Pcs in the preparation of pyridyl ligated derivatives,⁸⁶ which show remarkable stability in solution due to the robustness of the ruthenium-pyridyl linkage.

Some examples in which two Ru(II)Pcs are linked together by means of other photoactive units through ruthenium-pyridyl bonds have recently been reported. For instance, treatment of PDI, bearing two 4-pyridyl substituents at the imido positions, with Ru(II)Pc monocoordinated with CO affords triad 30 in good yields (Fig. 6).⁸⁷ Another related example describes the self-assembly of two Ru(II)(CO)Pcs with one appropriate squaraine molecule bearing two 4-ethenylpyridyl moieties to yield triad 31 (Fig. 6).⁸⁸ This ensemble was shown to absorb a large portion of the visible spectrum.

On the other hand, triad 32 (Fig. 6) bearing an orthogonal geometry was prepared by treatment of Ru(II)(CO)Pc with a hexakis-substituted C₆₀-pyridyl ligand.⁸⁹ This array exhibits electronic coupling between the two electroactive components (the two Ru(II)Pc units and the fullerene moiety) in the ground state.

Other supramolecular interactions have also been used as a recognition motif for the preparation of binuclear Pc ensembles, such as D-A contacts between appropriately substituted Pcs bearing electron-donating or electron-withdrawing groups. This supramolecular tool has been exploited in Torres' group for the construction of the photoactive supramolecular Pc-C₆₀ triad 33 depicted in Fig. 7.⁹⁰ Hetero-association between the complementary electron-deficient Pc 34 and electron-rich Pc 35, bearing also a covalently linked C₆₀ unit, was confirmed by different techniques, which provided evidence for the formation of a 1:1 D-A complex with a stability constant of about 10^5 M^{-1} in chloroform.

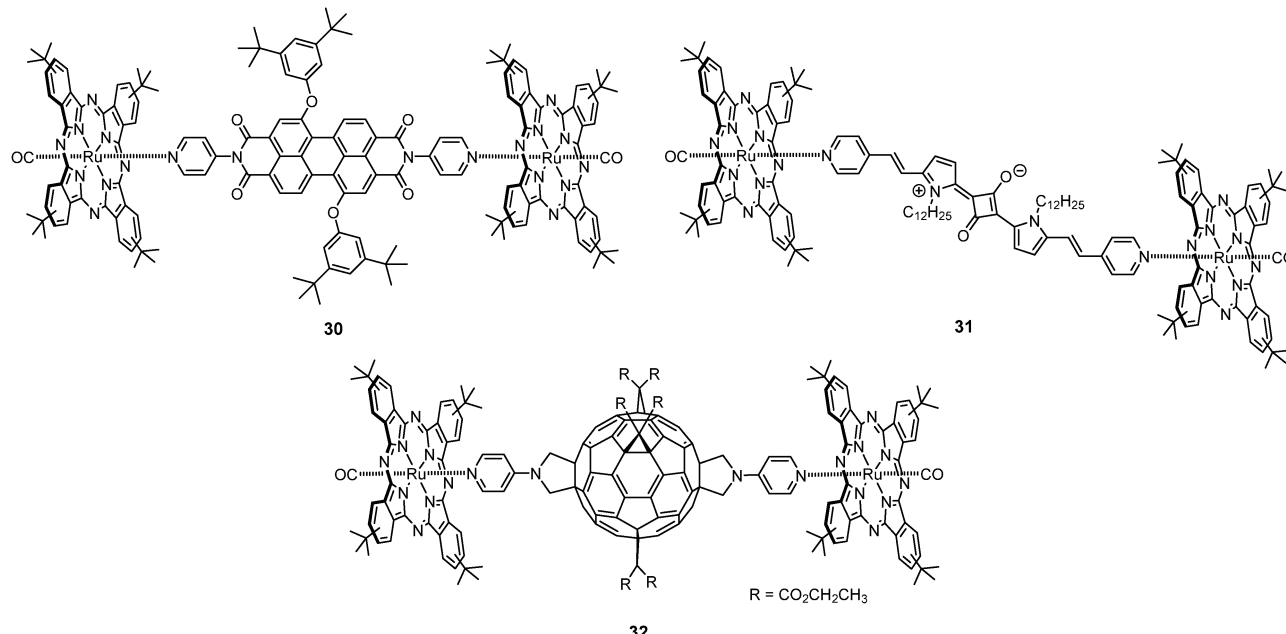


Fig. 6 Molecular structures of supramolecular triads Ru(II)Pc₂-PDI **30**, Ru(II)Pc₂-squaraine **31**, and Ru(II)Pc₂-C₆₀ **32**.

The self-assembly of Pcs functionalized at the periphery with crown-ether moieties was intensively studied in the late 1980's by different groups.^{91,92} In particular, tetra-15-crown-5-substituted Pcs were found to form cofacial dimeric supramolecular complexes in the presence of alkali cations with diameters exceeding those of the crown ether rings such as K⁺. In these complexes, four potassium ions were sandwiched between two crown-ether Pc units. This approach was recently used, together with metal-ligand interactions, to ensemble two Pcs and two C₆₀ moieties.⁹³

Thus, supramolecular system **36** (Fig. 7) consists of a cofacial Pc dimer held together by crown-ether-K⁺ interactions, which is bound through both Zn(II) metal centers to the pyridyl-functionalized C₆₀ component. Further stabilization by alkyl-ammonium cations-crown-ether interactions takes place in the ensemble.

Hydrogen-bonding interactions have also been used to create ensembles of two Pcs with other electroactive subunits. In particular, a melamine/PDI recognition motif has been employed as a new

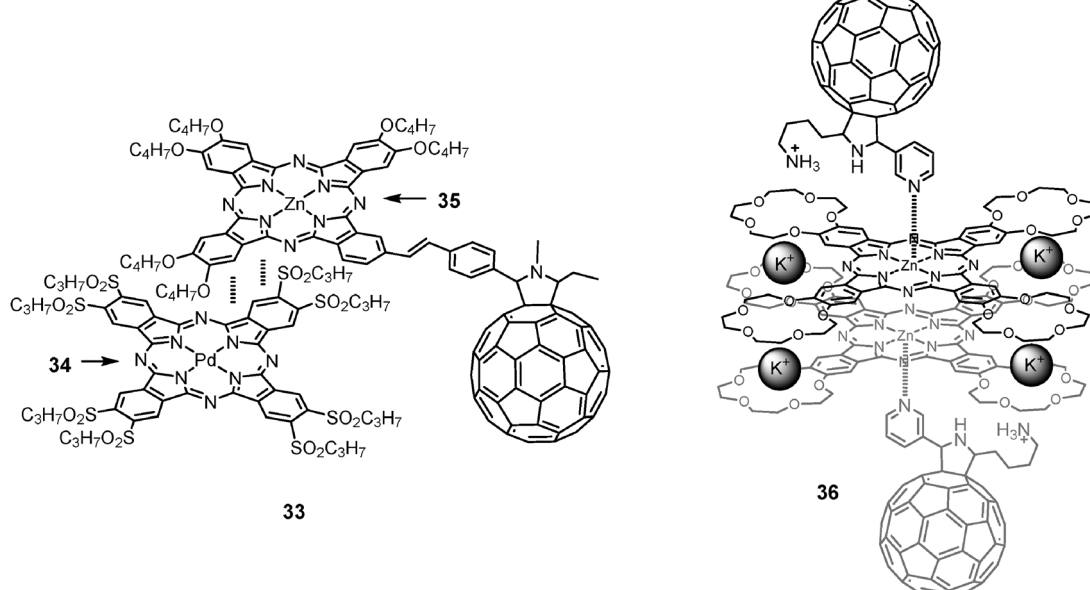


Fig. 7 Structures of heterosupramolecular triad **33** formed by D-A interactions between Pd(II)Pc **34** and Zn(II)Pc-C₆₀ dyad **35**, and crown-ether Pc₂-(C₆₀)₂ ensemble **36**.

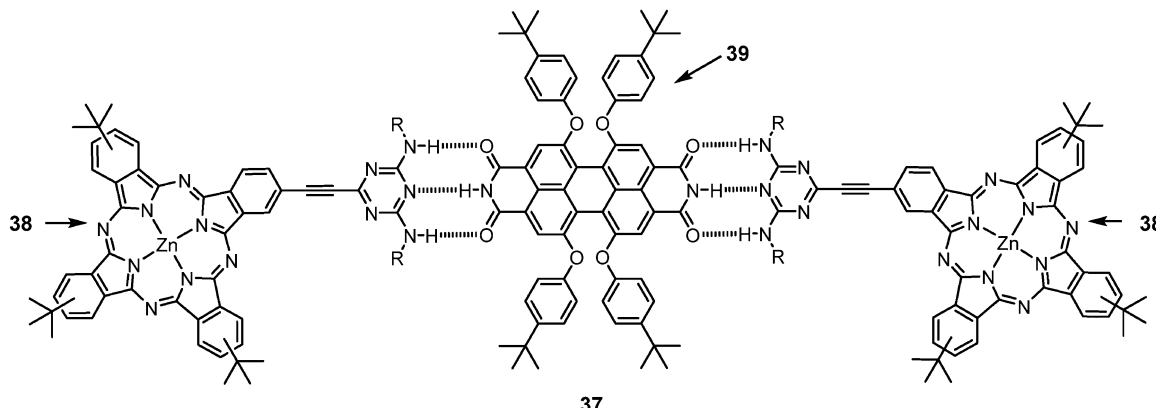


Fig. 8 Molecular structure of heterosupramolecular triad 37.

strategy to assemble Pcs in well-defined, hydrogen-bonding supramolecular architectures such as 37 (Fig. 8).⁹⁴ Thus, two Pc derivatives 38 that were functionalized with a ditopic melamine moiety strongly bind to each of the complementary diimide subunits in PDI 39 forming a stable supramolecular assembly. More recently, a related Pc unsymmetrically substituted with six strong donor thioalkyl chains and one melamine unit was assembled to a complementary PDI through three strong and highly directional hydrogen bonds.⁹⁵

2.5 Phthalocyanine–subphthalocyanine systems

A number of macrocyclic chromophores can be considered as Pc derivatives, for instance those with extended conjugation (*e.g.* Ncs, phenanthrenocyanines), those formed by replacement of one isoindole unit by another heteroaromatic moiety (*e.g.* triazolePcs, pyridinoporphyrazines) and those with a reduced (SubPcs) or increased (superPcs) number of isoindole units. Among all the Pc derivatives, SubPcs hold a privileged position. These lower Pc homologues are 14 π-electron aromatic compounds which comprise three *N*-fused, diiminoisoindole units in a cone-shaped geometry, and a central boron atom axially substituted with a halogen atom or other type of ligands. SubPcs are very promising candidates as photo- or electroactive systems.^{96–100} In particular, SubPc–Pc conjugates are perfectly suited for the study of intramolecular energy/electron-transfer processes for several reasons. First, the absorption of each chromophore perfectly complements that of the other; second, the energy level of their excited states and, therefore, of their optical transitions are very well suited for the efficient absorption and directional funneling, *via* energy-transfer processes, of photoexcitation energy; and finally, the redox gradient can be easily tuned by the introduction of different peripheral substituents on both macrocycles, and thus, control can be gained over the competition between photoinduced energy- and electron-transfer mechanisms.

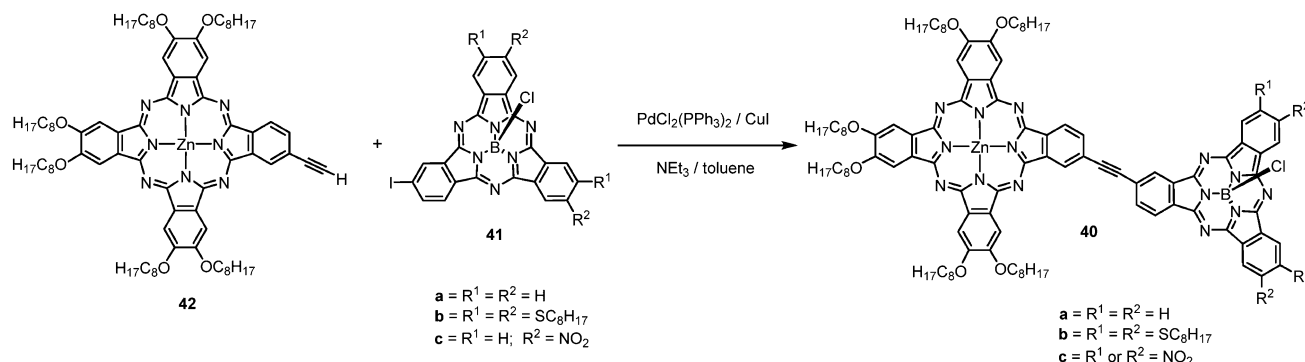
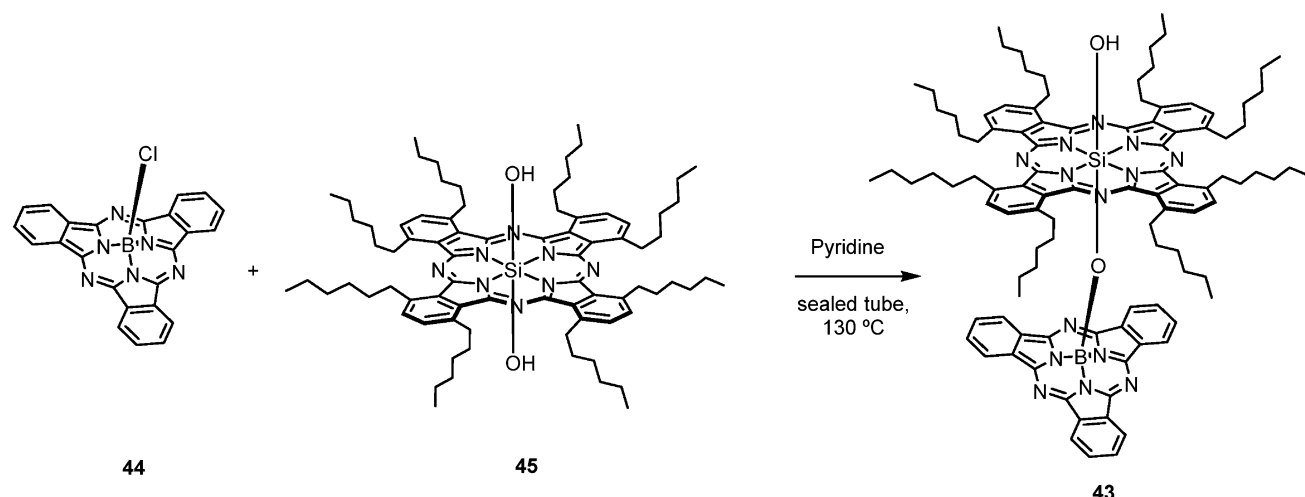
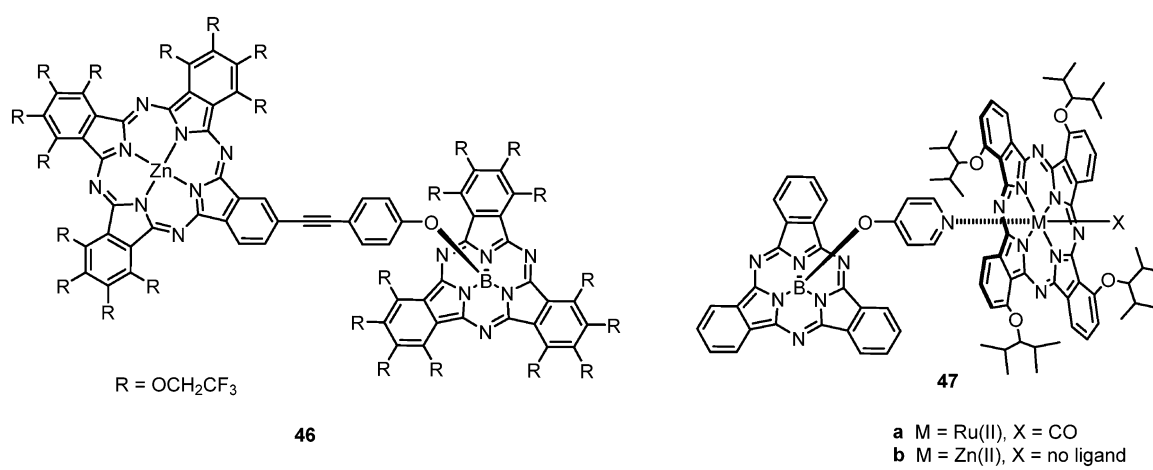
As for other Pc-based, binuclear ensembles, different strategies can be applied for linking both chromophores. For instance, dyads 40a–c (Scheme 8), in which both units are covalently linked through their peripheral positions by a conjugated ethynyl spacer, have been synthesized.¹⁰¹ Pd(II)-mediated, cross-coupling reaction

between different monoiodo-SubPcs (41a–c) and Pc 42 bearing a single ethynyl group afforded the target compounds. A remarkable dependence of the reaction rate on the SubPc peripheral substitution was noticed; electron-poor aromatic rings react much faster (40c > 40a > 40b).

Peripheral functionalization of SubPcs is sometimes difficult since the harsh reaction conditions for SubPc formation preclude the incorporation of a number of important functional groups. On the other hand, substitution of axial ligands of SubPcs is a feasible, modular approach towards the functionalization of these rings. Therefore, covalent bonding of SubPc and Pc cores can take place through the axial position of the participating rings.¹⁰² Cofacial Pc–SubPc dyad 43 having an oxygen atom linking the metal ions at the centres of the macrocycles was prepared by condensation reaction of ClSubPc 44 and Si(iv)(OH)₂Pc 45 (Scheme 9). The principal absorption bands arising from the SubPc and Si(iv)Pc components are evident in the UV-vis absorption spectra of dyad 43, but a small hypsochromic shift of the SubPc Q-band and a small bathochromic shift of the Si(iv)Pc Q-band are observed with regard to the monomeric reference compounds 44 and 45, respectively. These effects can be ascribed to differences in the axial environment more than to significant interactions of the π-electron orbitals of the component chromophores. The lack of interactions could be due to the cone-shaped structure of the SubPc unit, which avoids excitonic coupling even at such a short distance between the macrocycles. In accordance with this, the fluorescence spectrum of dyad 43 showed two bands at *ca.* 605 nm and *ca.* 780 nm, attributable to independent emissions from the SubPc and Si(iv)Pc components, respectively.

Very recently, a related alkynyl-linked SubPc–Pc system 46 (Fig. 9) was prepared through Pd(II)-catalyzed, Sonogashira coupling between a peripheral ethynyl moiety at the Pc and the *p*-iodofunctionalized position of an axial phenoxy ligand at the SubPc moiety.¹⁰³ A remarkable feature of this dyad is that both SubPc and Pc units are fully coated with trifluoroethoxy groups.

Following a supramolecular approach, SubPc–Pc dyads 47a,b (Fig. 9) were constructed through metal-ligand interactions between pyridiloxyl moieties linked at the axial position of the SubPc and the metal center of tetraisopropoxy-substituted

**Scheme 8** Synthesis of Pc-SubPc dyads **40a–c**.**Scheme 9** Synthesis of μ -oxo Pc-SubPc dyad **43**.**Fig. 9** Molecular structures of Pc-SubPc dyads **46** and **47**.

Zn(n)Pc (**47b**) and Ru(u)(CO)Pc (**47a**).¹⁰⁴ The complexation process was studied by 1H NMR and fluorescence spectroscopic methods, which confirmed the 1:1 binding stoichiometry between the chromophoric units. The K_{ass} , as determined by fluorescence

titration, were generally higher for **47a** [$(2.5\text{--}4.7) \times 10^4 M^{-1}$] than for **47b** [$(0.3\text{--}1.8) \times 10^4 M^{-1}$] (in **47b**). UV-vis spectroscopy experiments revealed negligible ground-state interactions between the two chromophores.

3. Phthalocyanine–porphyrin systems

The unique physicochemical properties that both Pcs and Pors present as individual chromophores have prompted, in recent years, to the preparation of several Pc-Por ensembles and their study.

As in the case of Pc-Pc assemblies, covalent and supramolecular Pc-Por systems have been prepared using, in some cases, synthetic strategies similar to the ones employed for the preparation of Pc-Pc systems (*e.g.*, metal-catalyzed coupling reactions or metal-ligand interactions between appropriately substituted Pc and Por macrocycles leading to covalent or supramolecular assemblies, respectively).

In this part of the review, we will present some of the most recent examples of covalent and supramolecular Pc-Por ensembles.

3.1 Covalent phthalocyanine–porphyrin systems

Since the first report, dated 1986, on the preparation of covalently linked, Pc-Por heterodimers,¹⁰⁵ a large number of covalent, Pc-Por ensembles have been prepared and studied.

In 2007, the groups of Torres, Cavaleiro and Guldi reported a series of *N*-bridged, Pc-Por heterodimers in which a Pc macrocycle was connected either at the β -pyrrolic (**48a–c**) (Scheme 10) or *meso* (**49**) (Fig. 10) positions of a Por unit.²⁹ Dyad **48a** was prepared following two different synthetic procedures. One synthetic route involved a statistical condensation reaction between 4-*tert*-butylphthalonitrile and 4-porphyrinylaminophthalonitrile **50**, which was obtained by a Buchwald-Hartwig amination reaction of Ni(II)Por **51** with 4-iodophthalonitrile, leading to Pc-Por dimer **48a** in 33% yield (Scheme 10). Alternatively, dyad **48a** could also be obtained by a Buchwald-Hartwig reaction between aminoPor **51** and a tri-*tert*-butyl-iodo-substituted Zn(II)Pc in 70% yield. Zn(II)Pc-Ni(II)Por derivative **48a** served as a precursor for the preparation of Pc-Por dyads **48b** and **48c** which were obtained by acid-promoted demetallation of the Por unit (**48b**) followed by treatment with Zn(OAc)₂ (**48c**). Immobilization of H₂-Zn(II)Por-Zn(II)Pc conjugates **48b** or **48c** onto single-walled carbon nanotubes (SWCNTs) has also been demonstrated, giving rise to the formation of stable, D-A Pc-Por-SWCNT hybrids.¹⁰⁶

In the case of the preparation of *meso*-linked Pc-Por **49** (Fig. 10), similarly to the case of Pc-Por heterodimer **48a**,

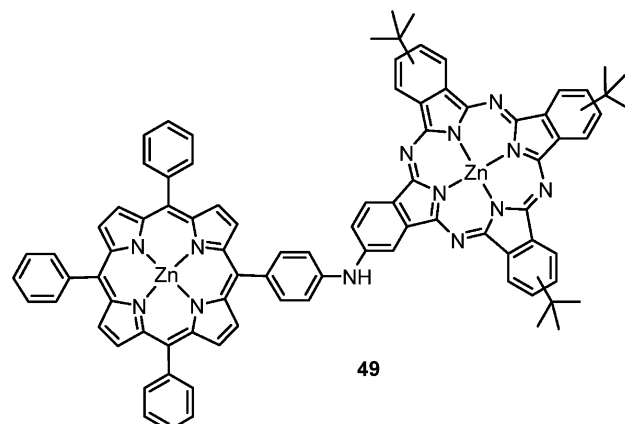
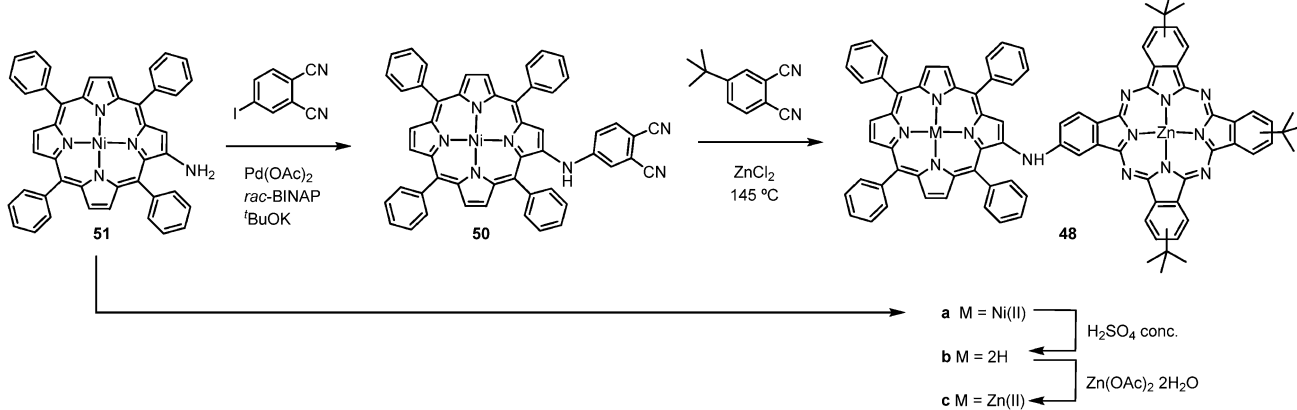


Fig. 10 Molecular structure of *N*-linked, Pc-Por dyad **49**.

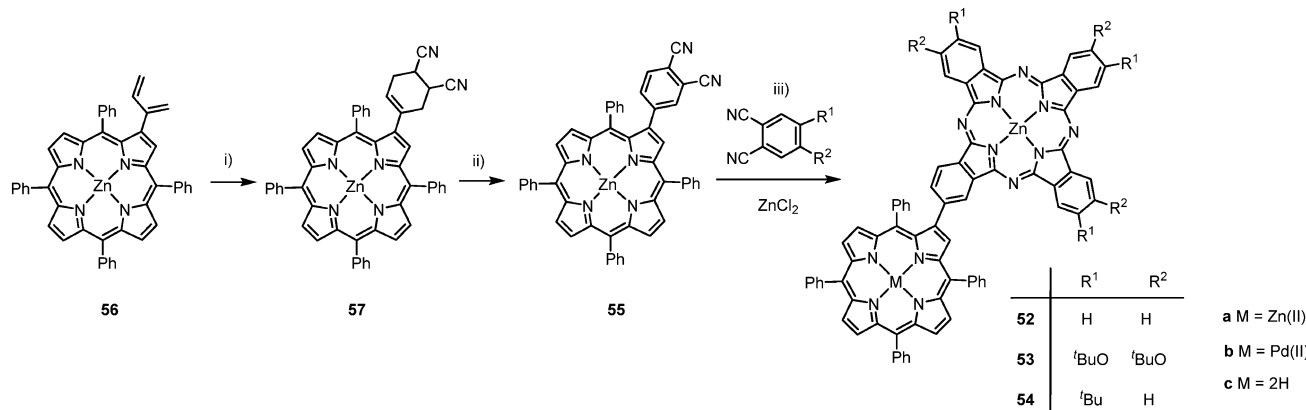
two synthetic strategies were used. In the first synthetic route, a Por-substituted phthalonitrile was prepared by Pd(II)-catalyzed coupling reaction between 4-iodophthalonitrile and a Zn(II)Por bearing an amino moiety at the *para* position of one of the four *meso*-phenyl rings, followed by statistical cross condensation of the resulting product with an excess of 4-*tert*-butylphthalonitrile, affording Pc-Por dyad **49** in 17% yield. Dimer **49** could also be prepared in 41% yield by direct, metal-catalyzed coupling of the same amino-substituted Zn(II)Por used above with a tri-*tert*-butyl-iodo-substituted Zn(II)Pc.

Ground state absorption spectra of Pc-Por dyads **48b** and **49** show the characteristic absorption features of the individual macrocycles, namely strong absorptions assigned to the Por and Pc Soret- and Q-bands. A red-shift (*ca.* 23 nm in the case of **48b**) of the Zn(II)Pc-based absorption was observed with respect to a Zn(II)Pc reference compound, as well as a hypsochromic shift of the Zn(II)Por bands, thus suggesting some degree of ground-state electronic communication between the two macrocycles. Photophysical studies with **48b** and **49** revealed efficient Por-to-Pc energy transfer phenomena (*vide infra*).¹⁰⁷

Some examples of Pc-Por dimers presenting a direct linkage between the two macrocycles have also been reported. Zn(II)Pc-Zn(II)Por dyads **52a–54a** having the Pc moiety directly bound to



Scheme 10 Synthesis of *N*-linked, Pc-Por dyad **48**.



Scheme 11 Synthesis of Pc–Por dyads 52–54. Reagents and conditions: (i) fumaronitrile, toluene, reflux, overnight; (ii) DDQ, toluene, reflux; (iii) DMAE–o-DCB, 145 °C, Ar, 24 h (for 52a, 53a and 54a).

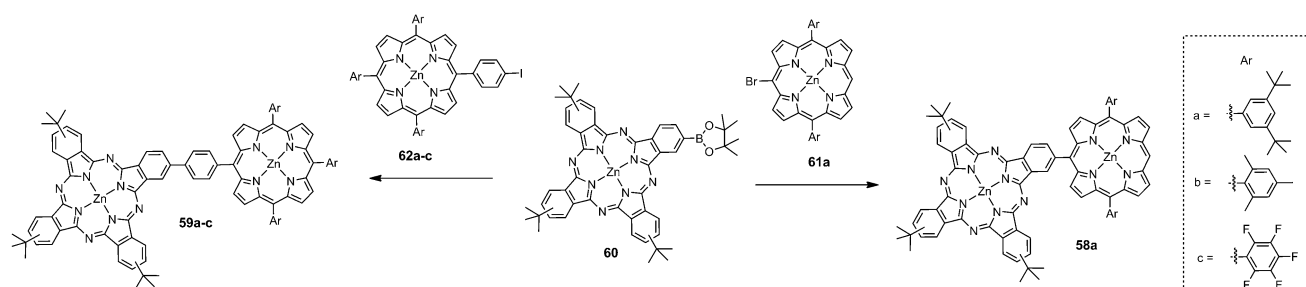
one of the Por β -pyrrolic positions have been synthesized (Scheme 11).¹⁰⁸ The synthesis of these dyads involves the use of a common Por-substituted phthalonitrile 55, which was prepared in 75% yield by Diels–Alder reaction of diene 56 with fumaronitrile, followed by the oxidation of the resulting adduct 57 with DDQ. Target Zn(II)Pc–Zn(II)Por dyads 52a–54a were obtained by statistical condensation of compound 55 with an excess of unsubstituted phthalonitrile (in the case of 52a), 4,5-dibutoxyphthalonitrile (in the case of 53a), or 4-*tert*-butylphthalonitrile (in the case of 54a) in the presence of ZnCl₂. For all these Pc–Por heterodimers, their electronic absorption spectra resulted to be almost identical to those of equimolar mixtures of the corresponding Pc and Por subunits. Moreover, the direct linkage between Pc and Por in dyads 52a–54a results in a hindered rotation between the two chromophores.

A metal-catalyzed, Suzuki cross-coupling reaction has been employed for the preparation of Pc–Por dyads 58a, 59a–c and 54a. This latter compound was prepared using a different synthetic strategy from the one mentioned above.¹⁰⁹ In such Pc–Por dyads, the Pc macrocycle was directly connected to a Zn(II)Por β (54a) or *meso* (58a, 59a–c) position, through the coupling of a common Zn(II)Pc-boronate derivative 60 with Por 61a (in the case of 58a), 62a–c (in the case of 59a–c) or a Zn(II)TPP macrocycle bearing a bromine atom at a β -position (in the case of 54a) with yields ranging from 30% to 65% (Scheme 12). Similar to the case of dyads 48b and 49, the absorption spectral features of dyads 54a, 58a and 59a–c resulted similar to those of

the individual Zn(II)Pc and Zn(II)Por subcomponents, thus suggesting the absence of significant ground-state electronic communication between the two macrocycles.

Another example of directly-linked Pc–Por heterodimers is represented by H₂Pc–Zn(II)Por 63 and Zn(II)Pc–Zn(II)Por 64 (Fig. 11).¹¹⁰ These systems are constituted by a Por macrocycle directly connected at one of its *meso* positions to a Pc macrocycle, and substituted at the opposite *meso* position with an Im group. In such systems, intermolecular π – π stacking between the Por and Pc macrocycles is precluded due to the orthogonal geometry adopted by the two closely-spaced chromophores. The pendant Im substituent in these Pc–Por dyads promotes, in noncoordinating solvents, the formation of stable, slipped cofacial supramolecular tetramers, that is [H₂Pc–Zn(II)Por]₂ (63)₂·s and [Zn(II)Pc–Zn(II)Por]₂ (64)₂·s, through the coordination of the imidazole moiety of dyad 63 or 64 to the Zn(II)Por macrocycle of another dimer, with extremely large K_{ass} (10^{11} – 10^{12} M⁻¹) (Fig. 11). The formation of self-assembled dimers (63)₂·s and (64)₂·s could be inferred by UV-vis analysis which revealed a broadening of both the split Zn(II)Por Soret bands and the Pc Q-band, broadening that is accompanied, in this latter case, by a 7–10 nm red-shift of the λ_{max} . The formation of supramolecular tetramers (63)₂·s and (64)₂·s was also confirmed by ¹H NMR spectroscopy.

The use of metal–ligand coordination has also been involved in order to obtain cofacial stacks of Pc–Por dyads ((65)₂c–(70)₂c) as a result of the antiparallel stacking of Pc–Por dyads (65–70) (Fig. 12).^{28,111}



Scheme 12 Synthesis of Pc–Por dyads 58a and 59a–c. Reagents and conditions: Pd₂(dba)₃, S-Phos, K₃PO₄, toluene, 90 °C.

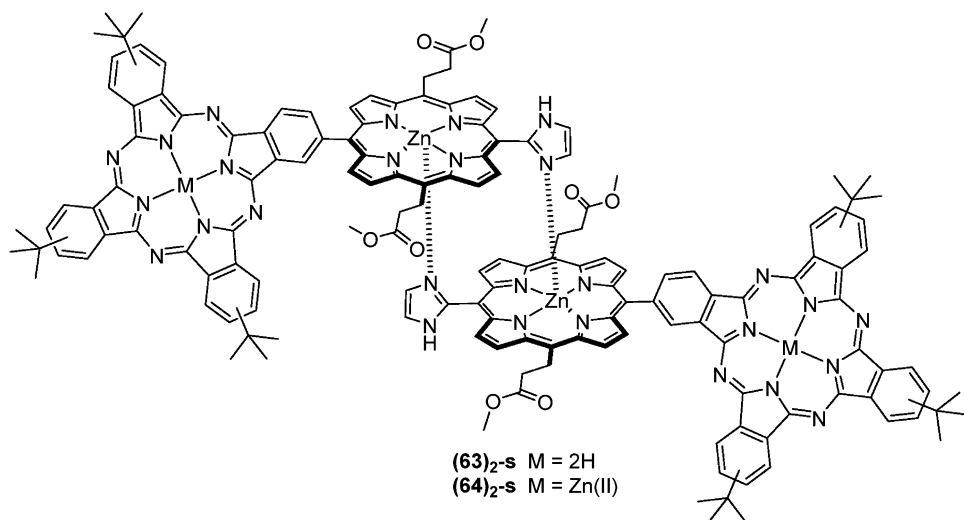


Fig. 11 Formation of slipped, cofacial tetramers $(63)_2\text{-s}$ and $(64)_2\text{-s}$ resulting from the assembly of Pc-Por dyads **63** and **64**, respectively.

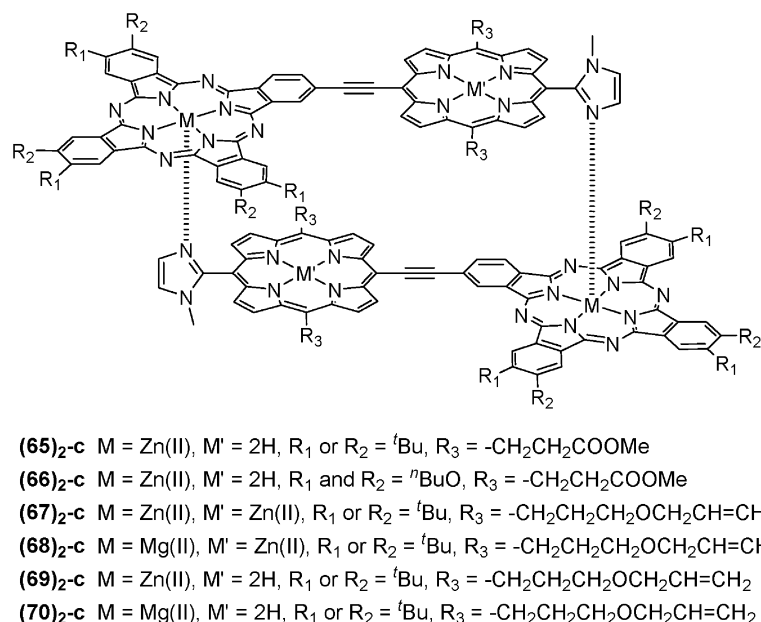
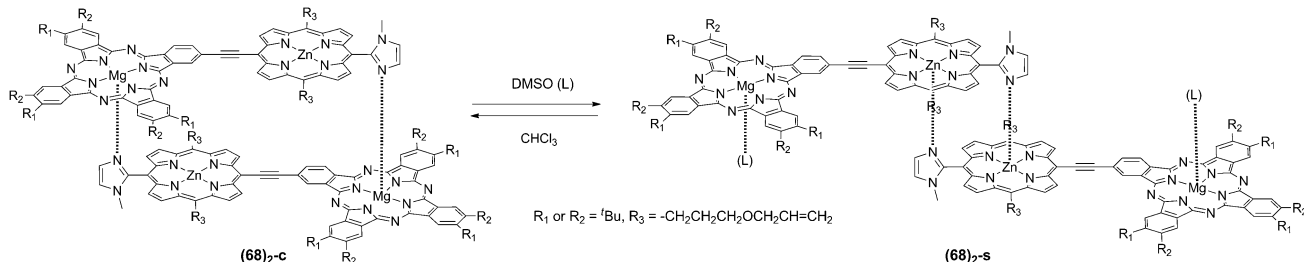


Fig. 12 Formation of cofacial, Pc-Por tetramers $(65)_2\text{-c}$ – $(70)_2\text{-c}$ resulting from the self-assembly of Pc-Por dyads **65**–**70**.

These dyads are constituted by one Im-substituted Por and one Pc connected, in this case, through an ethynylene spacer that allows free rotation of the two chromophores around the triple bond, which is not possible in dyads **63** and **64**. $\text{M}(\text{II})\text{Pc-H}_2\text{Por}$ dimers **69** and **70** were synthesized by using $\text{Pd}(\text{II})$ -catalyzed coupling reaction between an ethynyl-substituted $\text{Zn}(\text{II})$ or $\text{Mg}(\text{II})\text{Pc}$ and an iodo-substituted H_2Por bearing an Im moiety. Compounds **69** and **70** were subsequently converted to $\text{M}(\text{II})\text{Pc-Zn}(\text{II})\text{Por}$ dimers **67** and **68** by treatment with zinc acetate. On the other hand, a complementary synthetic strategy was employed for the preparation of $\text{Zn}(\text{II})\text{Pc-H}_2\text{Por}$ dimers **65** and **66** which were prepared by copper-free, Sonogashira coupling reaction between adequately substituted $\text{Zn}(\text{II})\text{Pcs}$ having an iodo group and an ethynyl-substituted H_2Por bearing an Im group.

For these series of Pc-Por dimers, complementary coordination of the Im group of a Pc-Por dyad to the $\text{Pc Zn}(\text{II})$ or $\text{Mg}(\text{II})$ metal center of a second dimer results in the formation of head-to-tail supramolecular tetramers as demonstrated by different techniques. For example, in the case of dyad **69**, GPC analysis using a noncoordinating solvent such as CHCl_3 showed a single peak corresponding to supramolecular tetrad **(69)₂-c**; neither monomer nor polymer was observed. The formation of such a supramolecular complex was also supported by MALDI-TOF mass spectrometry experiments, which showed a clear peak assignable to this supramolecular tetrad in addition to the dissociated dyad species. Further insight into the association ability of this dyad came from ^1H NMR spectroscopy in noncoordinating solvents which showed an upfield shift for



Scheme 13 Formation of slipped, Pc–Por stacks $(\mathbf{68})_{2\text{-s}}$ from cofacial Pc–Por stacks $(\mathbf{68})_{2\text{-c}}$ upon addition of DMSO.

the Im protons with respect to a reference, uncomplexed Im–Pc system, suggesting a ligand-to-metal coordination between the Im group and the Zn(II)Pc moiety. Finally, the stability of such tetrads was investigated by UV-vis titration experiments, which showed important spectral changes upon addition of 1-methylimidazole to the solution of the self-assembled tetrads. From these titrations experiments, a K_{ass} of 10^{14} M^{-1} was calculated.

Interestingly, UV-vis titration studies of CHCl_3 solutions containing self-assembled, cofacial dimer $(\mathbf{68})_{2\text{-c}}$ showed, upon addition of variable amounts of DMSO, the selective formation of a new stacked species $(\mathbf{68})_{2\text{-s}}$ (Scheme 13). This is a consequence of the preferred complexation of DMSO, a hard base, to the magnesium ion, a hard acid, with respect to the zinc ion, an intermediate acid. As expected, addition of 1-methylimidazole to a solution of $(\mathbf{68})_{2\text{-s}}$ resulted in the complete disassembly of the stacked complex and the formation of a Pc–Por having one 1-methylimidazole ligand on both zinc and magnesium centers.

Strong NLO properties involving two-photon absorption (2PA) and three-photon absorption (3PA) have also been reported for stacked complexes $(\mathbf{68})_{2\text{-c}}$ and $(\mathbf{70})_{2\text{-c}}$.¹¹²

Very recently, a wide-band capturing solar energy harvesting material constituted by a Pc–Por conjugate (**71**) having the two macrocycles connected by a semiflexible amide linker has been reported by the groups of Tkachenko and D’Souza (Fig. 13).¹¹³ Compound **71** was prepared by reacting an amino-functionalized tri-*tert*-butyl-Zn(II)Pc with a monocarboxyphenyl *meso*-substituted Zn(II)Por prior to conversion of the latter compound to its highly-reactive, acid chloride analog by treatment with thionyl chloride. Interestingly, Pc–Por dyad **71** has been employed for the preparation of a photoelectrochemical cell by modifying the

semiconducting TiO_2 surface with a ligand (4-carboxyphenylimidazole) capable of axially binding to the Zn(II)Por macrocycle. Although the overall performance of such a cell was relatively low compared to some of the well-engineered photocells, this method represents a new approach for the preparation of novel photovoltaic devices which function by a combination of multi-chromophoric systems and supramolecular interactions.

A Pc–Por dimer (**72**) in which the two chromophores are separated by a long and rigid, conjugated spacer has also been prepared (Fig. 13).¹¹⁴ In **72**, the presence of a π -conjugated, oligomeric phenylethynyl bridge reduces the symmetry of the Sn(IV)Cl₂Por and Zn(II)Pc chromophores, resulting in red-shifted and broadened absorption bands as compared to some Pcs and Por reference compounds, as well as in a splitting of the Zn(II)Pc-centered Q-band.

3.2 Supramolecular phthalocyanine–porphyrin systems

Supramolecular interactions have widely been used as an efficient and versatile method for the preparation of Pcs–Por heterodimers.^{22,115}

In this context, one of the most successful “supramolecular” approaches that has been used to prepare such dimers is represented by the metal–ligand axial coordination, relying on the ability of some ligands, such as pyridyl or Im moieties, to axially coordinate to the metal center of Pcs or Por macrocycles. Following this strategy, a series of Pcs–Por and Ncs–Por supramolecular ensembles have recently been prepared by the complexation of Im-substituted H₂Pors **73** to Pcs **74** or Ncs **75** (Fig. 14).^{116,117}

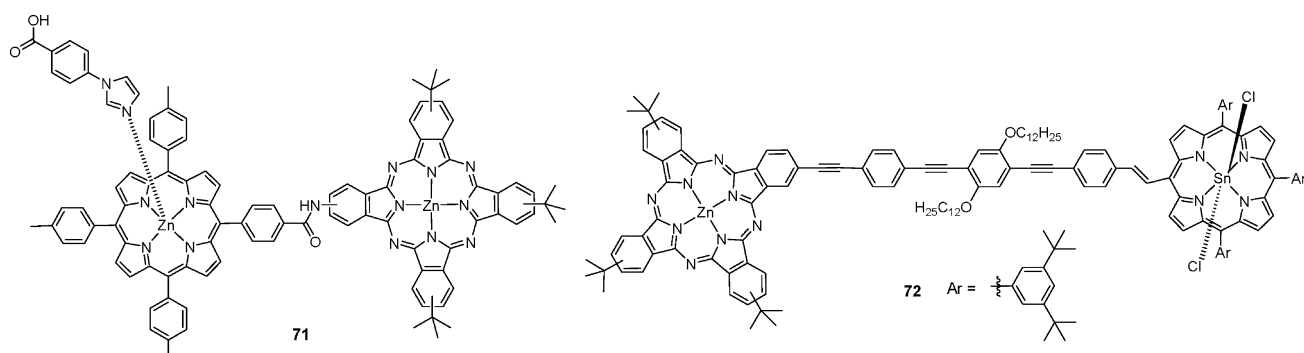


Fig. 13 Molecular structures of Pcs–Por dyads **71** and **72**.

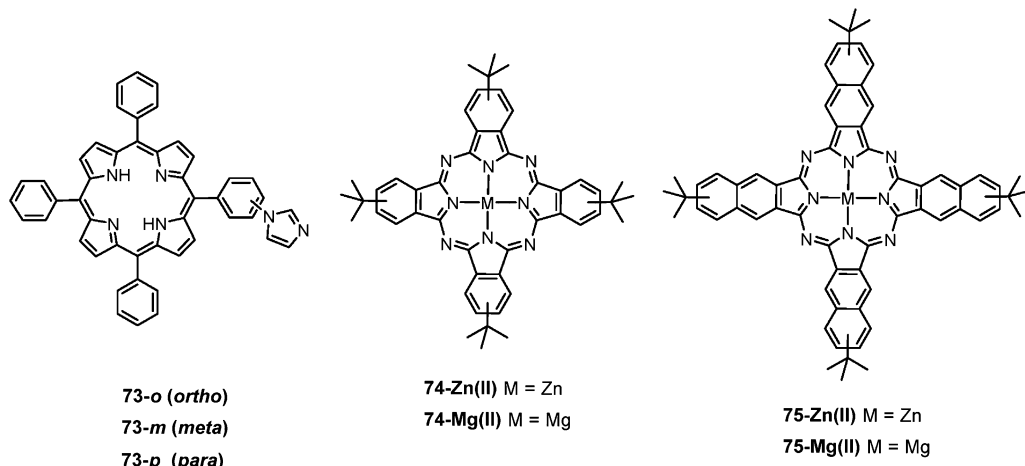


Fig. 14 Molecular structures of Im-substituted, H₂Pors **73-o**, **-m**, **-p**, Pcs **74-Zn(II)** and **75-Zn(II)** and Ncs **74-Mg(II)** and **75-Mg(II)**.

In such systems, the substitution pattern of the Im unit at the H₂Por *meso* phenyl ring has been changed from *ortho* (**73-o**), *meta* (**73-m**) and *para* (**73-p**) with the aim of obtaining a family of Pc-Por and Nc-Por dyads. The different relative orientations of the Por and the Pc or Nc macrocycles in such supramolecular ensembles are expected to influence the communication between the two chromophores. On the other hand, the employed Pes/Ncs were decorated with four *tert*-butyl substituents at their periphery in order to improve solubility and reduce self-aggregation. UV-vis studies on Pors **73** in a noncoordinating solvent such as *o*-DCB show the characteristic Por Soret band at around 432 nm, whereas in the case of Pc **74-Zn(II)** and Nc **75-Zn(II)** their absorption maxima were located in the visible (681 nm) or infrared (IR) (777 nm) region of the solar spectrum, respectively. The spectral features of Pc **74-Mg(II)** and Nc **75-Mg(II)** were quite similar to their zinc analogs, showing bands at 351, 618, and 681 nm while the spectrum of Nc was stretched into the near-IR region with peaks at 332, 690, 734 and 770 nm. Importantly, the Por band at 518 nm had little or no overlap with the absorption bands of either Pc or Nc providing a possibility for selective excitation of the donor H₂Por.

Addition of H₂Por **73-p** to a solution of Pc **74-Zn(II)** or Pc **74-Mg(II)** resulted, beside the normal increase of the H₂Por absorption peaks, in a diminishing of the intensity of the Pc Q-band and the raising of new bands with several isosbestic points indicating existence of only one equilibrium process in solution. A similar trend was observed when titrating Nc **75-Zn(II)** or Nc **75-Mg(II)** with H₂Por **73-p**. Job's plot experiments suggested the existence of a 1:1 complex formation between the H₂Por donor **73-p** and the acceptor macrocycles **74-Zn(II)** or **75-Zn(II)**, with K_{ass} of $8.23 \times 10^4 \text{ M}^{-1}$ and $1.53 \times 10^5 \text{ M}^{-1}$, respectively. The magnitudes of the K_{ass} for the Mg(II)Pc or Mg(II)Nc with Por **73-p** were generally smaller than those of the corresponding zinc analogs. The formation of a 1:1 supramolecular complex was also observed when titrating Pc **74-Zn(II)** or Nc **75-Zn(II)** with H₂Por **73-o** or H₂Por **73-m**, obtaining K_{ass} around 10^4 – 10^5 M^{-1} . The K_{ass} values resulted higher in the case of the complexes formed between Pc **74-Zn(II)** or Nc **75-Zn(II)**

and H₂Por **73-p** with respect to the same complexes formed employing H₂Por **73-o** or H₂Por **73-m**, probably due to the lower steric constraints present on the *para*-substituted H₂Por. Moreover, the binding constants of the Im-substituted Pors with Nc **75-Zn(II)** were found to be 2–3 times larger than those obtained for Pc **74-Zn(II)**, probably due to the higher electronic-richness of the Zn(II)Nc with respect to the Zn(II)Pe macrocycle.

More recently, a series of supramolecular Pc-Por dyads (**76**) have been prepared by the groups of Tkachenko and D'Souza featuring the axial coordination of (*ortho*-, *meta*- or *para*-) Im-substituted H₂Pors to a carbonyl Ru(II)(CO)Pc (Fig. 15).¹¹⁸ The replacement of a Zn(II)Pe for a Ru(II)Pc(CO) was aimed at increasing the stability constant of the resulting assemblies due to the stronger coordination between the ruthenium metallic center and the nitrogen Im ligand. Such Pc-Por dyads were obtained by reacting Ru(II)Pc(CO) with a stoichiometric amount of the appropriate Im-functionalized H₂Por followed by chromatographic purification. Importantly, the presence of the carbonyl group on the Ru(II)Pc macrocycle provides stronger ligation for the coordinated nitrogen ligand due to the π -acceptor ability of the carbonyl

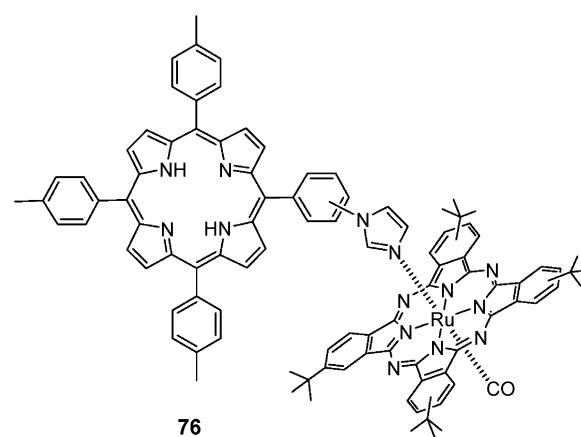


Fig. 15 Molecular structures of Pc-Por dyads **76** resulting from the complexation of *ortho*-, *meta*- or *para*-Im-substituted, H₂Pors to a Ru(II)(CO)Pc.

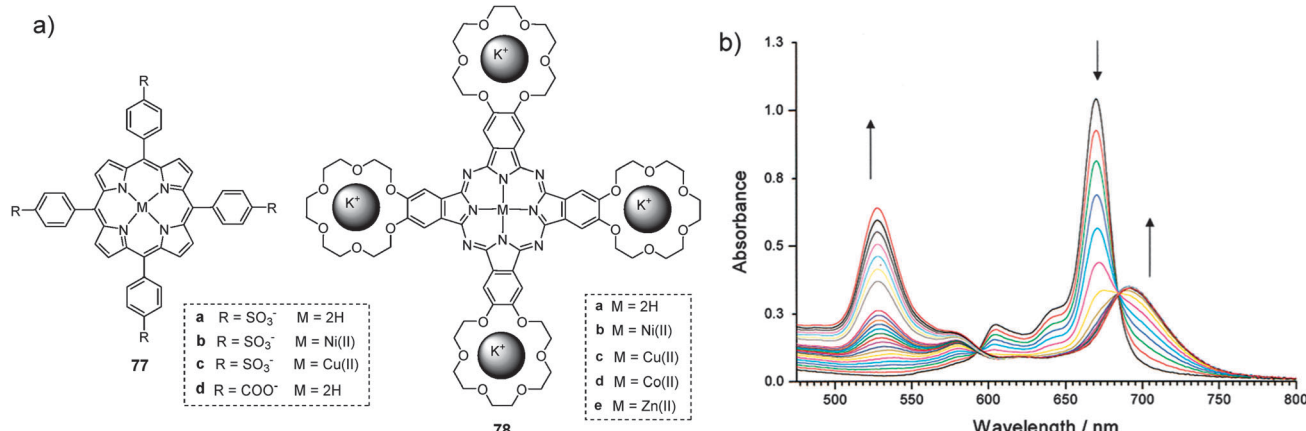


Fig. 16 (a) Molecular structures of K^+ -complexing, crown ether-substituted Pcs **78** and tetraanionic Pors **77**. (b) Evolution of the absorption spectrum of Ni(II)Pc **78b** upon addition of Ni(II)Por **77b** in DMSO. Reprinted from ref. 120. Copyright 2002 ACS.

the carbonyl ligand at one of the two axial Ru(II) coordination sites. UV-vis studies on these supramolecular complexes suggested small electronic communication between the two chromophores.

Electrostatic interactions have also been exploited in order to drive the formation of Pc-Por supramolecular dimers and oligomers. In this context, a family of Pc-Por complexes consisting of negatively charged tetrasulfonatophenyl Pors (**77a–c**) or a tetracarboxyphenyl Por (**77d**) ion pairing with crown ether substituted Pcs (**78**) bearing potassium ions into its four crown ether cavities have been prepared¹¹⁹ and studied (Fig. 16a).¹²⁰ The complexation of potassium ions by the crown ether residues imparts a tetracationic nature to the Pc supramolecular complex, thereby providing the potential for the K^+ -doped Pcs to interact *via* electrostatic interactions with tetraanionic Pors. CV and spectroelectrochemistry experiments indicate a degree of partial charge transfer character for the ground state.

For example, the titration of Ni(II)Pc **78b** with Ni(II)Por **77b** in DMSO resulted in a small blue shift of the Por Soret band, complete disappearance of the crown ether-substituted Pc

Q-band and the appearance of a new band in the red spectral region (Fig. 16b). In contrast to the metal-containing Pc and Por systems described above, titration of the H₂Por **77a** with free-base (**78a**), Co(II) (**78d**) or Zn(II) (**78e**) Pcs, showed different behavior.

Weak electrostatic interactions in solution between non-charged macrocycles such as an Al(III)ClPc and an Al(III)OHPor have also been studied.¹²¹ UV-vis and fluorescence studies on mixed solutions of the two macrocycles indicate the formation of a 1 : 1 Pc-Por heterodimer with a K_{ass} of $5.7 \times 10^4 \text{ M}^{-1}$, a value higher than that of the respective Pc-Pc or Por-Por homodimers, but considerably lower than the one obtained for strongly interacting Pcs and Pors bearing oppositely charged substituents ($\sim 10^7 \text{ M}^{-1}$).

More recently, the groups of Ermilov and Ng have used host-guest interactions between a tetrasulfonated Zn(II)TTP (**79**) and several Si(IV)Pcs axially-substituted with two permethylated β -cyclodextrin (CD) units (**80**) for the construction of Pc-Por supramolecular complexes (Fig. 17).¹²² UV-vis absorption and fluorescence measurements indicate that the two chromophores bind in a 1 : 1 manner in water with K_{ass} in the range

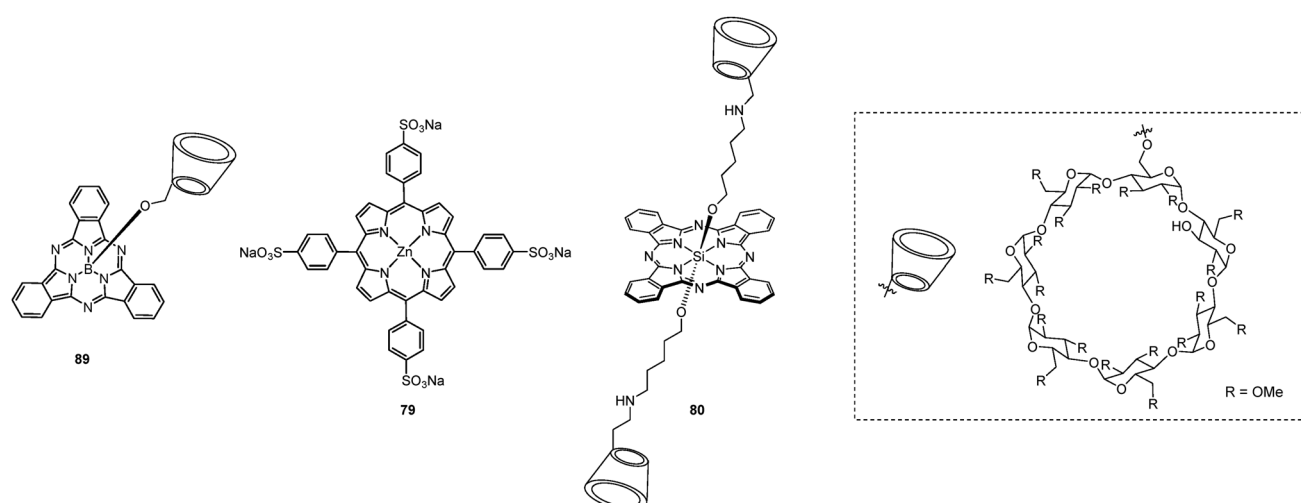


Fig. 17 Molecular structures of β -CD-substituted SubPc **89**, tetrasulfonated Zn(II)Por **79**, and β -CD-substituted Si(IV)Pc **80**.

of 1.1×10^7 to $3.5 \times 10^8 \text{ M}^{-1}$, as a result of the interaction between the negatively-charged sulfonated groups and the internal cavity of the β -CD.

3.3 Phthalocyanine–porphyrin systems connected to other electroactive moieties

Pc–Por ensembles connected, covalently or through supramolecular interactions, to one or more electroactive units have also been reported.

A triad system (**81**) constituted of a Zn(II)Por “input” unit, a H₂Pc “output” unit, and Fc as the redox-switching unit has been prepared (Fig. 18).¹²³ The synthesis of **81** involves a one-pot, Pd-coupling reaction between a Zn(II)TPP derivative bearing two iodo atoms, an ethynyl-substituted Fc compound, and an ethynyl-functionalized H₂Pc. The reaction gave a mixture of trimeric, dimeric, and monomeric species which were purified by using chromatography procedures to obtain the desired triad **81**.

Electrochemical studies on triad **81** showed electrochemical potentials close to those of the individual molecular components (Pc, Por and Fc), thus suggesting a relatively weak, ground-state coupling between these subunits in the array.

Very recently, some Pc–C₆₀–Por triads (**82**) presenting the three photoactive moieties covalently connected have been described.¹²⁴ Zn(II)Pc–C₆₀–Ni(II)Por triad **82a** was prepared in a 37% yield in a one-step synthesis *via* 1,3-dipolar cycloaddition of an azomethine ylide, generated *in situ* by a condensation reaction between a formyl Zn(II)Pc and glycine N-substituted with a Ni(II)Por macrocycle, to C₆₀ (Fig. 18). Next, Zn(II)Pc–C₆₀–H₂Por **82b** was obtained in a 95% yield by demetallation of the Por macrocycle in **82a** using a H₂SO₄ solution in dichloromethane. Finally, metallation of compound **82b** with Zn(AcO)₂ afforded Zn(II)Pc–C₆₀–Zn(II)Por triad **82c** in 91% yield. A modification of the synthetic route leading to triad **82a** replacing the formyl Zn(II)Pc for a diformyl Zn(II)Pc has allowed the authors to prepare Pc₂–(C₆₀)₂–Por pentads.

Recently, the groups of Torres, Cavaleiro and Guldi reported a series of supramolecular triads constituted by pyridyl-substituted C₆₀ ligands (**83** and **84**, Fig. 19) axially-coordinated to the Pc zinc center of tri-*tert*-butyl Zn(II)Pc–M(II)Por (M = Zn(II) (**54a**), Pd(II) (**54b**) and 2H (**54c**)) dyads, and their analog dyads having *tert*-butyloxy or no substituents (**53a–c** and **52a–c**, respectively) on the Pc macrocycle (Scheme 11).¹²⁵ Compounds **52a**, **53a** and

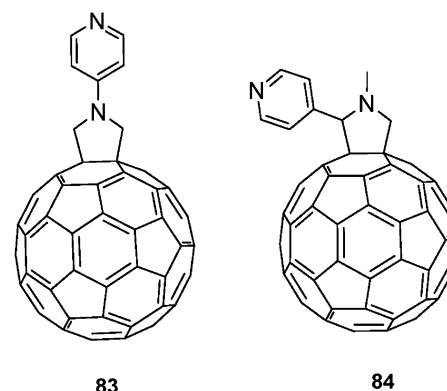


Fig. 19 Molecular structures of pyridyl-substituted C₆₀ derivatives **83** and **84**.

54a were obtained by statistical, cross-condensation of a H₂Por-substituted phthalonitrile with an excess of phthalonitrile, 4-*tert*-butylphthalonitrile, and 4,5-dibutoxyphthalonitrile, respectively, in a refluxing mixture of *o*-DCB and DMAE, in the presence of zinc chloride. Compounds **52c**, **53c** and **54c** were obtained in excellent yields (about 95%) through the demetallation of the Pors of compounds **52a**, **53a** and **54a** with trifluoroacetic acid in CH₂Cl₂. The absorption spectra of these compounds showed an additional band at 516 nm, which is assigned to one of the H₂Por Q-bands. Similarly to compounds **52a**, **57a** and **54a**, dyads **52b**, **53b** and **54b** were obtained by statistical condensation of Pd(II)Por-substituted phthalonitrile with adequate phthalonitriles in moderate yields (13–45%). Coordination of dyads **52–54** by fullerene derivatives **83** and **84** led to the formation of D–A, supramolecular hybrids through coordination of the pyridyl moiety of the fullerene species to the zinc metal center of the dyads’ Pc macrocycle, as corroborated by titration fluorescence studies and transient absorption measurements (*vide infra*).

The same groups also investigated the supramolecular interaction between fullerene derivative **83** and fused Pc–Por conjugates **85a,b** (Fig. 20).¹²⁶ The UV-vis spectrum of **85a** in toluene shows the characteristic absorption bands of the two chromophores, although a remarkable bathochromic shift of 20 nm is observed in the Por Soret band. The broadening, splitting, and red-shift of the Pc Q-band (from 677 nm to 685 and 709 nm) is also a consequence of the “desymmetrization” of the Pc, the enlargement of the π -conjugated system, and the intramolecular electronic coupling between the two macrocycles.

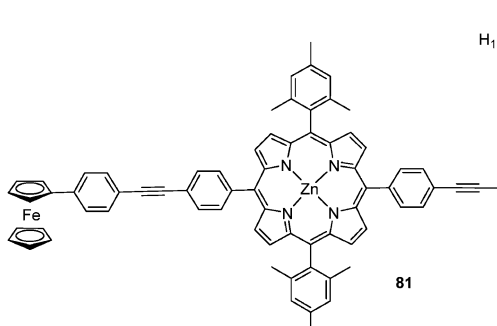
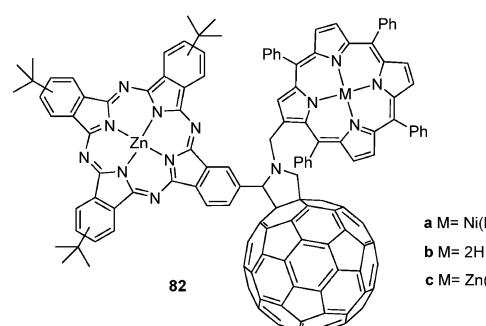
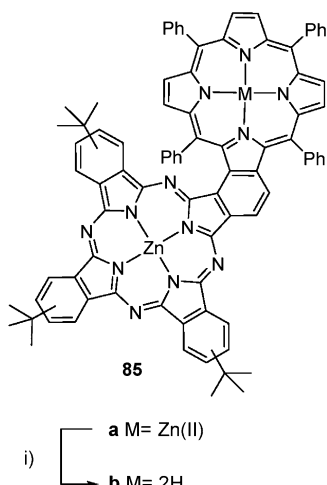
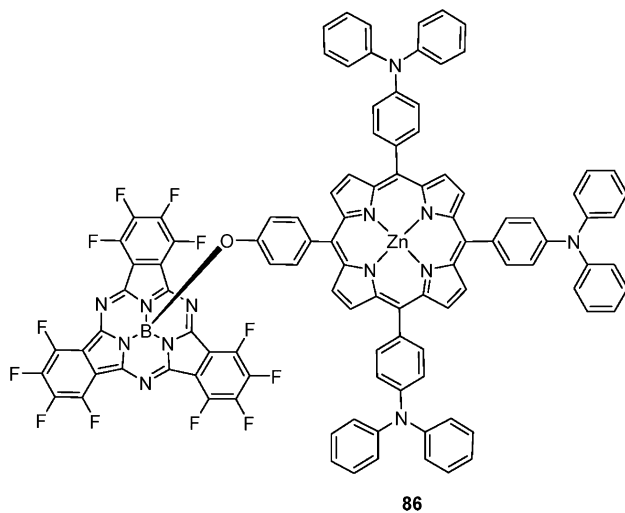


Fig. 18 Molecular structure of Pc–Por–Fc triad **81** and Pc–C₆₀–Por triads **82**.



**Fig. 20** Molecular structure of fused *Pc*–*Por* conjugates **85**.

The UV-vis spectrum of dimer **85b** shows an additional minor Q-band at 538 nm due to the H₂Por subunit. It is interesting to note that, while reported fused diPors and fused diPcs show a

**Fig. 21** Molecular structure of TPA-substituted Zn(II)Por-SubPc ensemble **86**.

planar geometry, **85a** and **85b** present a marked distortion as evidenced by molecular mechanic calculations (MM+). This fact contributes to the strong “desymmetrization” of the *Pc* observed in the UV-vis spectra of **85a** and **85b**, although it does not preclude the extension of the π-conjugated *Pc* system with the Por.

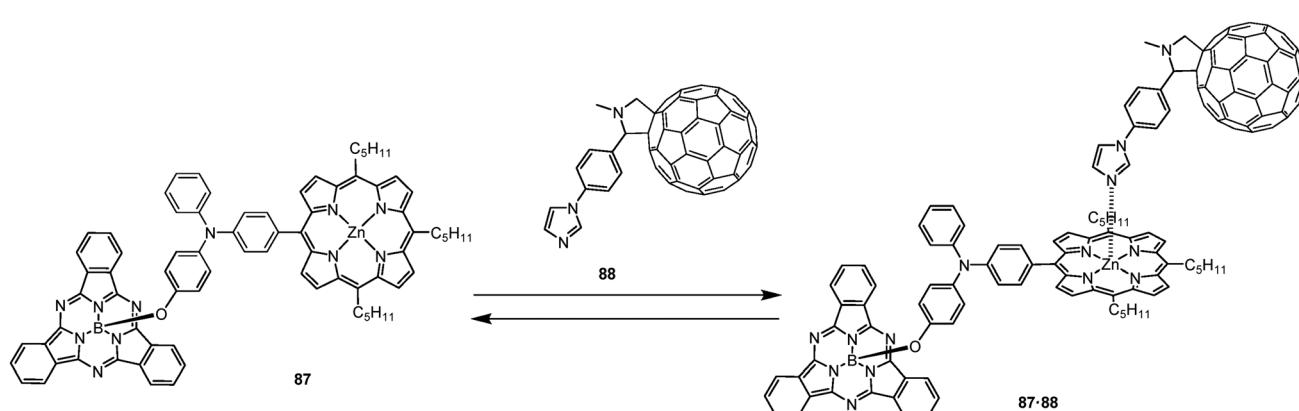
3.4 Porphyrin–subphthalocyanine systems

Few examples of SubPc–Por dimers have been reported to date. One of the first examples of such ensembles is represented by dyad **86**. This compound has been synthesized by reacting a triphenylamine (TPA)-substituted Zn(II)Por carrying a phenol group with a dodecafluoroSubPc axially substituted with a chloro atom (Fig. 21).¹²⁷ Computational studies on this dimer revealed that the HOMO is shared between the TPA moieties and the Por macrocycle, while the LUMO is localized on the F₁₂SubPc chromophore.

More recently, a SubPc–TPA–Zn(II)Por triad (**87**) has been prepared and its complexation by an Im-substituted C₆₀ **88** investigated by using different techniques (Scheme 14).¹²⁸

The absorption spectrum of **87** presents common features of both the electron-donor Zn(II)Por–TPA and the electron-acceptor SubPc subunits, suggesting negligible electronic interactions between these chromophores in the ground state. Upon addition of Im-substituted C₆₀ ligand **88** to a solution of **87**, a diminishing in the Por Soret band intensity, a 4 nm red-shift, and the appearance of an isosbestic point at 430 nm was observed suggesting the formation of a pentacoordinated Zn(II) complex in which the Im-substituted C₆₀ derivative is coordinating the Zn(II)Por metal center, forming self-assembled complex **87·88**. Analysis of the absorbance data upon titration allowed the authors to determine the K_{ass} of complex **87·88** which was 1.1 × 10⁴ M⁻¹.

A supramolecular complex formed by tetraanionic Por **79** and SubPc **89** (Fig. 17) has also been reported.¹²⁹ The β-CD-substituted SubPc **89**, which represents the first covalently-linked SubPc–CD conjugate, was synthesized in very low yields (about 5%) by treating the peripherally-unsubstituted Cl-SubPc with mono-6-hydroxy permethylated β-CD in the presence of triethylamine in refluxing *p*-xylene. The presence of the permethylated β-CD moiety greatly increased the solubility of

**Scheme 14** Complexation of SubPc-TPA-Zn(II)Por triad **87** by Im-substituted C₆₀ **88** leading to supramolecular tetrad **87·88**.

89 in common organic solvents and allowed it to be purified readily by chromatography. The absorption spectrum of **89** in ethanol showed no signs of aggregation. Next, the complexation of SubPc **89** with tetrasulfonated Zn(*ii*)TTP **79** in water was investigated by UV-vis analysis. These studies show that, upon increasing the mole fraction of SubPc **89**, the Por B band at 413 nm gradually decreases and shifts to 416 nm, while two isosbestic points at 325 and 460 nm are observed, indicating the formation of a supramolecular complex. Job's plot analysis suggests the formation of a 2:1 supramolecular complex (**89**)₂·**79**. A K_{ass} of $1.2 \times 10^{12} \text{ M}^{-2}$ in water was determined for complex (**89**)₂·**79** which indicates strong binding between the two components. More recently, as an extension of the above-mentioned work, a report has appeared in which compounds **79** and **89** have been investigated in the presence of a third chromophore, namely β -CD disubstituted Si(iv)Pc **80** (Fig. 17).¹³⁰ The UV-vis spectrum of a 1:1:1 mixture of **79**, **80** and **89** in water showed a number of intense absorptions covering a broad range from 300 to 700 nm, and was basically a superposition of the spectra of the three individual components except for the Por Soret band and the Pc Q-band which were shifted to the red by 3 nm and 8 nm, respectively. The intensity of the latter was also slightly reduced in the mixture. In this case photophysical (steady-state and time-resolved fluorescence and transient absorption) experiments were used in order to shed light onto the possible interactions between the three macrocycles in solution.

4. Porphyrin–porphyrin binuclear systems

4.1 *meso*- and β -linked binuclear porphyrins

Binuclear Por-based systems in which the constituent Pors are directly linked through their *meso*–*meso* positions are an attractive target in the search for electronic interactions between the component units. Different synthetic approaches have been applied for the construction of such systems, for instance, coupling reactions of monomeric Pors with AgPF₆, Suzuki–Miyaura cross-coupling reactions of boronic ester with halogen-containing macrocycles, and acid-catalyzed condensations of *meso*-formyl substituted Pors with *meso*-aryldipyrromethanes, among others.¹³

meso–*meso* diPors such as **90** (Fig. 22) present split Soret bands in their UV-vis spectra as a consequence of the exciton coupling between Por subunits, but the conjugative electronic interaction between the chromophores is weak because of the nearly perpendicular conformation.¹³¹ However, the electronic interactions between directly linked Por units can be modulated as a function of the dihedral angle; therefore a decrease in the dihedral angle of *meso*–*meso* diPors, from an average of 90° to an oblique geometry, leads, indeed, to an enhancement in the electronic coupling between the subunits. This enhancement has been observed in permanently distorted, *meso*–*meso*-linked diPors **91** (Fig. 22), which are bridged by a strap of variable length.¹³² Shortening of the strap length causes a gradual decrease in the dihedral angle between the Pors and concomitant increasing distortion of the constituent rings, which is proved by red-shifting of the exciton split Soret band together with the growth of a new high-energy band, as well as changes in the resonant Raman spectra. INDO/SSCI calculations predict that these facts are due to charge transfer states located close to the excitonic Soret transitions, which are intensified upon a decrease in the dihedral angle.

Encouraged by this observation, the same authors undertook the task of modulating the dihedral angle in *meso*–*meso*-linked Zn(*ii*) diPors **90** through coordination with α,ω -diaminoalkanes (H₂N(CH₂)_nNH₂).¹³¹ In particular, they observed that, upon the addition of 1,7-diaminoheptane (**7DA**), a 1:1 complex was formed, which showed absorption (and also fluorescence) spectral features similar to those of permanently distorted *meso*–*meso*-linked diPor **91**. It was then assumed that the association of **7DA** with **90** took place through two amino groups coordinated to the two Zn(*ii*) centers, hence forcing a tilt of the two Pors from a dihedral angle of about 90° to a decreased one. Furthermore, these torsional changes can be effected in a reversible manner, since the addition of acetic acid to a solution of complex **7DA**–**90** restores the original absorption and fluorescence spectra of **90**.

Another illustration of how axial ligand coordination of *meso*–*meso* linked diPors can be used to modulate the electronic properties of the conjugate is exemplified with the coordination of butadiynyl-linked diPor **92** with bidentate ligands (Scheme 15).

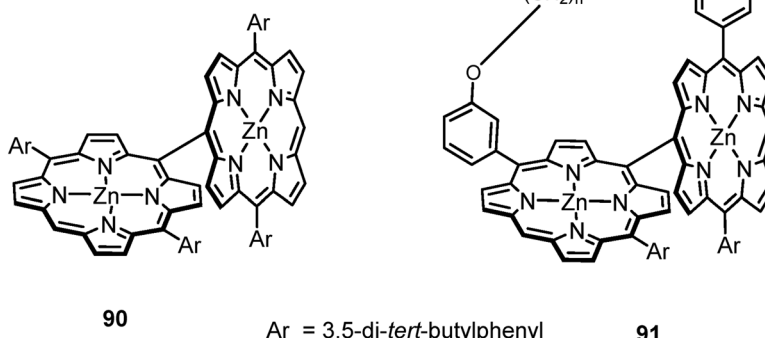
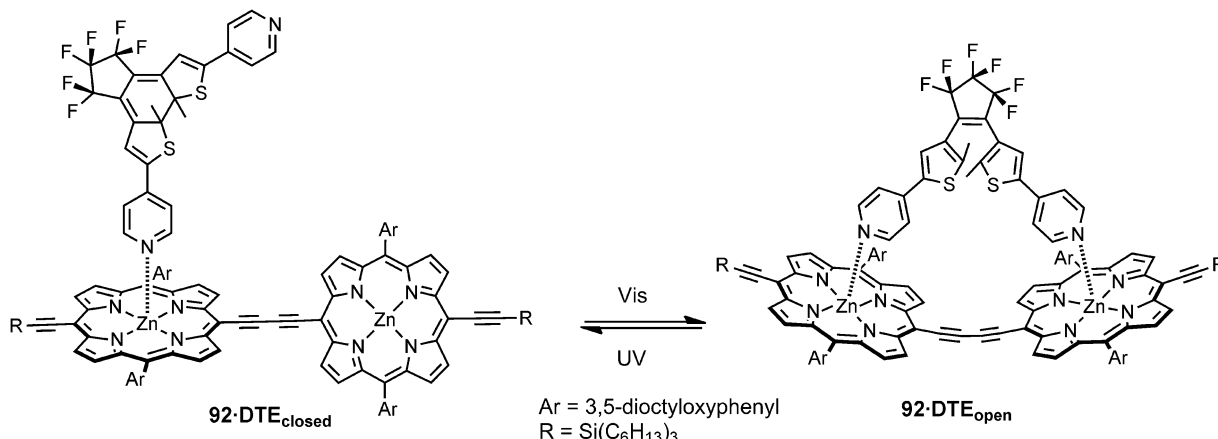


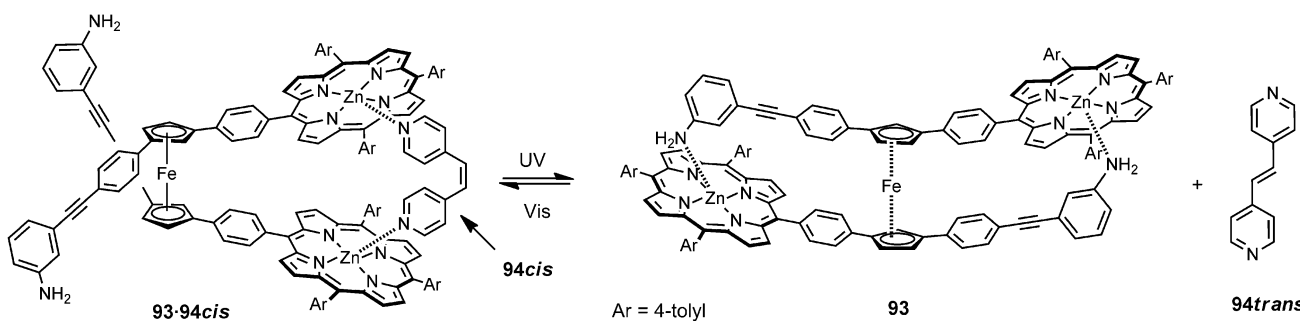
Fig. 22 Distorted *meso*–*meso* linked diPors **90** and **91**.

**Scheme 15** Isomeric forms of 92-DTE complex.

The very low rotational barrier imposed by the butadiyne link in the dimer allows a broad distribution of conformations, and all the Por-Por dihedral angles are populated at room temperature. It has been shown that when a bidentate dipyridylpyrrole ligand is added to 92, a stable 1 : 1 complex is formed in which the Por macrocycles of the dimer are essentially coplanar.¹³³ Encouraged by this result, the same authors have undertaken the complexation of pyridine-appended dithienylethene (**DTE**), which is a well-known photochromic molecule, with the *meso-meso*-linked Por dimer **92** (Scheme 15) in the search for photoresponsive molecular memories.¹³⁴ **DTE** is reversibly switched between its closed and open isomeric forms by irradiation with 302 nm UV- and 450 nm visible light, respectively. The open isomer possesses much more conformational flexibility than the closed form and, therefore, **DTE-open** is able to adopt a conformation that is well-suited for a chelated 1 : 1 complex with **92**, whereas **DTE-closed** cannot easily coordinate to both Zn(II) centers of the same dimer molecule because of geometrical incompatibilities. In fact, the absorption spectrum of 1 : 1 **92-DTE-open** complex strongly suggests a structure where the Por macrocycles adopt a mutually planar conformation. The spectrum recorded after irradiation of this complex at 302 nm indicates the formation of the monodentate, non-planar **92-DTE-closed** ensemble. Subsequent exposure to broadband visible light restores the original absorption spectrum, thus showing that the process is fully reversible.

An intriguing case described by Aida and coworkers is the manipulation of the conformations of diPor systems comprising a Fc unit as a rotary module.¹³⁵ Photoresponsive Por dimers **93** were prepared in which the Por units are linked through their *meso* positions to the Fc unit (Scheme 16). Additionally, each cyclopentadienyl ring of the Fc moiety is covalently linked to an aminodiphenyl arm. The conformation of this diPor is externally locked by the coordination of the *cis* form of the bidentate 1,2-bispyridylethylene **94** to each of the Zn(II) atoms complexed in the Por cavity (one-to-one complex **93-94cis**). Upon UV-irradiation, the bidentate ligand isomerizes to the *trans* and is released from the host, thus causing an internal rotation through the Fc axis to afford the internally locked state **93**, as each aniline unit coordinates to the Zn(II) metal of one Por. The backward photochemical isomerization of **93** in the presence of **94trans** results in switching of **93** to its externally locked state **93-94cis**. In a related example, the Fc spacer was doubly-linked to an azobenzene unit through the same positions linked to the aminodiphenyl arms in the previous example.¹³⁶ By means of UV-vis irradiation cycles, the azobenzene unit changes its conformation from *trans* to *cis*, respectively, thus causing the molecule to rotate around the Fc moiety in a reversible, pedal-like fashion.

The large conjugated character of *meso-meso*-butadiyne-linked Zn(II)Por dimers and, thus, their red-shifted absorption at around 700–750 nm and their 2PA¹³⁷ cross sections render them potential sensitizers for one- and two-photon PDT.

**Scheme 16** Photochemically controlled conformational switching of **93**.

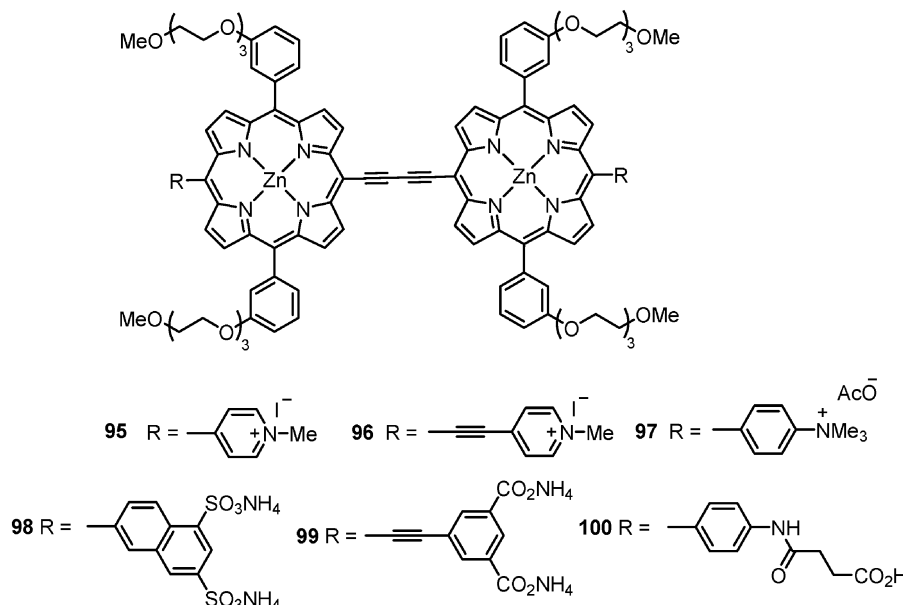


Fig. 23 Structures of hydrophilic conjugated Zn(II)Por dimers 95–100.

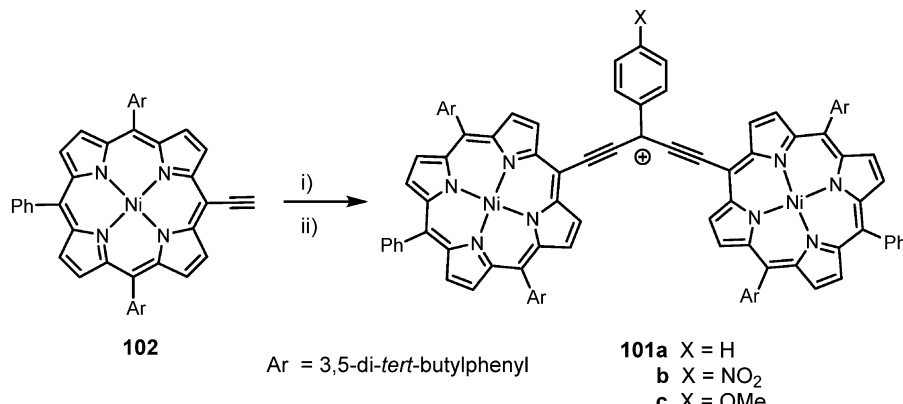
However, for such an application, water solubility is compulsory for reproducible delivery into cells, this requirement representing a difficult challenge considering the large hydrophobic core of *meso*-*meso*-butadiyne-linked diPors. For conferring water-solubility to these molecules, four polar triethoxylglycol substituents have been appended along the sides of each dimer, together with charged cationic (*methylpyridinium* and *trimethylammonium*) (compounds 95–97 in Fig. 23) and anionic (*sulfonate* and *carboxylate*) (compounds 98–100 in Fig. 23) substituents at the *meso*-positions.¹³⁸ The photophysical properties and intracellular uptake of this series of hydrophilic conjugated Por dimers have been investigated.¹³⁹ Using fluorescence microscopy, the accumulation of the photosensitisers in adenocarcinoma cells was monitored. Por dimers with positively charged substituents partition into cells more efficiently than the negatively charged dimers. In addition, one-photon and two-photon excited PDT results show that these Por dimers are very efficient one-photon PDT sensitizers, with efficiencies approaching those of drugs used clinically for PDT, especially in the case of dimer 96 functionalized with two terminal *N*-methylpyridinium moieties.¹⁴⁰ The latter molecule, in particular, has shown an unprecedented wavelength-dependent effect in the production of singlet oxygen.¹⁴¹ It also behaves as a fluorescent molecular rotor being sensitive to the viscosity of the media; thus, intracellular viscosity changes in single cells can be quantified by means of fluorescence measurements. Using this tool, the authors have shown that there is a dramatic increase in the viscosity of the immediate environment of the rotor on photoinduced cell death. They provide insight into the dynamics of diffusion in cells, which is pertinent to drug delivery, cell signaling and intracellular mass transport.¹⁴²

In an attempt to obtain Por dimers with an enhanced electronic delocalization, resonance-stabilized carbocationic systems such as **101a–c** have been prepared,¹⁴³ which emulate common dyes, such as cyanines and rhodamines. These systems have

been called “porpho-cyanines”, and were found to have effective delocalization,¹⁴⁴ over approximately 18 conjugated bonds, significantly longer than traditional cyanine dyes. Porphocyanines **101** were synthesized as shown in Scheme 17, through deprotonation of the terminal acetylene **102** and reaction with 0.5 equivalents of methyl benzoate derivatives, followed by addition of trifluoroacetic acid to generate the carbocation. These compounds show intense NIR absorption maxima located in the 1100–1340 nm range. Interestingly, extending the length of the acetylenic link between Pors brings about even more red-shifting of the maximum absorption wavelength, up to *ca.* 1620 nm.¹⁴⁵ The mid-IR absorption exhibited by these carbocationic systems, together with their large ultrafast third-order nonlinearities, makes them promising materials for all-optical switching.

Additional changes over the conjugated structure of butadiynyl-linked diPors include the insertion of Pt(II) between the sp C atoms *via* σ coordination of two Por-acetylidyne ligands to the metal centre.¹⁴⁶ Pt(II)-acetylidyne π -conjugated oligomers and polymers have received much attention because of their potential applications in electronic and optoelectronic devices. For this reason the effects of the Pt(II) bridge on the π -conjugation between Por units has been addressed. Electrochemical and UV-vis absorption measurements on these Pt(II)-diacetylidyne bridged Por dimers show that conjugation is reduced with regard to parent butadiyne-bridged diPors.

Recently, other types of conjugated Por dimers, such as *meso*-*meso*-(*E*)-ethene-1,2-diyl-linked diPors, have also been prepared by Suzuki coupling of porphyrinylboronates and iodo vinyl-Pors.¹⁴⁷ Electronic absorption and steady state emission studies, together with theoretical geometry and spectral calculations, led the authors to conclude that the ethenediyl-linked dyads exist in solution in a family of conformations that differ in the extent of conjugation across the bridge, due to differing



Scheme 17 Synthesis of cations **101a–c**. (i) $\text{XC}_6\text{H}_4\text{CO}_2\text{Me}$ (0.5 equiv.); $\text{LiN}(\text{SiMe}_3)_2$ (4 equiv.), THF; (ii) trifluoroacetic acid (2% by vol.), CHCl_3 .

dihedral angles between the Por and alkene planes. (*E*)-Azoporphyrins, namely, Por dimers linked through azo-bridges by their *meso* positions, are also an interesting class of π -extended diPors since they combine the porphyrinoid conjugation with the potential photoreactivity of the azo linkage. Stronger interactions between the Por rings across the azo bridge than across ethene and ethyne linkers have been found.¹⁴⁸ Carbazole¹⁴⁹ and pyrrole¹⁵⁰ linked Por dimers, as well as 1,2-,¹⁵¹ 1,3- and 1,4-¹⁵² phenylene-linked diPors have also been prepared by means of metal-catalyzed, cross-coupling methodologies. In many cases, the structural features of the aromatic spacer impart a cofacial nature to the diPor system. Cofacial diPors holding spacers such as tris-anthracenic units,¹⁵³ or structurally simpler biphenylene, anthracene, dibenzofuran, dibenzothiophene or dimethylxanthene bridges have been prepared following classical synthetic protocols based on acid-catalyzed condensations.¹⁵⁴ Cofacial, “Pacman”-type, Por dimers, in which two Por rings are held in a face-to-face arrangement by a calixarene platform, have also been described.¹⁵⁵

On the other hand, much effort has been devoted to the synthesis of chiral diPors because of their many important applications. Chiral Pors have been used as catalysts in asymmetric synthesis, as sensors for chiral recognition, and as mimics for enzymatic processes.^{156,157} Several approaches can

be applied for chiral diPor synthesis. The most straightforward method is to attach chiral building blocks to preformed Por synthons, the chiral unit also performing as a bridge between the two macrocyclic units. For instance, commercial (−)-2,3-*o*-isopropylidene-D-threitol has been coupled to a *meso*-substituted bromoPor,¹⁵⁸ and two chiral BINOL spacers have been employed to link two Por rings in an offset face-to-face geometry with an interplanar distance of 5.8–7.2 Å, thus creating a chiral cavity which is suitable for hosting aromatic molecules (**103** in Fig. 24).¹⁵⁹ Apart from that, chirality can be achieved in *meso*–*meso* linked diPors by intramolecular chiral induction. Stereoselective synthesis of the chiral *meso*–*meso*-linked Por dimer **104** (Fig. 24) was achieved by using a chiral BINOL moiety as a remote chiral auxiliary, which controls the chirality of the diPor bond formed after oxidative coupling of the two subunits.¹⁶⁰ For instance, a 2.2 : 1 ratio of SS/SR diastereoisomers of **104** was obtained with (S)-BINOL as remote auxiliary when the intramolecular oxidative coupling was performed at low temperatures. The two diastereoisomers of **104** were separated by achiral column chromatography. This elegant example is the first one reported in which the two atropisomers of a directly, *meso*–*meso* linked chiral diPor were isolated without utilizing chiral chromatography.

In the last few years, Pors have proved to be realistic candidates for replacing the costly and environmentally unfriendly

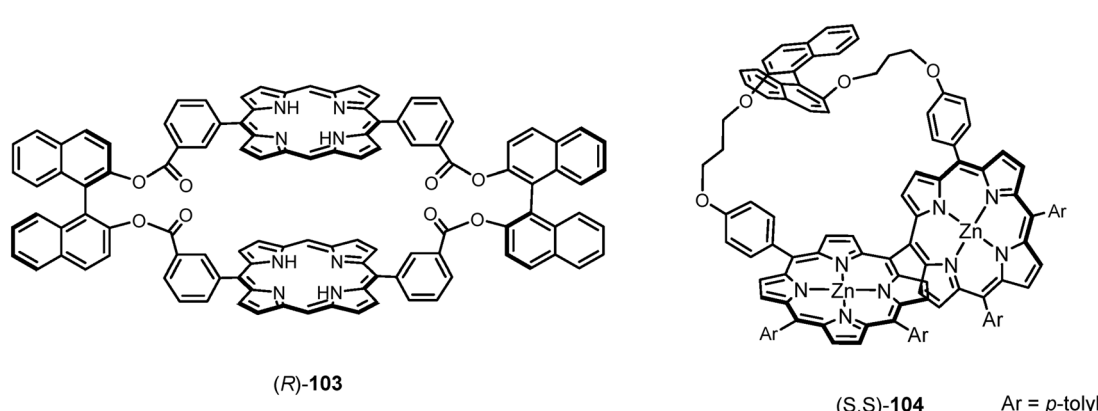


Fig. 24 Chiral diPors **103** and **104**.

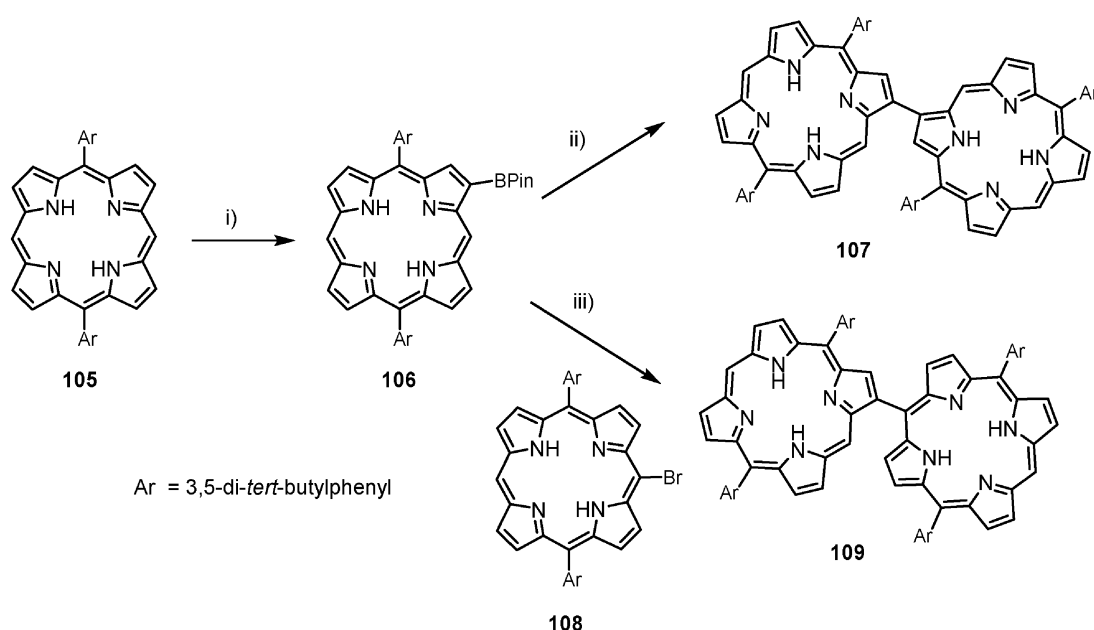
ruthenium-based sensitizers in dye sensitised solar cells (DSSCs).¹⁶¹ Incorporating multichromophore light harvesting arrays with increased absorption cross sections would have the advantage that efficient DSSCs with thinner dye-sensitised films can be prepared. In this regard, directly *meso-meso* linked Por dimers are interesting candidate dyes to improve light-harvesting capability in DSSCs as the Soret band becomes broader by splitting into two bands due to strong exciton coupling between Por moieties. In the meantime, the extinction coefficients of the Q-bands also increase due to the reduced symmetry of Por dimers. In this regard, some directly *meso-meso* linked Por dimers tethered at two or four pyrrolic positions¹⁶² or at one free *meso*-position^{163,164} with carboxylic acid moieties to anchor onto the TiO₂ surface have been prepared and studied. Efficiencies of up to 5.2% have been achieved with some of these systems.¹⁶⁴

As in the case of *meso-meso* linked multiporphyrinic molecules, β - β directly linked diPors are receiving much attention since the interactions among coupled moieties are the basis of fundamental biological processes. The research on these types of compounds was triggered by the finding that the conditions of direct borylation of aromatic compounds *via* C-H bond iridium-catalyzed activation can be successfully applied to Por chemistry. Osuka and co-workers found that treatment of 5,15-bis(3,5-di-*tert*-butylphenyl)Por (**105**) with bis(pinacolato)-diborane (B(pin)) in the presence of catalytic amounts of an iridium complex provided Por **106** in moderate yields (Scheme 18).¹⁶⁵ The borylation took place exclusively at the β -position adjacent to the unsubstituted *meso*-position of the Por core, namely, the sterically less hindered β -position. Exhaustive tetraborylation could also be carried out on 5,15-diarylPor **105**. β -Borylation provides useful building blocks for the synthesis of Por-containing ensembles. In fact, as a proof of concept, the same authors

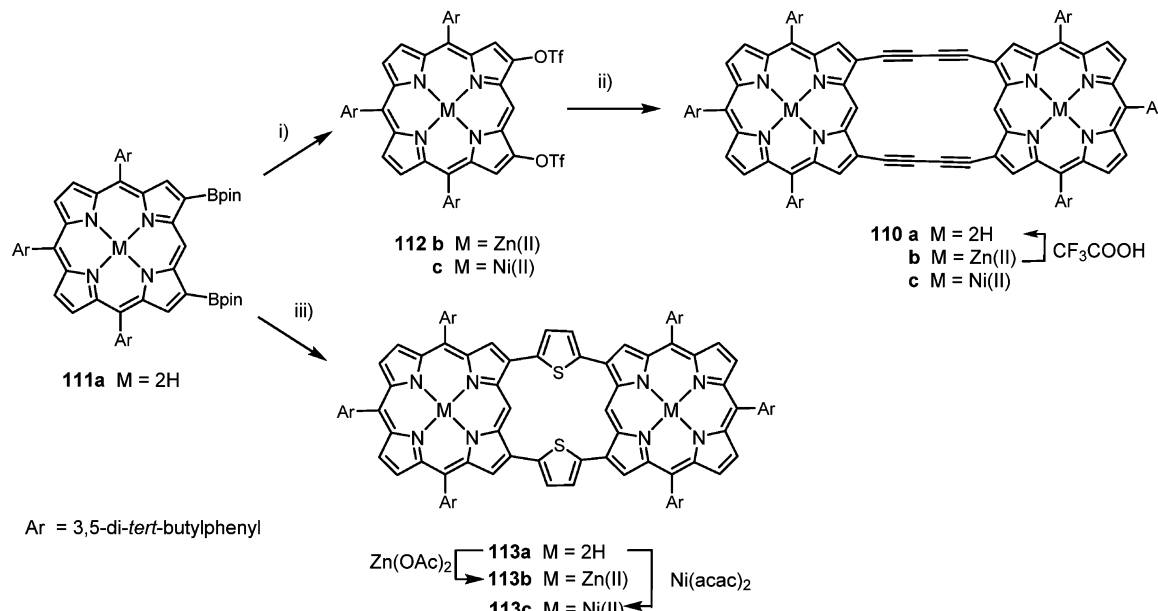
reported the Pd(II)-catalyzed oxidative dimerization of **106** to give the β - β -linked diPor **107** in good yield (Scheme 18). In addition, Suzuki–Miyaura coupling between **105** and *meso*-bromoPor **108** afforded the *meso*- β -linked diPor **109**.

Whilst the chirality of other diPor systems relies on unsymmetric substitution patterns (their basic bisPor framework has a plane of symmetry and is therefore achiral), directly β , β -coupled bisPor exhibits axial chirality *per se*, independently of their substitution. The first example of isolation of enantiopure β , β -linked Por dimers was reported in 2006.¹⁶⁶ The dimers were prepared by Suzuki–Miyaura cross-coupling of a tetraphenyl (or tetratosyl) Por borylated at the β -position with the corresponding β -monobrominated Por derivative. The resulting bisPor Zn(II) complexes could be separated by HPLC on a chiral stationary phase into their atropoenantiomers, (*i.e.*, (*p*)- and (*m*)) which, indeed, showed mirror-imaged circular dichroism curves. Following the same protocol, other metallated (Cu(II), Ni(II), Pd(II), etc.) β , β -coupled bisPor were prepared.¹⁶⁷ It was shown that the configurational stability of the Por–Por axis strongly depends on the nature of the central metals.

As shown in previous sections, covalently linked π -conjugated Por dimers show interesting electronic features, which depend on the extent of overall π -conjugation, which is a function of molecular co-planarity. In this regard, doubly β -to- β butadiyne-bridged diPors **110a–c** are very interesting compounds since they possess a robust, enforced, overall planar conformation.¹⁶⁸ These compounds were prepared from bis(β -borylated)-H₂Por **111a**, which was first treated with Oxone, and then with PhNTf₂ and Cs₂CO₃ to yield trifluoromethanesulfonyl derivatives **112b–c** after metallation (Scheme 19). Installation of ethynyl groups was conducted through standard Sonogashira coupling with trimethylsilylacetylene followed by desilylation; then a



Scheme 18 Synthesis of β - β linked diPors **107** and **109**. Reagents and conditions: (i) bis(pinacolato)diborane, $[\text{Ir}(\text{cod})\text{OMe}]_2$ (cat), 4,4'-di-*tert*-butyl-2,2-bipyridyl, 1,4-dioxane; (ii) O_2 , $\text{Pd}(\text{OAc})_2$, 1,3-bis(diphenylphosphino)propane, DMSO-toluene; (iii) Pd_2dba_3 , PPh_3 , Cs_2CO_3 , DMSO-toluene.



Scheme 19 Synthesis of β - β linked diPors **110a–c** and **113a–c**. Reagents and conditions: (i) (1) oxone, THF–acetone–H₂O, RT, 1.5 h; (2) PhNTf₂, Cs₂CO₃, DMF, RT, 12 h; (3) Zn(OAc)₂ or Ni(acac)₂, CHCl₃, MeOH, RT, 2 h; (ii) (1) Me₃SiCCH, Pd(PPh₃)₄, CuI, Et₃N, DMF, toluene, 70 °C, 3 h; (2) K₂CO₃, THF, MeOH, RT, 2 h; (3) Cu(OAc)₂, THF, pyridine, RT, 24 h; (iii) 2,5-dibromothiophene, Pd₂(dba)₃, PPh₃, Cs₂CO₃, CsF, toluene–DMF–H₂O, reflux, 48 h.

Cu(II)-mediated oxidative coupling reaction furnished the corresponding butadiyne-linked Por dimers **110a–c**. Interestingly, TPA cross-section values of these double-linked dimers almost double those of related monobutadiynyl-linked diPors. π -Conjugation through thienylene linkages in Por dimers has been also studied. DiPors **113a–c** were prepared from β , β -diborylPor **111a** and 2,5-dibromothiophene under Suzuki–Miyaura cross-coupling conditions (Scheme 19).¹⁶⁹

Metal–ligand coordinative interactions are a useful tool to construct β - β linked diPors. For instance, β - η^1 -palladio- and Pt(II)Por (**114a,b** in Fig. 25) were formed by regioselective metallation at the β carbon of *meso*-phosphanylporphyrins.¹⁷⁰ The coplanar Por dimers linked by peripherally fused phosphametallacycles through their β and *meso* positions were found to exhibit characteristic optical and electrochemical properties derived from the p _{π} –d _{π} orbital interaction.¹⁷¹ Oppositely, Pt(II)- (and also Pt(IV)-) bridged cofacial diPors such as **115** in

Fig. 25 have been constructed by metallation at the *meso* position of a β -pyridyl Por.¹⁷² The Pt center forces the two Por macrocycles to be in close proximity by the stable two Pt–C σ -bonds supported by the pyridyl groups. These Pt-bridged cofacial diPors such as **115** have inherent helical chirality, and the authors succeeded in separating the enantiomers by chiral HPLC. In addition, β , β' -doubly-2,6-pyridylene-linked Por dimer **116** was prepared by Suzuki–Miyaura coupling reactions and, in a second step, it was readily metallated *via* *meso*-C–H bond activation with the assistance of the pyridyl nitrogen atoms to produce the corresponding Pd(II) complexes.¹⁷³ Interestingly, diPor **116** exhibits remarkably bent conformations due to constraints arising from double β , β' -2,6-pyridylene bridges. On the other hand, the functionalization of two neighboring β -pyrrolic positions of a Por by a fused N-heterocyclic carbene ligand and subsequent metallation of this external coordination site by Pd(II) affords another type of metal-bridged diPors.¹⁷⁴

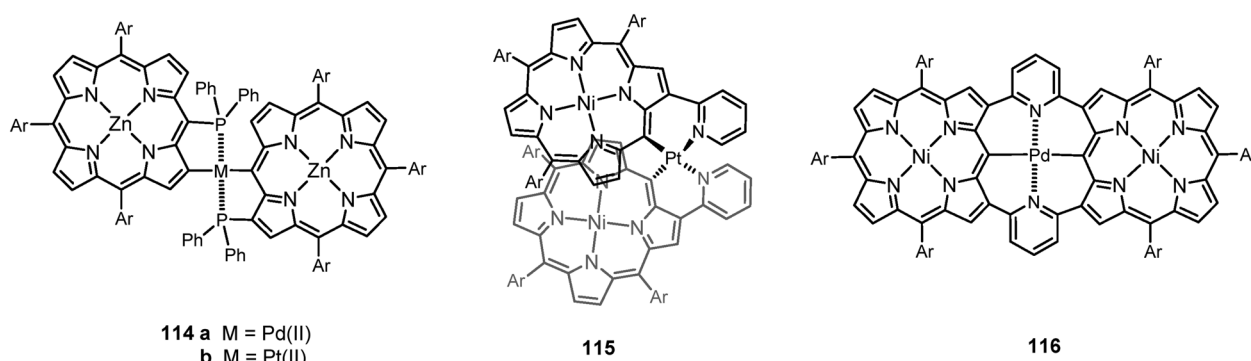


Fig. 25 Structures of (a) β - η^1 -Pd(II)- and Pt(II)-diPors **114a,b**; (b) Pt(IV)-bridged cofacial diPor **115**; and (c) Pd(II)-bridged diPor belt **116**.

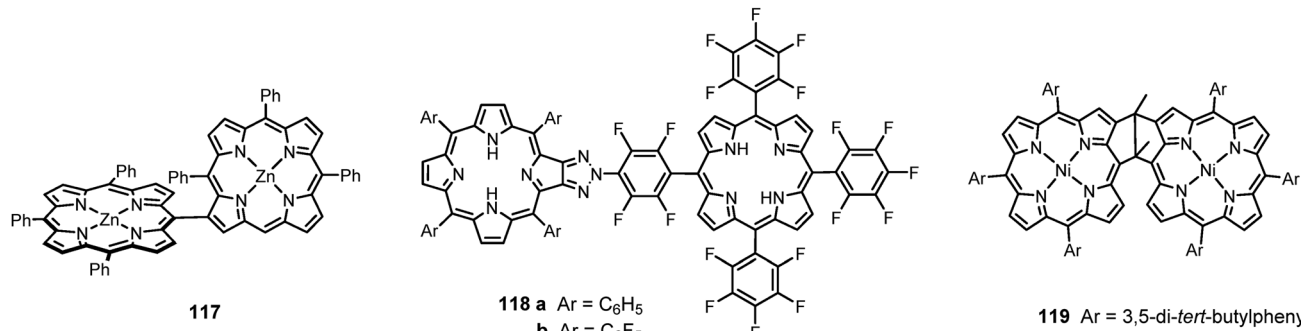


Fig. 26 *meso*-to- β linked diPors **117** and **118a,b** and *meso*-*meso*, β - β diPor **119**.

Similarly to the above-mentioned examples of metal-bridged diPors, in which both *meso*- and pyrrolic positions are involved, the dimerization of *meso*-bromoPors using Pd-catalyzed homo-coupling conditions in the presence of a Lewis acid provides directly linked *meso*- β diPors such as **117** (Fig. 26).¹⁷⁵ In this unprecedented example, the coupling formally involves the C-H bond cleavage at the β -position that is remote from the initially brominated *meso*-position, where the coupling reaction is probably initiated. Importantly, the dimerization was perfectly regioselective. The structural and electronic features of **117** are similar to other previously reported *meso*- β -linked diPors, which were prepared by condensation reaction of a tetraphenyl-porphyrin derivative featuring a formyl group at the β -position and different *meso*-substituted dipyrromethanes.¹⁷⁶ In all the examples, the UV-vis absorption spectra showed split Soret bands, as a consequence of the exciton coupling in line with the directly linked dimeric structure. Worth mentioning is the isolation of a *meso*- β directly linked Ni(II)diPor after treatment of a [36]octaphyrin with Ni(acac)₂.¹⁷⁷ This conversion was serendipitously found during the study on the nickel(II) metallation of the expanded Por.

Other interesting examples of Por dimers with *meso*-to- β linkages involve the previous formation of either a triazole¹⁷⁸ or a pyrrolidine¹⁷⁹ ring fused to one of the pyrrolic components of a Por core, followed by *N*-arylation or *N*-alkylation reaction with other appropriately functionalized Por monomers. Following this approach, interesting bisPors such as **118a,b** (Fig. 26) have been obtained.¹⁷⁸ Also, a diPor system **119** (Fig. 26) with a *meso*-to-*meso*- β -to- β linkage has also been reported. The preparation of such a compound involves SmI₂-mediated pinacol coupling of a β -acetyl-Por followed by treatment with concentrated sulfuric acid and trifluoroacetic acid.¹⁸⁰ In the final diPor system, the two Pors are held close in a conformationally restricted manner. Photophysical experiments and quantum mechanical calculations indicate that the π -conjugation extends to the whole molecule, being an interesting example of homoconjugation *via* two alkyl linkages.¹⁸¹

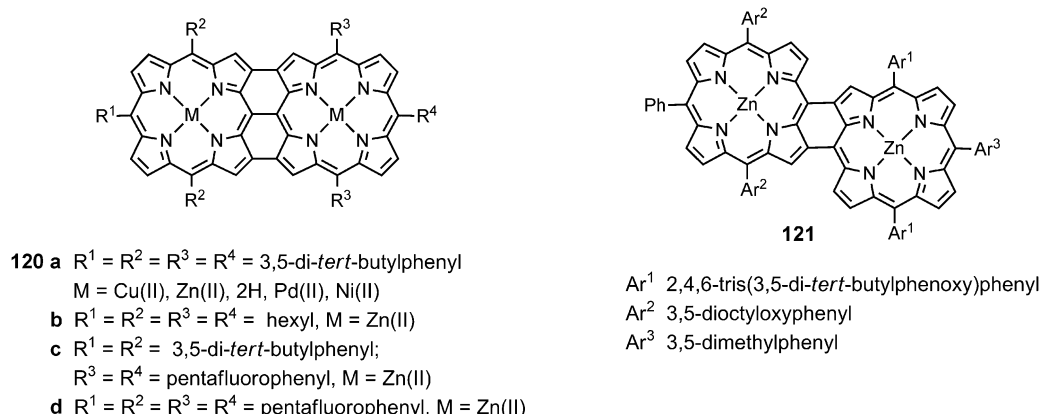
4.2 Fused, binuclear porphyrins

Fusion reactions allow for the connection of two π -electronic systems by two or more bonds in a single step. This strategy is highly useful for constructing rigid and planar structures,

which would be effective for π -conjugation and suppression of energetic decay in the photoirradiated excited state. Fusion of two Por units through aromatic rings such as benzene,¹⁸² pyrazine,¹⁸³ or AQ¹⁸⁴ leads to large π -systems, which show split Soret bands and substantially bathochromically shifted Q-bands. Por dimers fused with shared benzene or AQ units are prepared by retro-Diels–Alder reaction of bicyclo-connected Por–Por precursors. In the case of the pyrazine-fused systems, their synthesis proceeds by oxidative dimerization of β -aminoPors.

In addition to those highly conjugated dimeric structures, particular attention has been paid to *meso*-*meso*, β - β , β - β triply linked Por dimers **120** (Fig. 27), since they hold great potential as molecular wires in nanoscale electronic devices. In such a type of array, conjugation is fully extended over the whole covalent ensemble, which results in extremely low-energy electronic absorption bands that reach into the IR region.¹⁸⁵

These compounds were first reported in 2000 by Osuka and co-workers (**120a** in Fig. 27),¹⁸⁶ and their synthesis was carried out by oxidation of *meso*-*meso* linked diPors with, for instance, Sc(OTf)₃ and DDQ.¹⁸⁷ Since then, different structural variations of the so-called “Por tapes” have been pursued, as well as other oxidative methods to prepare these triply fused diPors such as the phenyliodine bis(trifluoroacetate)-mediated oxidation of mononuclear Zn(II) Pors with one free *meso*-position.¹⁸⁸ For instance, bulky aryl substituents installed at the *meso* positions of the Por monomer in the former reported example (5,15-bis(3,5-di-*tert*-butylphenyl)) have been replaced by alkyl substituents in order to enhance the self-assembling nature of the tapes by π - π stacking (**120b**).¹⁸⁹ Hybrid Por tapes (**120c**) consisting of a donor core of 3,5-di-*tert*-butylphenyl-substituted Zn(II)Por and an acceptor pentafluorophenyl-substituted Zn(II)Por were prepared by a synthetic route involving the cross-condensation reaction of a Ni(II)-porphyrinylidipyrromethane and pentafluorobenzaldehyde, followed by appropriate demetallation, remetallation with a Zn(II) salt, and oxidative ring-closure.¹⁹⁰ Interestingly, these hybrid Por tapes show slightly larger TPA values than the parent homoleptic ones composed exclusively of donor Por components.¹⁹¹ Electron deficient Por tapes, such as hexakis(pentafluorophenyl)-substituted *meso*-*meso*, β - β , β - β triply linked Zn(II)-diPor¹⁹² **120d**, and others containing CN groups attached to peripheral *meso*-aryl substituents¹⁹³ were also prepared and their electronic properties investigated.

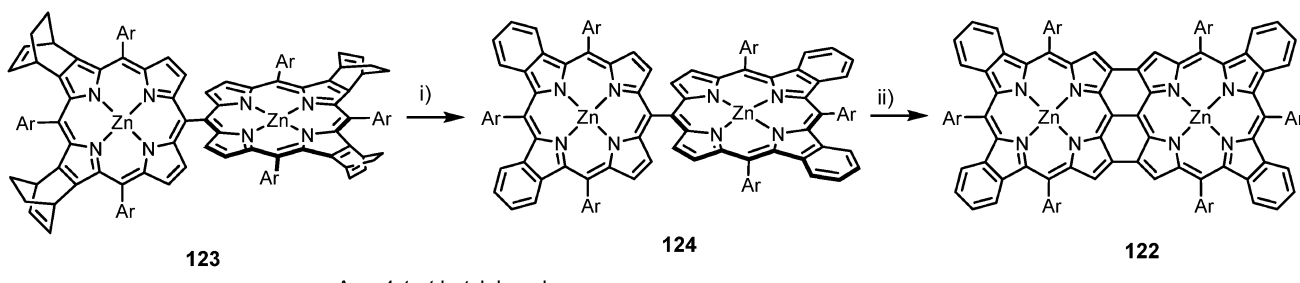
**Fig. 27** "Por tapes" 120a-d and 121.

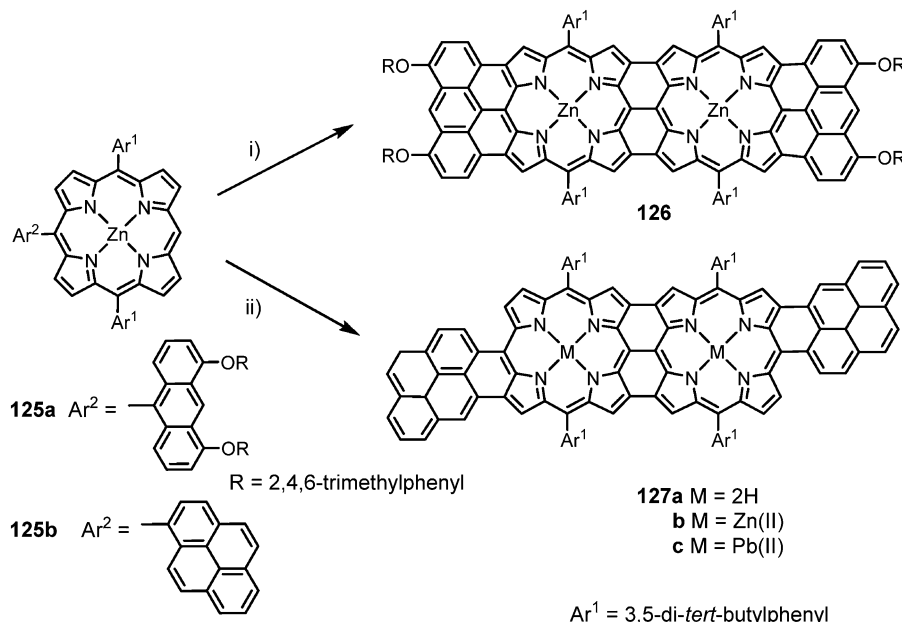
Additionally, *meso*- β doubly linked ensembles 121 were synthesized by oxidation of *meso*- β singly linked Por dimers having a free *meso*-position, with DDQ-Sc(OTf)₃.¹⁹⁴ It is worth mentioning that the crystal structures of some of these compounds reveal that the component Por cores are almost coplanar. The electronic communication between the two Por macrocycles is quite strong in these triply (and also doubly) fused arrays, and all of them present extremely low HOMO-LUMO gaps, with the lowest energy absorption bands reaching the infrared region (*ca.* 1050 nm). Another remarkable feature of these Por tapes is that, after installing peripheral alkoxy chains at the periphery, the molecules organize into liquid crystalline phases which show intrinsic electron transport properties.¹⁹⁵ In contrast, liquid crystalline phases formed by fused metalloPor dimers functionalized with semifluoroalkyl side chains behave as p-type semiconductors.¹⁹⁶

Further enlargement of the π -electronic network of *meso*-*meso*, β - β , β - β triply linked diPors has also been undertaken by different means. Certainly, Por tapes composed of three or more Pors have a large π -electronic network and give absorbances, which extend into the mid-NIR region (*ca.* 1.5 μm). However, these derivatives are difficult to synthesize, have low solubility, and are indeed far from the scope of this review, which is focused on Por dimers. Nevertheless, the conjugation of Por dimers can be additionally extended through several modes of substitution involving the *meso*, (β,β), (β,meso) and (β,meso,β) positions. For diPors substituted with two alkyne groups at the

terminal *meso* positions, the Q-band is red-shifted by 130 nm ($\lambda = 1181$ nm) relative to the parent dimer.¹⁹⁷ Extending the conjugation in Por dimers by benzannulating β,β -pyrrolic positions such as 122 in Scheme 20 red-shifts the Q-band up to 1169 nm.¹⁹⁸ This compound is prepared by the initial retro Diels-Alder reaction of bicyclo[2.2.2]octadiene-fused *meso*-*meso*-linked diPor 123 that affords the dibenzofused porphyrin dimer 124, which is further oxidized with DDQ-Sc(OTf)₃ to the target diPor 122. Notably, this compound shows larger TPA cross sections than normal diPor tapes.

Recently, it has been shown that anthracene rings can be fused to Por dimers through the (β,meso,β) mode by oxidative ring closure of a mononuclear Por 125a with an anthracene moiety linked to its *meso*-position, using Sc(OTf)₃/DDQ (Scheme 21).¹⁹⁹ In order to circumvent problems of insolubility and aggregation, the anthracene moiety was designed to bear bulky 2,4,6-trimethylaryl ether substituents. The spectrum of anthracene end-capped fused dimer 126 extends well into the near-IR with a λ_{max} at 1495 nm. The effect of aromatic ring fusion to Por tapes in a (β,meso) mode has also been explored. For instance, pyrene-(β,meso)-fused diPor 127 holds the advantage of displaying out-of-plane-distortion, which is known to improve solubility and processability in conjugated aromatics. Starting from the Por derivative 125b, having one pyrene ring linked to one *meso* position and one unsubstituted *meso*-carbon, pyrene-fused Por dimer 127 was successfully obtained (Scheme 21).²⁰⁰ The increase in conjugation of the Por dimer by

**Scheme 20** Synthesis of 122. Reagents and conditions: (i) 210 °C, 0.1 mmHg for 30 min; (ii) DDQ-Sc(OTf)₃.



Scheme 21 Synthesis of **126** and **127**. *Reagents and conditions:* (i) DDQ-Sc(OTf)₃, CH₂Cl₂; (ii) FeCl₃, CH₂Cl₂, then aq HCl (M = 2H); Zn(OAc)₂, MeOH, CH₂Cl₂, (M = Zn(II)); Pb(OAc)₂, pyridine, CH₂Cl₂, (M = Pb(II)).

adding two fused pyrene rings results in a large bathochromic shift of the Q-band up to 1323 nm.

4.3 Supramolecular ensembles of covalent and noncovalent porphyrin dimers

In this section we will review some recent works on the self-aggregation of appropriately functionalized, covalent Por dimers and Por monomers leading to the formation of supramolecular multiPor and Por-Por ensembles, respectively.

Among the supramolecular interactions that have been used for such a scope, coordinative, metal-ligand interactions are probably the most used and versatile ones, especially considering the large variety of metal atoms that metalloPors can incorporate in their central cavity.²⁰¹

In this context, a considerable number of metalloPor systems bearing peripheral coordinating ligands, mainly nitrogenated bases such as pyridyl, Im, aminopyrimidyl, and amino groups, have been reported and their self-aggregation ability studied. For such systems, by carefully modulating some parameters such as the directional angle and basicity of the ligand(s) nitrogen(s) lone pair as well as steric factors around the metalloPor macrocycle, a large variety of supramolecular structures have been obtained such as cofacial, linear, branched, cyclic, dendritic, and polymeric metalloPor assemblies.

For example, supramolecular Por dimers (**(128)₂,(129)₂**)²⁰² and tetramers (**(130)₂,(131)₂**)²⁰³ have been obtained from the spontaneous self-assembly in a noncoordinating solvent such as CHCl₃ of *meso*-triazolyl-appended Zn(II) Por monomers (**128,129**) and dimers (**130,131**), respectively, these latter compounds are prepared by Cu(I)-catalyzed, 1,3-dipolar cycloaddition of benzyl azide to *meso*-ethynylated Zn(II)Pors (Fig. 28). GPC and ¹H NMR and UV-vis spectroscopies clearly demonstrate the formation of

metal-ligand coordination complexes, with K_{ass} as high as 10^{11} M^{-1} in the case of dimer (**129**)₂.

A similar assembly strategy has been used for the preparation of supramolecular Por dimers (**(132)₂** and **(133)₂**) from bis Im-substituted, *meso-meso* linked H₂Por-Zn(II)Por **132** and butadiyne-linked H₂Por-Zn(II)Por **133**, respectively (Fig. 29).²⁰⁴ The 2PA and higher-order nonlinear absorption properties of (**132**)₂ and (**133**)₂ were investigated over femtosecond time scales using an open-aperture Z-scan method, revealing, in the case of the self-assembled butadiyne-linked Por dimer (**133**)₂ a 2PA cross section almost 20 times larger than that of the *meso-meso*-linked Por dimer (**132**)₂. These results suggest that the butadiyne connection, which brings about a significant expansion of the Por-Por π -system, is probably the predominant factor in the observed 2PA cross section enhancement. Supramolecular polymers with a mean molecular weight of $M_n = 1.5 \times 10^5$ Da could also be obtained by zinc metallation of the free-base Por macrocycle in dimer **133**, leading to a further increase of the 2PA cross section. Finally, 3PA was observed in the case of supramolecular Por tetrad (**133**)₂, an observation which is the first of this kind in Por chemistry.

In 2007, Satake, Kobuke and coworkers reported an interesting self-aggregating, monoIm-substituted Por dimer **134**, whose fluorescence could be switched between two states (a fluorescent and a less-fluorescent state) as a response to changes in Por dimer binding ability (Scheme 22).²⁰⁵

In fact, whereas in noncoordinating solvents Por dimer **134** mainly adopts a stacked conformation (**134**)₂-s which is poorly fluorescent, addition of pyridine to this stacked assembly induces its almost quantitative transformation to the extended species (**134**)₂-e. This process, which can be reverted by addition of acetic acid and subsequent heating, is accompanied by an

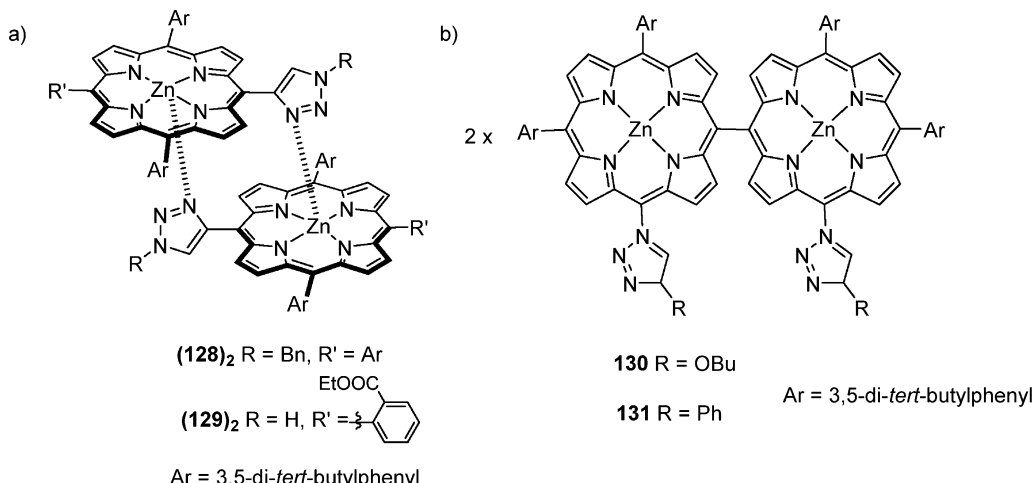


Fig. 28 Molecular structures of (a) cofacial Por dimers $(\mathbf{128})_2$ and $(\mathbf{129})_2$ resulting from the self-assembly of meso-triazolyl-appended Zn(II) Por monomers $\mathbf{128}$ and $\mathbf{129}$ and (b) Por dimers $\mathbf{130}$ and $\mathbf{131}$ able to self-assemble giving rise to tetrads $(\mathbf{130})_2$ and $(\mathbf{131})_2$.

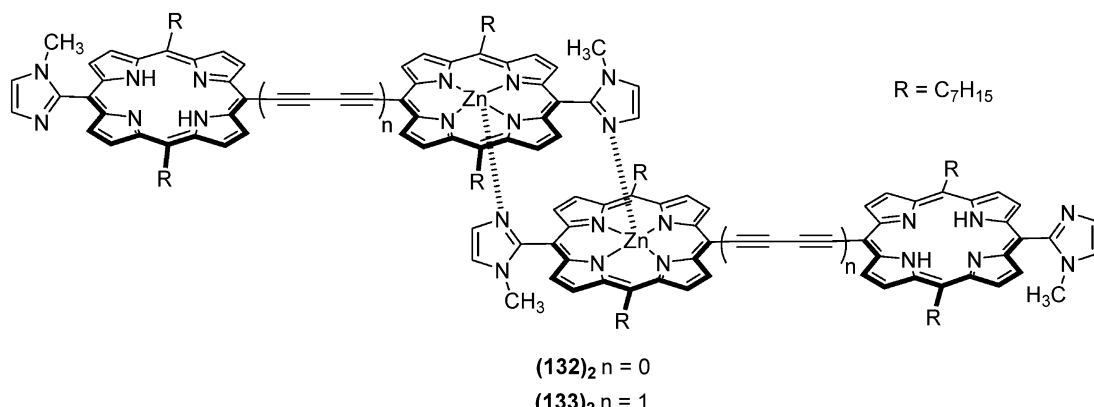
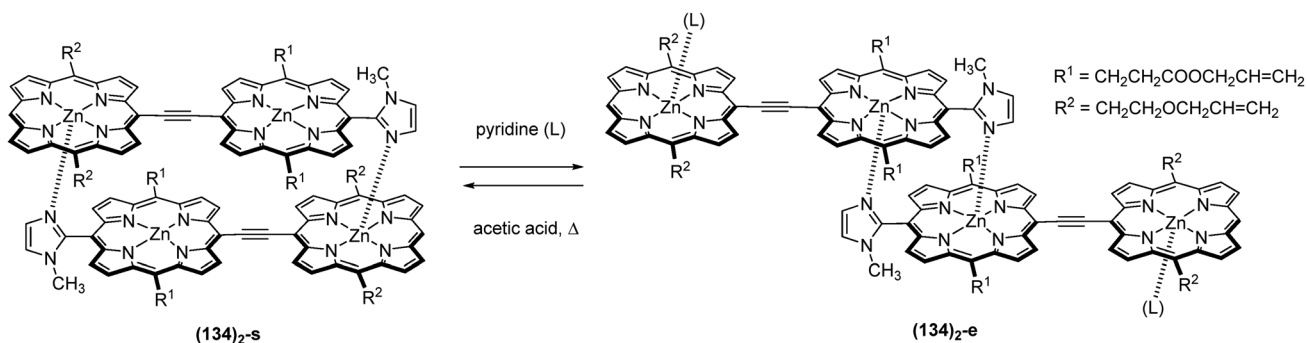


Fig. 29 Molecular structures of Por tetramers $(\mathbf{132})_2$ and $(\mathbf{133})_2$ resulting from the self-assembly of bis Im-substituted, meso–meso linked $\text{H}_2\text{Por-Zn(II)}\text{Por}$ $\mathbf{132}$ and butadiyne-linked $\text{H}_2\text{Por-Zn(II)}\text{Por}$ $\mathbf{133}$, respectively.



Scheme 22 Molecular structures of the stacked $(\mathbf{134})_{2-s}$ and extended $(\mathbf{134})_{2-e}$ conformation resulting from the self-aggregation of Por dimer $\mathbf{134}$.

increase in the fluorescence intensity by a factor of 7. In both supramolecular complexes, which structural features have unequivocally been elucidated by ^1H NMR spectroscopy, the interconversion rate can be regulated by controlling the dimer-to-external ligand ratio and/or the temperature. A covalent version of $(\mathbf{134})_{2-e}$ in which the two central, stacked Por

macrocycles have covalently been linked by metathesis reaction between the terminal alkenes on R^1 using Grubbs' catalyst has also been reported.²⁰⁶

A combination of Zn(II)-Im interactions and metathesis reaction has also been used by the group of Kobuke in order to prepare Por tetramer $\mathbf{135a}$ (Fig. 30) which was obtained from

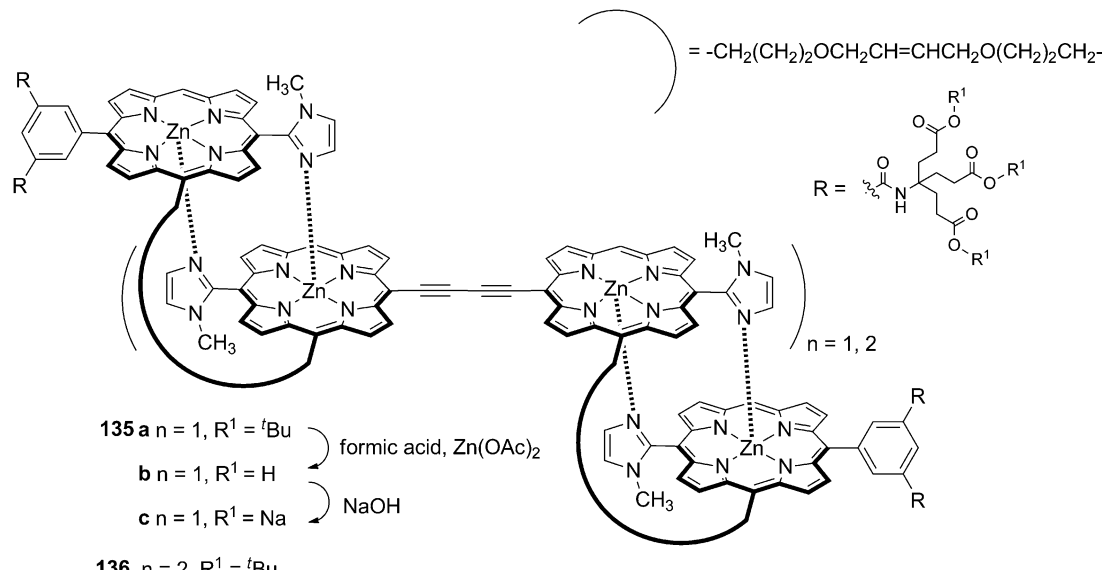


Fig. 30 Molecular structures of multiPor systems **135** and **136**.

a supramolecular precursor constituted by a covalent, bis-Im-substituted, butadiyne-bridged Zn(II)Por dimer axially coordinated to two, mono-Im-functionalized Zn(II)Por monomers.²⁰⁷ Por tetramers **135b** and **135c** could be easily obtained from compound **135a**. Interestingly, water-soluble compound **135c** showed good 2PA cross-section values and it was found to generate, upon two-photon excitation, singlet oxygen, cytotoxic for tumor cells in PDT.

High 2PA cross-section values were also obtained for a multiPor conjugate (**136**) presenting two covalently connected Por dimers in its central part, which is obtained by a stepwise elongation process employing the same Por components used for the synthesis of **135** (Fig. 30).²⁰⁸

Formation of Im-Zn(II) interactions have also been used to obtain cyclic, supramolecular Por assemblies by the slipped-cofacial, self-aggregation of a Zn(II)Por dimer (**137**) bearing two terminal Im units (Fig. 31a).

GPC showed that Zn(II)Por dimer **137** forms, in noncoordinating solvents, a polymeric mixture with broad molecular weight

distributions. Although the distribution of **137** was broad, the curve showed a distinctly longer elution time, indicating the formation of oligomeric species of small molecular weight, due to intramolecular cyclization species. This is in stark contrast to what is observed in the case of linear, *meso-meso*-coupled Zn(II)Por dimer complexes, which formed giant linear arrays.²⁰⁹ Further studies demonstrated that the cyclic coordination complex, formed in nonpolar solvent, could be broken in polar solvents by competitive coordination, in a reversible process, but in this case under high-dilution conditions. AFM and STM studies of these oligomeric species deposited on solid substrates confirmed the circular structure of the assembly, whereas small-angle X-ray scattering measurements in solution allowed the authors to determine the exact aggregation number, which in this case resulted to be six (Fig. 31b).²¹⁰ In this case, crucial for the formation of such cyclic structure is the presence of a 1,3-phenylene spacer connecting the two Im-substituted Zn(II)Por macrocycles, which maintains the two macrocycles with a 120° spatial orientation. Pentameric supramolecular

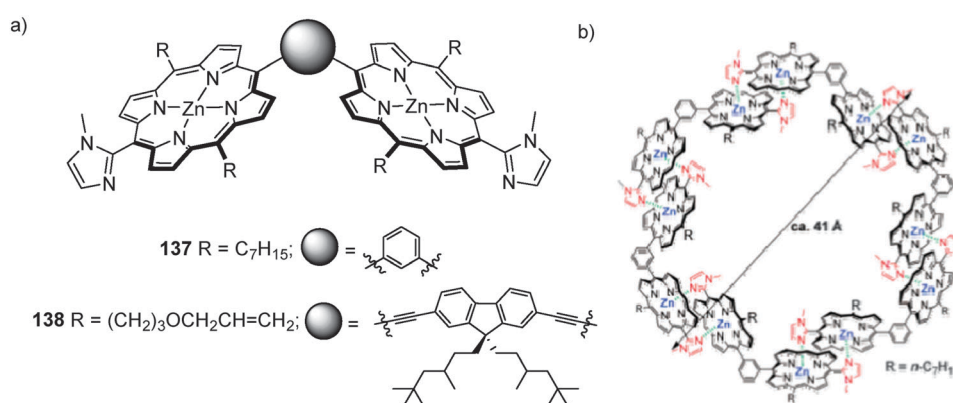


Fig. 31 Molecular structures of (a) Zn(II)Por dimers **137** and **138** bearing two terminal Im units and (b) cyclic, supramolecular ensemble resulting for the self-assembly of six Zn(II)Por dimers **137**. Reprinted from ref. 210. Copyright 2003 ACS.

nanorings based on the self-assembly of gable Por dimer **137** could also be obtained by a sequence of dissociation–reassociation processes.²¹¹ Interestingly, in these self-assembled, supramolecular nanorings, the distances and orientations between the metal Por units as well as the overall cyclic structure strongly resemble those of the natural light-harvesting complexes.

The 2PA properties of supramolecular Por nanorings have also been investigated similar to the case of the linear, supramolecular Por assemblies. Por dimer **138**, which contains a bridging fluorene unit and pendant terminal alkene units in the Por *meso* positions (Fig. 31a), formed, when dissolved in a nonpolar solvent, long and linear polymers which, by gentle heating, gradually converted to smaller, cyclic supramolecular arrays. Ring closing metathesis reaction was then carried out on these cyclic, supramolecular structures giving rise to covalent species which were separated by GPC in distinct fractions containing from 11 to 19 Por dimers. High 2PA values have been observed for these large, multiPor arrays as a result of their covalent, cyclic structure reinforced by metal–ligand cooperative intramolecular interactions between the Por units.²¹²

Gable-type Zn(II)Por dimer **139** in which the two macrocycles have been connected by a phenanthroline linker has also been prepared and used as a bifunctional receptor for free-base, *meso*-5,10-bis(4-pyridyl)-15,20-diphenyl H₂Por **140** (Fig. 32).²¹³

¹H NMR spectroscopy studies evidenced the quantitative formation of the triPor ensembles **139–140**, in which the two fragments are held together by two axial pyridyl-Zn interactions. The remarkable stability of this complex, with a K_{ass} of about $6 \times 10^8 \text{ M}^{-1}$ as determined by UV-vis absorption and emission titration experiments in toluene, is due to the almost perfect geometrical match between the two interacting units, as revealed by the X-ray crystal structure of the complex.

Three-dimensional, supramolecular Por boxes formed *via* enantiomeric, self-sorting assembly of (3 or 4)-pyridyl-appended, *meso–meso* linked Zn(II)Por dimers have also been synthesized.²¹⁴ Crucial for the formation of such box-shaped assemblies is the dihedral angle formed between the two Por macrocycles.

In 2004, the groups of Kim and Osuka reported the spontaneous self-assembly, in noncoordinating solvents such as CHCl₃, of a series of 4-pyridyl-appended, *meso–meso* linked Zn(II)Por dimers (**141**), giving rise to supramolecular Por boxes (Fig. 33a).²¹⁵ Interestingly, the formation of such boxes from achiral Por dimers proceeds *via* a homochiral, self-sorting process of Por atropisomers **141** giving rise to two enantiomerically pure supramolecular boxes (Fig. 33b). These boxes display strong Cotton effects in their circular dichroism spectra and K_{ass} as high as 10^{21} M^{-3} as a result of eight-point, simultaneous coordinative interactions.

Supramolecular boxes have also been obtained employing *meso–meso* Zn(II)Por dimers presenting, at a *meso* position of each of the two Por macrocycles, a 3-pyridyl (**142**),²¹⁶ a (5-azaindol-2-yl) (**143**),²¹⁷ or a cinchomeronimide (**144**)²¹⁸ unit. Interestingly, the self-sorting process of Por dimer **144** led to the formation of supramolecular cages of different sizes such as trimers, tetramers and pentamers. This structural variety arises from the different relative arrangements that the two 3-pyridyl fragments in **144** can adopt, which ultimately control the size of the resulting aggregates.

More recently, Tsuda, Kim and coworkers documented the self-aggregation ability of *meso–meso* linked Zn(II)Por dimers **145** presenting a mono- or a di-butadiyne linker as a bridging unit between the two Por macrocycles.²¹⁹ Different from *meso–meso* linked Zn(Por) dimers **141–144**, Por dimers **145** present free rotation around the linear linkers thus giving rise to two possible self-assembled Por boxes resulting from the assembly of orthogonal, similar to Por boxes in Fig. 33b, or planar Por–Por conformers. In such supramolecular constructs, the different lengths of the linkers and the dihedral angle between the Por moieties (90° in the case of orthogonal conformers and 0° in the case of planar conformers) significantly influence the π-conjugation between Por units and strongly affect the photochemical properties of these ensembles – *vide infra*.

Beside Por-based supramolecular boxes, supramolecular prism-shaped assemblies have also been obtained *via* coordinative self-assembly of two 1,3,5 triethynylpyridyl-substituted benzene (L)

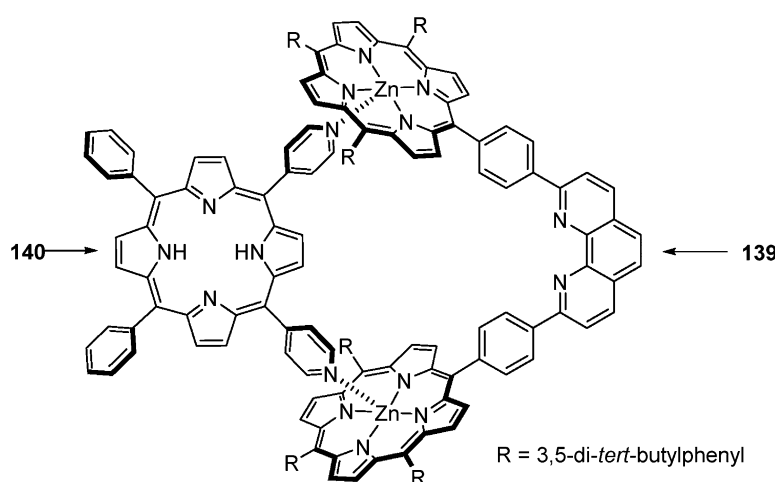


Fig. 32 Molecular structure of the supramolecular assembly **139–140** resulting from the complexation of *meso*-5,10-bis(4-pyridyl)-15,20-diphenyl H₂Por **140** to Zn(II)Por dimer **139**.

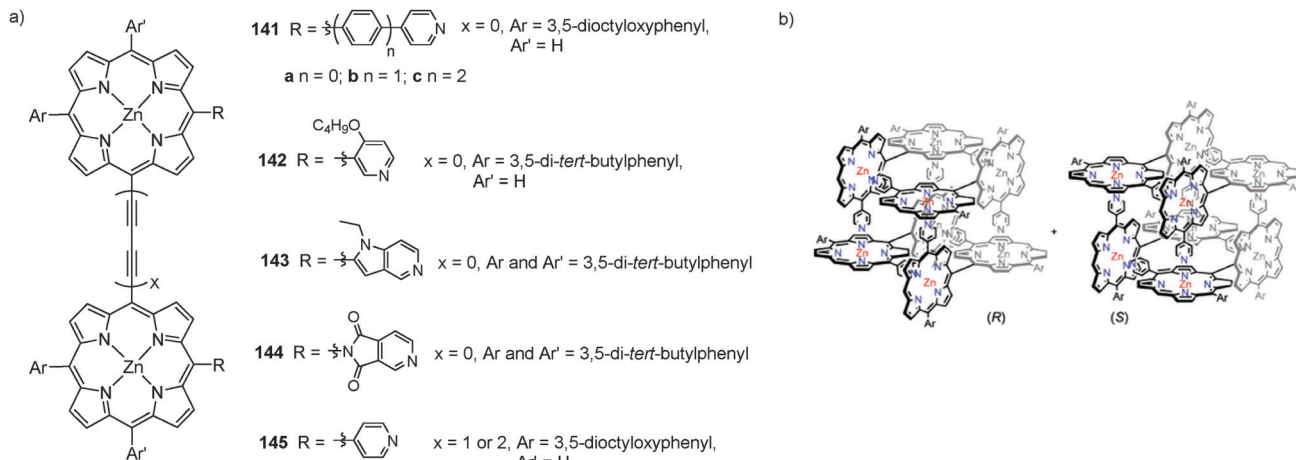


Fig. 33 Molecular structures of (a) *meso*-*meso* linked Zn(II)Por dimers 141–145 bearing two, *meso*-substituted pyridyl fragments and (b) (R) and (S) enantiomeric boxes resulting from the homochiral self-sorting of Por dimer 141a.

molecules and three Zn(II)Por (D) dimers.²²⁰ These supramolecular complexes have been structurally characterized by different techniques suggesting a L₂:D₃ stoichiometry of the assembly.

Although Zn(II)Pors and nitrogenated ligands are by far the more frequently used building blocks for the preparation of self-assembled Por dimers by metal-ligand interactions, metalloPors different from zinc and/or no-nitrogenated ligands have also been explored for this scope.

In 2007, Matano and coworkers reported the synthesis and self-aggregation properties of *meso*-phosphoryl-substituted Zn(II)Pors 146 and 147.²²¹ Pors 146 and 147, which have been prepared by copper-catalyzed, carbon-phosphorus cross-coupling reactions, have been found to undergo self-organization through oxo-zinc coordination leading to cofacial Por dimers (146)₂ and (147)₂ (or oligomers) (Fig. 34a). In both types of aggregates, the σ⁴-phosphorus center with a polarized Por-oxo bond defines the orientation and distances of the Por chromophores. Structural proofs of the formation of cofacial, partially overlapped Zn(II)Por dimers was obtained by variable-temperature NMR studies (¹H and ³¹P) and single crystal X-ray determination, whereas absorption and fluorescence studies allowed us to

determine the *K*_{ass} of supramolecular dimers (146)₂ and (147)₂ that was found to be $1.4 \times 10^4 \text{ M}^{-1}$ and $5.9 \times 10^6 \text{ M}^{-1}$ in toluene, respectively. These findings demonstrate the potential utility of phosphoryl groups as peripheral coordinating ligands for the formation of Por-based supramolecules.

Co(II)Por dimer (148)₂ with a ‘picket fence’ structure has been prepared from a mono(Im)-substituted Co(II)Por 148 via nitrogen–cobalt, metal-ligand interactions (Fig. 34b).²²² UV-vis, resonance Raman and ESR spectral measurements showed that the supramolecular dimer (148)₂ is able to bind to two dioxygen molecules reversibly, with an affinity that resulted to be lower than that of the corresponding monomer, probably due to steric hindrance and the orientational effect of the axial ligand.

4.4 Binuclear porphyrins connected to other electroactive moieties

Conjugates based on Por dimers acting as electron donors and an acceptor moiety, are an interesting class of D–A systems. In such ensembles, the presence of the two chromophores doubles the light-harvesting capability. This is especially important for photonic applications, since upon photoexcitation,

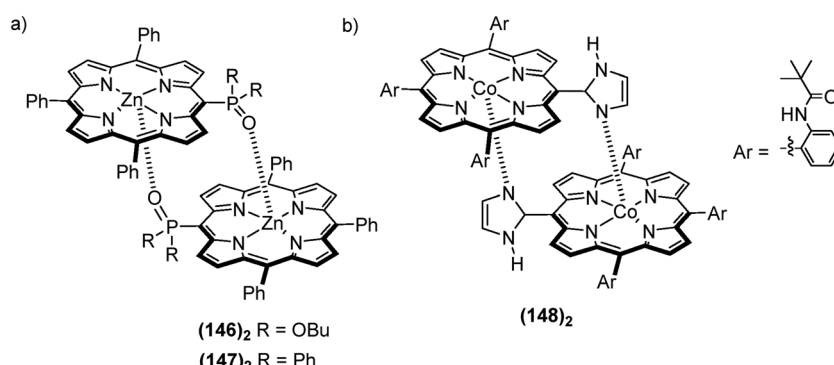


Fig. 34 Formation of cofacial Por dimers (a) (146)₂ and (147)₂ and (b) (148)₂ resulting from the self-assembly of *meso*-phosphoryl-substituted Zn(II)Por dyads 146 and 147, and *meso*-Im-substituted Co(II)Por 148, respectively.

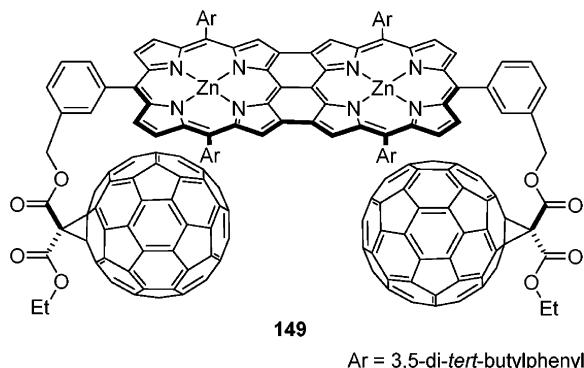


Fig. 35 Molecular structure of conjugate **149** constituted by two C_{60} units covalently attached to a triply-fused Zn(II)Por dimer.

both electron-donor moieties can donate to the fullerene moiety, thus helping to ensure a high quantum yield of CS even though the driving force for electron transfer is relatively small (*vide infra*).

In 2007, the groups of Diederich, Echegoyen and Armaroli reported a D-A conjugate (**149**) constituted by two C_{60} units covalently attached and spatially close to a triply-fused Por dimer (Fig. 35).^{223,224} The synthesis of **149** involved the preparation of a *meso*-*meso* linked Zn(II)Por dimer, which was then converted into its fused analog by oxidative ring closure using DDQ and $Sc(OTf)_3$. The latter triply-fused Por dimer was then functionalized with two malonate units and the resulting product subjected to a Bingel-Hirsch, cyclopropanation reaction with C_{60} furnishing the target conjugate **149**. Interestingly, a detailed electrochemical study of **149** showed that this D-A ensemble is capable of undergoing nine reversible redox processes involving a total of fifteen electrons. Moreover, photophysical investigations demonstrate that **149** does not exhibit any classical behavior documented for numerous Por-fullerene dyads (*vide infra*).

The 1,3 dipolar cycloaddition reaction between azomethine ylides and fullerenes, also known as the Prato reaction and one of the most widely used synthetic methods of fullerene functionalization,²²⁵ has also been used to prepare covalently-linked, Por_2-C_{60} trimers such as **150** (ref. 226) or **151** (ref. 227) (Fig. 36). Whereas compound **150** was prepared by a single Prato reaction between a C_{60} molecule and a Por dimer bearing an aldehyde moiety on the Por-Por bridging unit, in the case of trimer **151** a double 1,3 dipolar cycloaddition reaction between C_{60} and a gable-type Por dimer having two aldehyde units was carried out, resulting in a product with C_2 symmetry and a *trans*-2 substitution pattern at the fullerene sphere.

Moreover, both systems present a conformationally-constrained geometry, strongly pronounced in the case of trimer **151**, in which the Pors and fullerene are joined in a cyclic arrangement, that in principle, further constrains the relative motion of these two moieties by limiting rotations around bonds.

Very recently, a covalently-linked, multifullerene Ni(II)Por dimer (**152**) has been prepared in a so-called “molecular LEGO” approach using a synthetic route involving a short sequence of [4+2]-cycloaddition and cheletropic SO_2 -extrusion reactions (Fig. 37).²²⁸ This hexafullereno-diPor conjugate, which represents the first example of a transition metal complex of a regularly structured multi-modular molecular assembly of two Pors and six fullerenes, can be considered as a reversibly chargeable reservoir of a large number of electrons.

Covalent Por dimer conjugates connected to two distinct electroactive units have also been prepared such as covalent, D-A system **153a** reported in 2007 by the groups of Anderson and Albinsson (Fig. 38).²²⁹ Compound **153a**, constituted by a butadiyne-linked, Zn(II)Por dimer which is covalently connected at its ends to Fc and C_{60} moieties, has been used to test the influence of conformational heterogeneity on the electron transfer dynamics. It was found that when dimer **153a** was forced to adopt a planar conformation (N.B. in the uncomplexed form, **153a** can

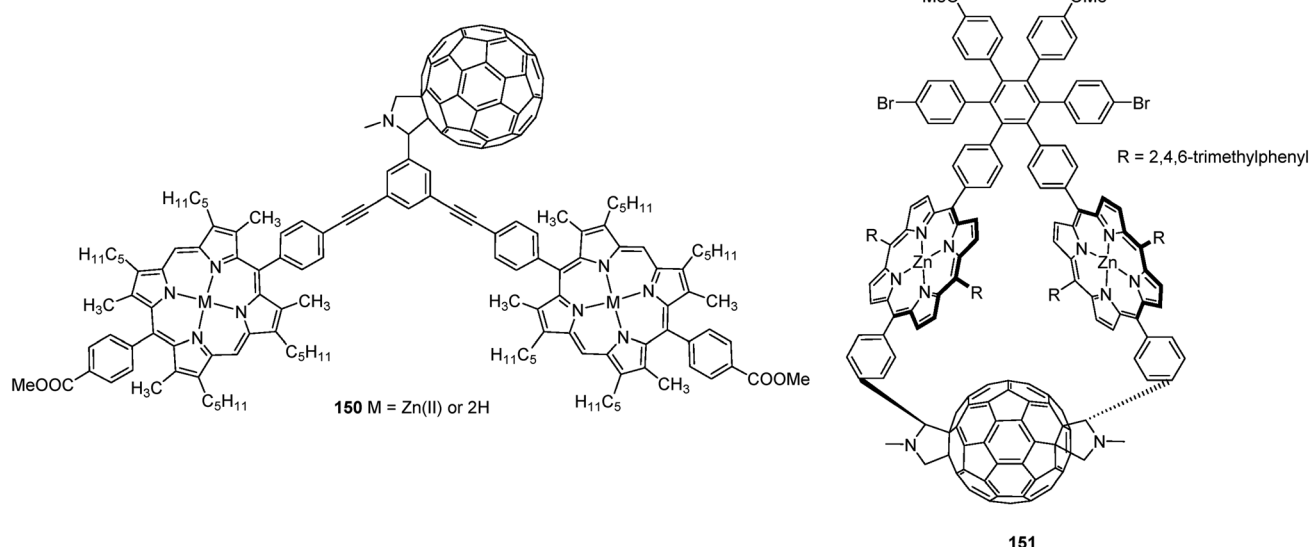


Fig. 36 Molecular structures of covalent, Por_2-C_{60} trimers **150** and **151**.

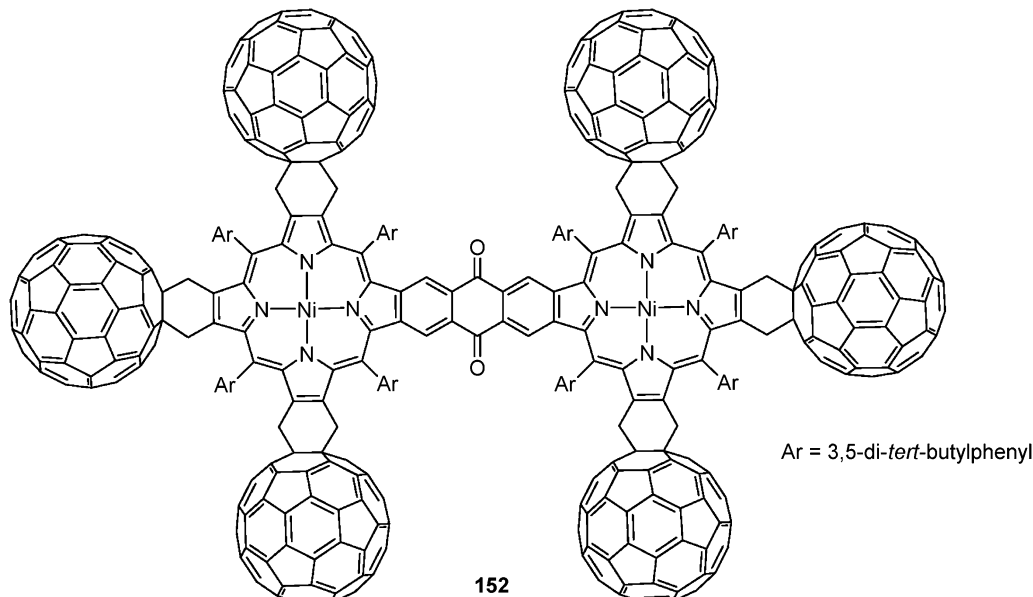


Fig. 37 Molecular structures of covalently-linked, hexafullereno-diPor conjugate 152.

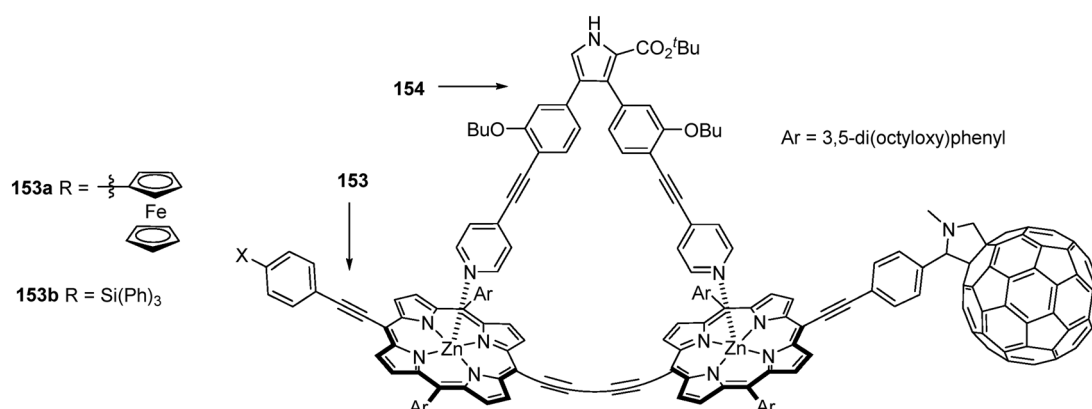


Fig. 38 Molecular structures of the supramolecular complex resulting from the coordination of bidentate ligand 154 to $\text{Zn}(\text{II})\text{Por}_2\text{-C}_60$ derivatives 153a,b.

adopt both a planar and a perpendicular conformation) by means of axial coordination of bidentate dipyridyl ligand 154, important changes in the CR rate were observed with respect to the unconstrained system 153a (*vide infra*). This study clearly evidenced the possibility of modulating some of the physical properties of a D-A system by controlling its conformational freedom, in this case by using reversible, supramolecular interactions.

In 2006, Kobuke and coworkers reported some supramolecular (155–157) and covalent, D-A Por dimers functionalized with Fc and/or C_{60} electroactive units (Fig. 39). Similarly to several Por dimer complexes mentioned above, zinc–nitrogen interactions between mono-Im-substituted $\text{Zn}(\text{n})\text{Pors}$ have been used for the preparation of supramolecular Por dimers 155–157 in which the two Pors adopt a slipped-cofacial arrangement.²³⁰

Whereas homodimers 155 and 156 could be easily obtained by self-assembly of $\text{Zn}(\text{n})\text{Por}$ dimers bearing an Fc or a C_{60} moiety, respectively, heterodimer 157 was prepared by using a

reorganization procedure. This consisted of dissolving equivalent amounts of homodimers 155 and 156 in pyridine in order to dissociate them into the respective monomeric species. The pyridine solvent was then evaporated obtaining, along with compounds 155 and 156, heterodimer 157, containing Fc as an electron donor and C_{60} as an electron acceptor. Supramolecular dimers 155–157 were then covalently fixed by using ring-closing metathesis reaction between the allyloxycarbonylethyl substituents appended at two of the Por *meso* positions, and the covalently linked, homo- and heterodimers separated by GPC. Whereas UV-vis investigation of the covalently-linked analog of heterodimer 157 in benzonitrile indicated no significant electronic interaction among the three chromophores (Por dimer, C_{60} and Fc) in the ground state, efficient and electronic communication was suggested in the excited state – *vide infra*.

In the same year, a series of supramolecular, Fc- and nonamethyl Fc-functionalized Por homodimers were prepared using the

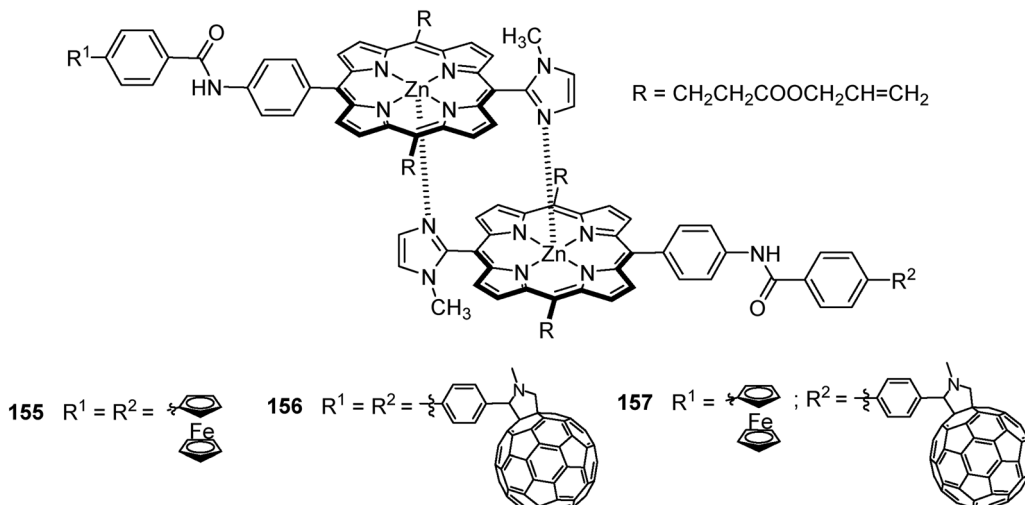


Fig. 39 Molecular structures of slipped-cofacial Zn(II)Por dimers bearing two Fc (155), two C₆₀ (156), and one Fc and one C₆₀ (157) moieties.

same Im-to-zinc complementary coordination strategy used for the preparation of compounds 155 and 156.²³¹ Structural variations in the bridging units connecting the peripheral Fc derivatives to the Por macrocycles (single bond, phenylene-ethynylene or phenylene-ethylene spacers) were also realized. In such systems, the interaction between the two ferrocenyl units across the coordination dimer proved to be weak and a single oxidation wave was observed in CV and differential pulse voltammetry.

Recently, a cyanine-like, squaraine moiety has also been used by Webster and coworkers both as an electroactive moiety and a bridging unit between two Por macrocycles.²³² The linear and NLO properties of this highly π -conjugated, Zn(II)Por dimer have been investigated showing increased 2PA cross section values across an unprecedented long wavelength range covering most of the near-infrared and considerably higher than its separate Por and squaraine constituents.

Besides C₆₀, Fc and squaraine, SWCNTs²³³ or carbon nanohorns (CNHs)²³⁴ have also been used as molecular platforms for the covalent grafting of free-base Por dimers. In the case of the SWCNT-based hybrid material, its synthesis involved the preparation of an amino Por dimer, which was then transformed *in situ* into the reactive diazonium species and finally reacted with octadecylamine-modified SWCNTs. On the other hand, a condensation reaction between a monocarboxylic acid-substituted H₂Por dimer and amino-functionalized CNHs has been used in order to prepare the CNH-based material. Both hybrid materials, which were found to be soluble or dispersible in several organic solvents, were fully characterized by using diverse techniques such as UV-vis and Raman spectroscopies, thermogravimetric analysis, and TEM.

The photovoltaic properties of D-A conjugates constituted by Por dimers covalently connected to C₆₀ or Fc derivatives have also been investigated.

In this context, in 2013 the groups of Matsuo and Nakamura reported a Mg(II)Por₂-C₆₀ covalent triad which was axially coordinated to an Im-substituted carboxylic acid (ICA), and in

turn layered on an ITO surface.²³⁵ A study of the photovoltaic properties of the resulting Mg(II)Por₂-C₆₀/ICA/ITO ensemble showed a quantum yield of the photocurrent conversion of 7.8%, ten times higher than the one of a device fabricated using an analogous Zn(II)Por₂-C₆₀ triad. In general, Mg(II)Pors have an important disadvantage, that is, a considerable instability due to their high-lying HOMO levels, which render them easily oxidized by singlet oxygen. However, in this case, the possibility of a rapid quenching of the photoexcited Mg(II)Por via electron transfer to the covalently-linked C₆₀ moiety, followed by fast electron injection from the fullerene onto the ITO semiconductor, considerably increase the stability of such a Mg(II)Por-based material, thus leading to efficient photon-to-electron conversion.

Supramolecular interactions have also been widely used in order to prepare D-A complexes based on covalent Por dimers and fullerenes, mainly C₆₀. In this context, two main strategies have been used in order to prepare such assemblies, that is, the covalent functionalization of the fullerene sphere with one or more ligands able to axially coordinate to one or both Por metal centers, or the use of dispersion forces such as π - π and van der Waals between unsubstituted fullerenes and Por dimers presenting well-defined geometrical features.

In 2009, the groups of Ana and Thomas Moore and Devens Gust employed a “two-point binding” strategy based on the zinc-nitrogen axial coordination in order to complex a dipyridyl-substituted C₆₀ derivative to a hexaphenylbenzene unit substituted with two bis(phenylethynyl)anthracene moieties absorbing light in the 400–500 nm range, two boron-dipyrromethene (BODIPY) entities, which absorb in the 450–550 and 330–430 nm range, and two Zn(II)Por macrocycles. The resulting multichromic, D-A system was able to harvest light from the ultraviolet throughout the visible region up to 650 nm.²³⁶

Using the same ‘two-point’ coordinate bonding between a dipyridyl-substituted C₆₀ and a Zn(II)Por dimer, a simpler Por₂-C₆₀ supramolecular system has been prepared and its photophysical properties investigated.²³⁷

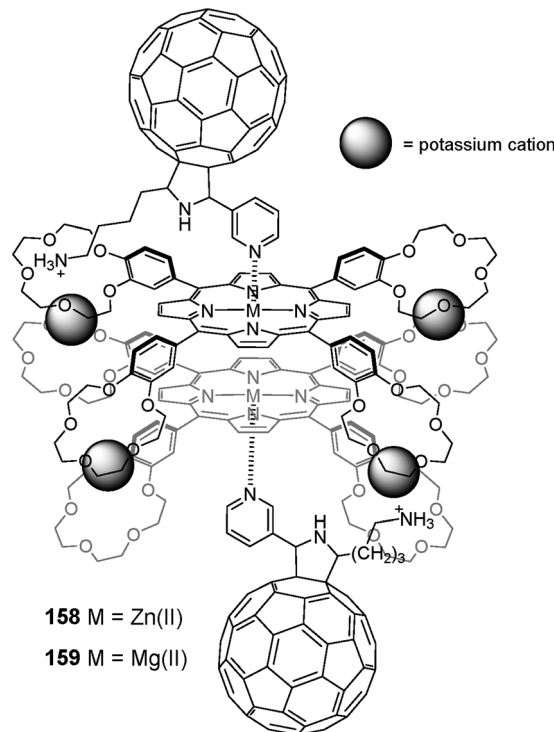


Fig. 40 Molecular structures of supramolecular ensembles Zn(II)Por₂-(C₆₀)₂ **158** and Mg(II)Por₂-(C₆₀)₂ **159**.

Structurally interesting, multicomponent supramolecular ensembles resulting from the complexation of two fullerene derivatives functionalized with both a pyridine and a terminal ammonium moiety to two crown ether-containing Zn(II)Pors (**158**)²³⁸ or Mg(II)Pors (**159**)²³⁹ have also been reported by the groups of D'Souza and Ito (Fig. 40). Supramolecular complexes **158** and **159** are held together by a combination of metal–ligand interactions between the pyridine group on the fullerene derivative and the Por metal central atom and cation–crown ether interactions between the four crown ether substituents on the

two Por rings and four potassium ions, leading to the formation of a cofacial Por–Por dimer. A further contribution to the stability of the complex is obtained *via* the interaction of the terminal alkylammonium moieties present on the fullerene derivatives to one of the crown ether macrocycles. Importantly, this latter complexation occurs without destroying the 4 K⁺/Por–Por stacked dimer. Both supramolecular ensembles **158** and **159** exhibited enhanced electron transfer properties with an important stabilization of the charge-separated state as a consequence of the cofacial, stacked arrangement adopted by the two Por macrocycles, as observed in Pc–Pc analog **36** (Fig. 7) (*vide infra*).⁹³ Within this strategy, perhaps the most popular design has been the covalent linkage of two Por macrocycles by rigid or semi-rigid spacers to form what are often termed as molecular “tweezers”.²⁴⁰ Such tweezer-like receptors possess an open structure, which is sufficiently flexible to adapt to the fullerene guest.

In 2000, the first report by Boyd and Reed *et al.* on the use of jaw-like, fullerene receptors based on Por dimers appeared.²⁴¹

Few years later, Aida and coworkers reported the first example of “supramolecular peapods” composed of linear, Zn(II)Por supramolecular nanotubes encapsulating fullerenes such as C₆₀ and C₇₀.²⁴² The formation of such nanotubes, whose structural features were determined by using several spectroscopic (UV-vis, ¹H NMR and IR) and microscopic (TEM) techniques, results from the self-aggregation of compound **160** composed of an acyclic Zn(II)Por dimer having six carboxylic acid functionalities and two large [4th generation]-poly-(benzyl ether) dendritic wedges, which are intended to increase the solubility of the carboxylic acid-appended metalloPor (Fig. 41a). A combination of intermolecular, hydrogen bonding interactions between the carboxylic acid groups of adjacent molecules, as well as π–π stacking interactions between fullerene and the two Por units of each tweezers, is responsible for the formation of these discrete, supramolecular architectures presenting a high aspect ratio and good thermal stability.

Zn(II)Por dimers **161** (ref. 243) and **162** (ref. 244) constitute two recent examples of molecular tweezers based on Por dimers

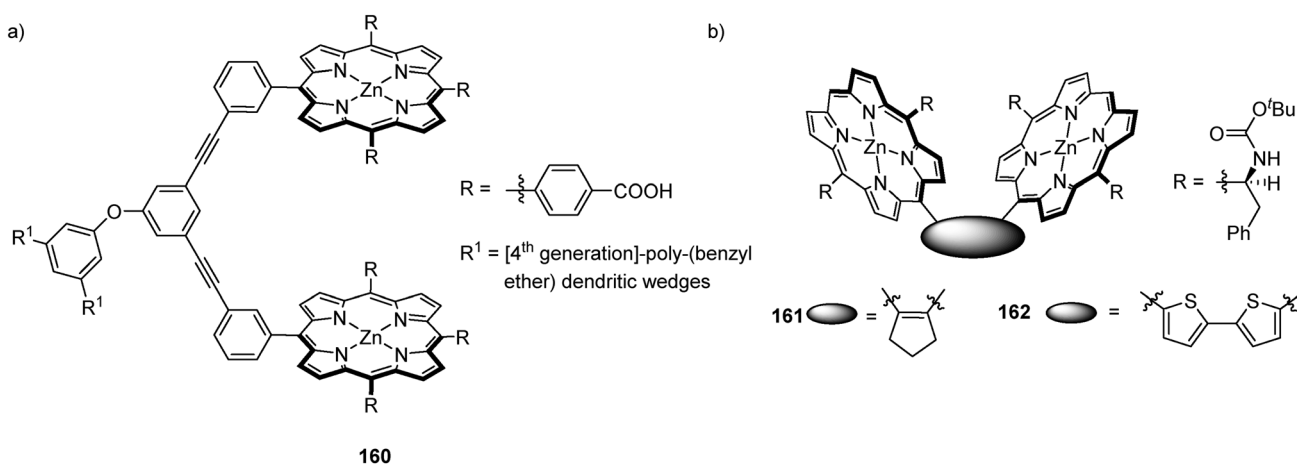


Fig. 41 Molecular structures of acyclic Zn(II)Por dimer tweezers (a) **160** and (b) **161** and **162**. For these latter compounds, only the (S) enantiomers have been represented.

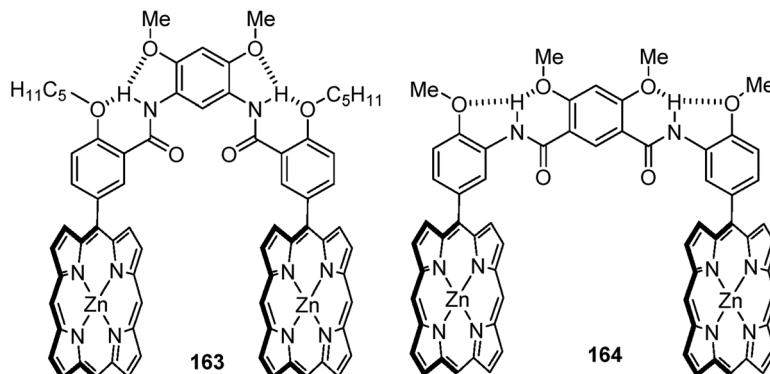


Fig. 42 Molecular structures of tweezer-like Por dimer receptors **163** and **164**.

able to bind C_{60} and C_{70} in solution (Fig. 41b). These two systems, which present either a cyclopentenyl (**161**) or a bisthiophenyl (**162**) bridging unit, possess different bite angles, which result in different fullerene binding abilities. As a consequence, receptor **161** is able to discriminate among C_{60} and C_{70} in solution ($K_{\text{ass}} C_{70}/K_{\text{ass}} C_{60} = 6.53$), while **162** is unable to produce even a moderate value of selectivity ($K_{\text{ass}} C_{70}/K_{\text{ass}} C_{60} = 2.0$).

Hydrogen bonding interactions have also been used by the group of Li in order to introduce a higher degree of preorganization into the tweezer-like design of Por dimers **163** and **164** (Fig. 42).²⁴⁵ In **163** and **164**, intramolecular hydrogen bonding interactions result in a *syn* conformation of both Por units, thus enhancing the ability of this receptor to associate fullerenes. UV-vis titrations allowed determining the K_{ass} of **163** and **164** towards C_{60} , which resulted to be, in toluene at room temperature, 1.0×10^5 and $2.7 \times 10^4 \text{ M}^{-1}$, respectively. A one order of magnitude increase in the K_{ass} was observed when

titrating **163** and **164** with C_{70} . The stronger fullerene binding ability of receptor **163** with respect to **164** clearly evidences that even small structural changes in the receptor binding pocket, such as the modification in connectivity of the amide groups between **163** and **164**, can result in important changes in the receptor binding constants.

Calix[4]arenes have also been used by the groups of Reed, Boyd and Armaroli as spacer units in Por dimer-based fullerene receptors. These tweezers have shown efficient binding for C_{60} and C_{70} with K_{ass} , for the most effective receptor, of 2.5×10^5 (for C_{60}) and $2.5 \times 10^6 \text{ M}^{-1}$ (for C_{70}) in toluene at room temperature.²⁴⁶

In 2008, the group of Morin described an interesting example of Por dimer tweezers (**165**), in which the two Por macrocycles were not covalently but mechanically linked, making use of a [3]rotaxane architecture (Fig. 43).²⁴⁷ In **165**, the extremely high conformational flexibility provided by the mechanical bond as

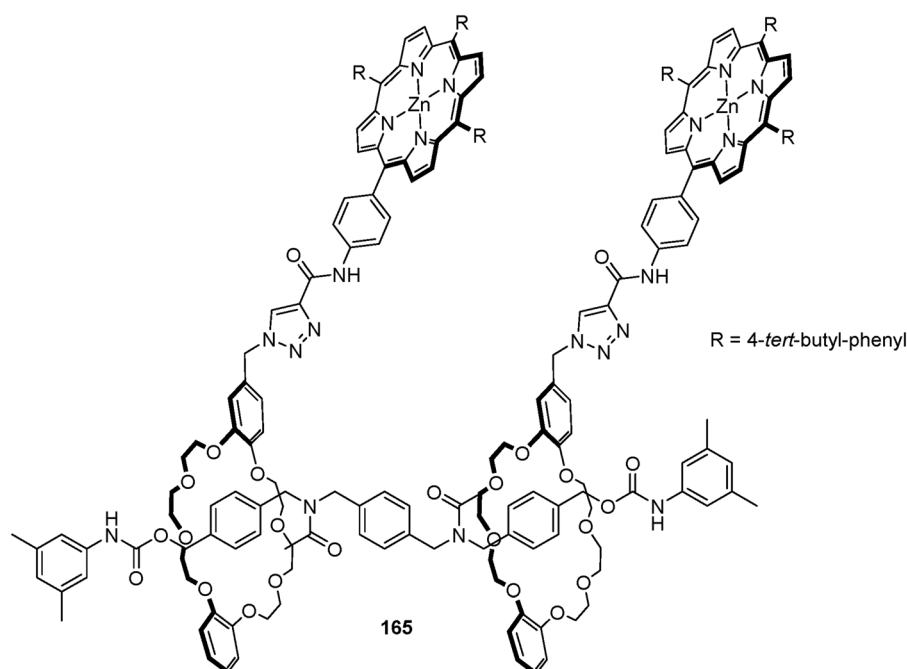


Fig. 43 Molecular structure of Zn(II)Por dimer receptor **165** based on a [3]rotaxane architecture.

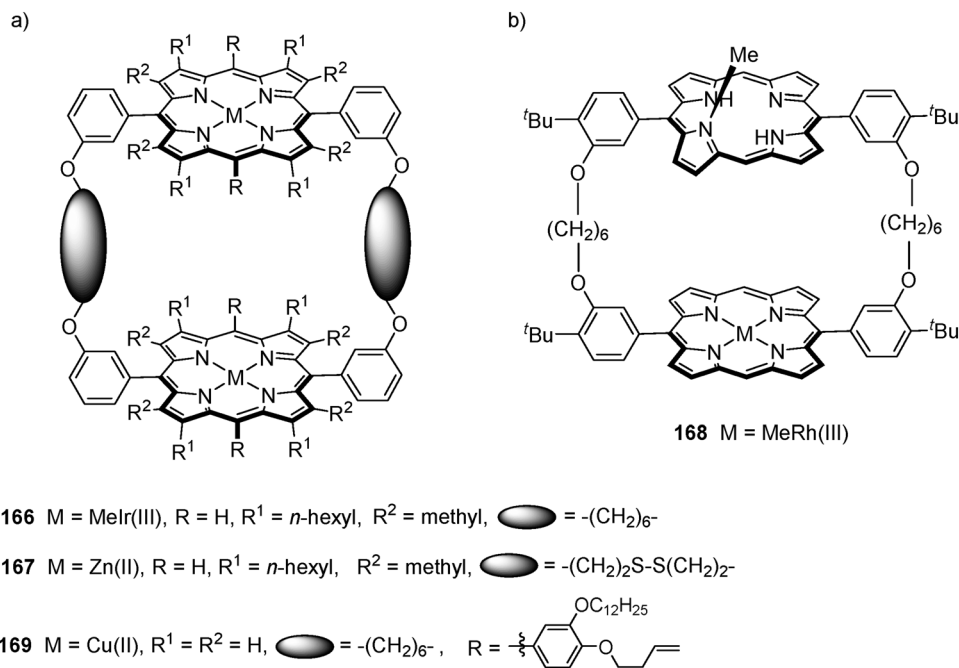


Fig. 44 Molecular structures of cyclic Por dimer receptors **166–169**. In the case of Por dimer **168** only one enantiomer has been represented.

compared to the “classical” covalent bond where rigid and covalent spacers are employed, resulted in a significant decrease in the C₆₀ *K*_{ass} (5×10^3 M⁻¹ in toluene at room temperature). However, this example illustrates that “unconventional” spacers can also be used for the preparation of molecular tweezers.

Although Por-based tweezers have shown to effectively complex fullerenes in solution, to date, some of the most efficient Por dimer-based hosts for fullerenes feature macrocyclic architectures. The extraordinary binding ability of such cyclic receptors, which are often more demanding from the synthetic point of view than their acyclic counterparts, is the result of a high degree of preorganization coupled to a good complementarity in size and shape between the host cavity and the fullerene guest, thus maximizing the host–guest interactions.

In 1999, Aida, Saigo and coworkers synthesized a cyclic Zn(II)Por dimer, which resulted to be the best C₆₀ receptor described at that time, with a *K*_{ass} of 6.3×10^5 M⁻¹ in benzene at room temperature. Since that report, a large variety of cyclic metalloPor receptors have been prepared and studied, most of them reviewed in a comprehensive account published in 2007.²⁴⁸ In light of this, in the following part we will mainly focus on some of the most recent examples.

In 2007, Tashiro, Aida and coworkers reported a cyclic MeIr(III)Por dimer (**166**) able to effectively complex C₆₀ with a *K*_{ass} of 1.3×10^8 M⁻¹ in *o*-DCB at room temperature, which still constitutes the highest stability constant value for a C₆₀–guest complex, and which exceeds by more than 3 orders of magnitudes the one obtained for a MeRh(III)Por analog of **166** (Fig. 44a).²⁴⁹ Single crystal X-ray diffraction studies showed that MeIr(III)Por dimer **166** binds in a η^2 fashion to a 6:6 C–C bond of C₆₀, a process that has also been observed in solution by ¹³C NMR studies at low temperatures. Such a combination of host–guest

size complementarity and dynamic, chemical entrapment of the fullerene by the reactive cage are probably responsible for the high *K*_{ass}.

The preparation of optimal Por dimer-based macrocycles for fullerene recognition has also been tackled by Sanders and coworkers using a different synthetic perspective, that is, using dynamic combinatorial chemistry.²⁵⁰ In this context, the authors prepared a mononuclear Zn(II)Por dithiol derivative that could be efficiently dimerized in the presence of a bipyridine or a 1,4-diazabicyclo[2.2.2]octane template to afford the cyclic Zn(II)Por dimer **167** (Fig. 44a).²⁵¹ Receptor **167** was able to effectively complex C₆₀, both in solution and in the solid state as demonstrated by ¹H NMR and X-ray crystal determination (Fig. 45). However, this spherical guest could not be used to template the formation of **167**, since reactive R-S[•] thiy radical species are generated during the receptor synthesis, which are incompatible with the presence of radical scavengers such as fullerenes.

More recently, a fullerene templating approach has successfully been employed for the preparation of Por-based cyclic receptors.²⁵² In this case, the fullerene guest preorganizes the Por monomers before the metathesis cyclization reaction and, thus, displaces the equilibrium toward the best fullerene host, which in this case resulted to be the Por trimer species.

Enantioselective recognition of chiral fullerenes has also been exploited by using cyclic and chiral Por dimer receptors. In this context, a chiral receptor (**168**, Fig. 44b) has been prepared by Tashiro, Aida and co-workers, which features a C₁-symmetric N-methylPor unit as an asymmetrically distorted π -electronic component. Host **168** was able not only to strongly bind to the smallest chiral fullerene, C₇₆ (*K*_{ass} = 1.5×10^7 M⁻¹), but also to discriminate between the two fullerene enantiomers of a racemic mixture as demonstrated by ¹H NMR studies.²⁵³

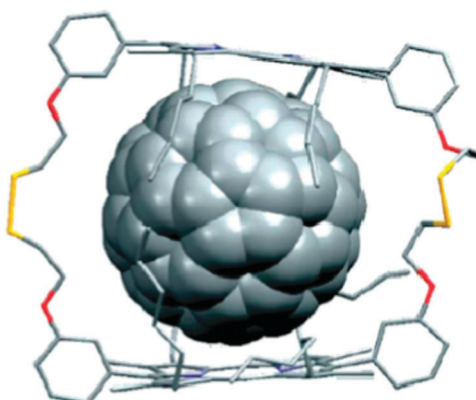


Fig. 45 X-ray crystal structure of the inclusion complex between Por dimer receptor **167** and C₆₀ (hydrogen atoms omitted for clarity). Reprinted from ref. 251. Copyright 2005 Royal Society of Chemistry.

Although strongly interacting with C₇₆, chiral compound **168** did not show any enantioselectivity, making it a good receptor for quantifying the enantiomeric excess in chiral fullerene mixtures, where the binding constants of the host for both enantiomers are identical.

More recently, the same group reported a second generation of chiral Por dimer hosts structurally similar to **168**, in which the alkylated Por macrocycle has strongly been distorted with the aim of increasing the discrimination ability of the resulting chiral guest for an enantiomeric mixture of C₇₆.²⁵⁴ This hypothesis was confirmed in the single enantioselective extraction of a racemic mixture of C₇₆ by one of these distorted Por dimers obtaining a 7% enantiomeric excess.

Very recently, endohedral fullerenes have also been used as guest molecules for cyclic Por dimer hosts. In 2011, Aida, Kato and coworkers have reported the complexation of an endohedral metallofullerene by a cyclic Cu(II)Por dimer (**169**).²⁵⁵

The host **169** complexes the paramagnetic La@C₈₂ in its cavity to form an inclusion complex which is the first ferromagnetically-coupled inclusion complex featuring paramagnetic La@C₈₂. This latter complex is transformed into a caged complex by ring-closing olefin metathesis of its side-chain olefinic termini, thus mechanically trapping the endohedral metallofullerene. Interestingly, this closure is accompanied by a change in the nature of the cage to ferromagnetic, thus opening the interesting possibility of modifying the mode of coupling between metal spins by changes in the cluster geometry.

In a more recent report, the groups of Tani and Fukuzumi investigated the electrochemical and photophysical properties of the supramolecular complexes resulting from the complexation of cyclic, free-base (**170**) and Ni(II)Por (**171**) dimers to another endohedral fullerene, that is, a lithium ion encapsulated C₆₀ molecule (Li⁺@C₆₀) with a *K*_{ass} of the order of 10⁵ M⁻¹ in benzonitrile (Fig. 46a).²⁵⁶

A few years earlier, the group of Tani, independently, published an interesting work describing, besides the expected C₆₀ inclusion property of Por dimers **170** and **171**, the ability of these systems to self-aggregate giving rise to the formation of supramolecular nanotubes.²⁵⁷ The presence of two pyridyl moieties on each Por macrocycle was crucial for the formation of these 1-D nanostructures through a combination of hydrogen bonding interactions between the pyrrole β-hydrogens and the pyridyl nitrogens and π–π interactions between adjacent pyridyl rings (Fig. 46b). In the case of Por dimer **171**, this arrangement is also maintained when C₆₀ is cocrystallized with the host, as clearly demonstrated by single crystal X-ray studies. Conductivity studies carried out on such supramolecular “peapods” revealed high and anisotropic conductivity ($\sigma = 0.72 \text{ cm}^2 \text{ V}^{-1} \text{ s}^{-1}$) along the nanotube axis as a result of the 1-D fullerene supramolecular organization.²⁵⁸

Surprisingly, a very different organization resulted from the cocrystallization of C₆₀ and Por dimer **170**.²⁵⁹ In this case, the

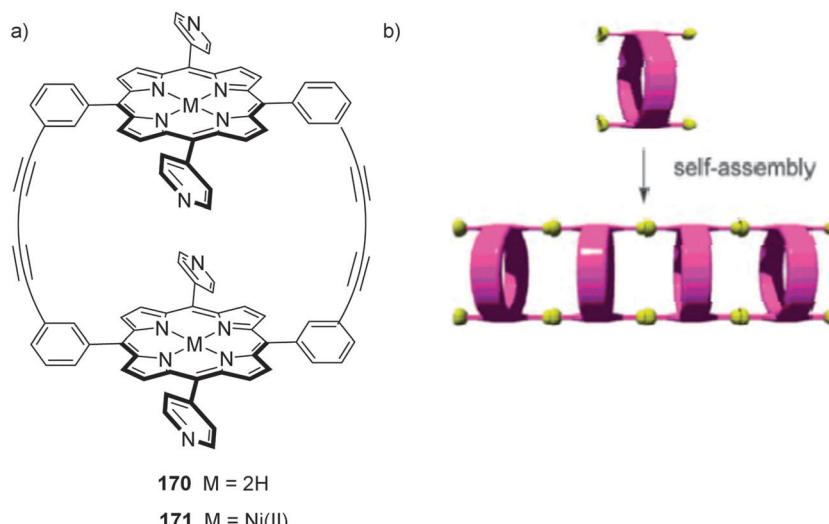


Fig. 46 (a) Molecular structures of cyclic Por dimers **170** and **171**. (b) Schematic representation of the strategy for the formation of a tubular assembly with cyclic Por dimers **170** and **171**. Reprinted from ref. 257. Copyright 2007 Wiley-VCH.

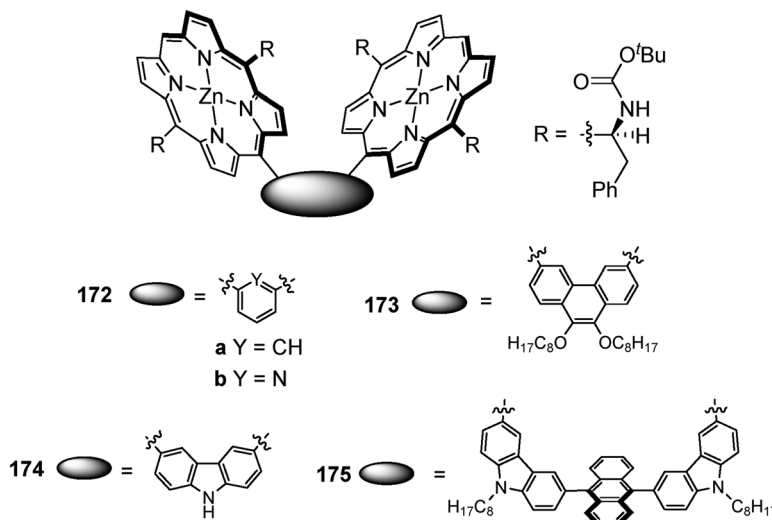


Fig. 47 Molecular structures of Zn(II)Por dimer nanotweezers **172–174** and nanocaliper **175**. For these compounds, only the (S) enantiomers have been represented.

formation of supramolecular nanotubes was no longer observed in the solid state, replaced by a zig-zag organization of the fullerenes. This structural modification was accompanied by a decrease in conductivity ($\sigma = 0.13\text{--}0.16 \text{ cm}^2 \text{ V}^{-1} \text{ s}^{-1}$) and a lower anisotropy. In the same work, the photovoltaic properties of both C₆₀·**170** and C₆₀·**171** were evaluated by constructing photoelectrochemical cells, which showed an IPCE value of 17% and a power conversion efficiency (η) of 0.33%. More recently, the formation of inclusion complexes between [6,6]-phenyl-C₆₁-butyric acid methyl ester and cyclic Por dimers **170** and **171** was also achieved as revealed by solution and X-ray crystal investigation.²⁶⁰

Similar to fullerenes, SWCNTs have also been complexed *via* supramolecular interactions by using covalently linked, Por dimers as demonstrated by Komatsu and coworkers in a series of seminal papers. These authors prepared a family of chiral, gable-type, Por dimer nanotweezers, having *m*-phenylene (**172a**),²⁶¹ 2,6-pyridylene (**172b**),^{262,263} 3,6-phenanthrene (**173**),²⁶⁴ and 3,6-carbazoleylene (**174**)²⁶⁵ as bridging units, which were able to discriminate diameter and/or (*n,m*)²⁶⁶ of SWCNTs according to the size and shape of the cleft made by two Pors and a spacer in between (Fig. 47). The use of chiral units on the Por macrocycles also resulted in different binding affinities of the nanotweezers to the left- and right-handed helical SWCNT isomers thus forming complexes with different stabilities that could be readily separated. Finally, optically enriched SWCNTs were obtained by uncomplexing the “gable-type” Por dimers. For such systems, it was rationalized that the nanotweezers with smaller bite angles accepted smaller diameter SWCNTs (<1.0 nm) deeper in the cleft, enabling precise differentiation of the nanotube diameter. However, an important limitation in selectivity was found by using such nanotweezers when trying to sort SWCNTs with larger diameters. In fact, a larger dihedral angle, or shallow cavity, needed to complex SWCNTs with large diameters, is accompanied by a decrease in the selectivity toward the SWCNT diameter. These studies suggested that nanotweezers with a longer spacer and narrower angle

exhibited better (*n,m*) selectivity than those with the shorter spacer and wider angle.²⁶⁷ Based on this theory and with the aim of complexing SWCNTs with diameters larger than 1.0 nm, Komatsu and co-workers, very recently, designed an “evolved” version of the Por dimer nanotweezers, called “nanocaliper” (**175**) (Fig. 47), which was able to recognize the diameter, handedness, and metallicity of SWCNTs simultaneously.²⁶⁸ The main features of the newly designed host receptor are a long spacer with more than 1.4 nm consisting of three aromatic moieties, with a nearly parallel orientation of the two Por units; restricted conformation by biaryl linkages of the Por–carbazole and carbazole–anthracene; strong interaction of two Pors and anthracene with the surface of a SWCNT through π – π stacking interactions; and, similar to the previous systems, stereogenic centers at the periphery of the Por units discriminating the helicity of SWCNTs. Nanocaliper **175** allowed us to obtain optically-active SWCNTs with >1.0 nm in diameter and, unexpectedly, to enrich metallic SWCNTs. The optically active metallic SWCNTs are identified for the first time, in addition to the optically active semiconducting SWCNTs with such large diameters.

5. Photophysics of homo- and heterobinuclear ensembles of phthalocyanines and porphyrins

The development of electron D–A models, which are able to mimic photosynthetic processes such as light harvesting, unidirectional energy transfer, charge transfer, and charge shift, is of great interest. In this context, the preparation of homo- and heterobinuclear systems based on Pcs and Pors is very appealing due to the excellent light-harvesting features of these ensembles. Implementation of electroactive units to these conjugates leads to D–A systems with improved energy/charge transfer abilities. A photophysical analysis of some representative examples compiled in this review will be presented with the

aim of rationalizing which effect the structural and electronic features of these D-A systems have on the photoinduced electron/energy transfer dynamics.

5.1 Binuclear phthalocyanines connected to other electroactive moieties

Photoinduced electron transfer processes in $\text{Zn}(\text{II})\text{Pc}_2\text{-PDI}$ 22 in Fig. 4 were investigated.⁸¹ A long lived charge separated state was achieved by addition of Mg^{2+} to benzonitrile solutions of $(\text{Zn}(\text{II})\text{Pc})_2\text{-PDI}$, in which PDI forms a complex with magnesium ($\text{Zn}(\text{II})\text{Pc}_2\text{•}^+\text{-PDI}\text{•}^-/\text{Mg}^{2+}$). As the low-lying triplet excited state of PDI precludes the formation of a long-lived charge-separated state, addition of Mg^{2+} stabilizes the charge separated state by lowering its energy and increasing the reorganization energy of electron transfer. In doing so, time resolved absorption spectra confirm the presence of long lived charge separated states (270 μs ; $[(\text{Zn}\text{Pc})_2\text{•}^+\text{-PDI}\text{•}^-/\text{Mg}^{2+}]$). On similar grounds, the tightly coupled $\text{Zn}(\text{II})\text{Pc}_2\text{-PDI}$ array 23 in Fig. 4 yielded a 517 ps lived radical ion pair state in toluene-pyridine after excitation of the $\text{Zn}(\text{II})\text{Pc}$ unit.⁸² While in conjugate 22 linkages at the imido positions are realized, in the latter compound, it is the linkage through ethynyl bridges at the bay position that affords CR *via* recovery of the singlet ground state.

Ethynyl-bridges are also employed to assemble Pc-Pc conjugates to C_{60} . The photophysical properties of multicomponent $\text{Zn}(\text{II})\text{Pc}_2\text{-}(\text{C}_{60})_2$ nanoconjugates 24 (Scheme 7) have also been investigated.⁸³ Steady state fluorescence assays, in which different solvent polarities were probed, reveal that quenching of the Pc fluorescence takes place, which is due to intramolecular electron transfer. This process is accelerated in polar media, although the quantum yield of CS is reduced. Additionally, femtosecond laser flash photolysis revealed relatively short lifetimes of the charge-separated state ($10^{-10}\text{-}10^{-9}$ s). Such a short lifetime is explained on grounds of close proximity between the electro- and photoactive $\text{Zn}(\text{II})\text{Pc}$ and C_{60} units in 24, thus facilitating through space charge transfer.

In a series of $\text{Zn}(\text{II})\text{Pc}_2\text{-AQ}$ triads linked by ethenyl spacers (27–29 in Fig. 5), electronic communication was ensured by changing the aggregation status.⁸⁴ In these series, only the connecting positions of the $\text{Zn}(\text{II})\text{Pcs}$ to the central AQ differ. As such, these triads show a dependence of their redox and photoinduced CS properties on the molecular topology and solvent environment. 1,5- and 2,6-connections, that is, 27 and 29, respectively, evoke efficient π -conjugation between the $\text{Zn}(\text{II})\text{Pcs}$ and the AQ unit, and lead to *J*-type aggregate formation in solution, while a 1,8-connection (28) forces cofacially π -stacking of $\text{Zn}(\text{II})\text{Pcs}$ out of the AQ plane. Time resolved absorption measurements confirm that photoexcitation of the $\text{Zn}(\text{II})\text{Pc}$ component in all the isomeric forms results in the formation of the $\text{Zn}(\text{II})\text{Pc}\text{•}^+\text{-AQ}\text{•}^-$ charge separated state. Interestingly, the kinetics of these electron transfer reactions are greatly dependent on the aggregation status of the triads. In particular, in the case of 27 and 29, monomeric species are present in THF, but aggregates are formed in benzonitrile, leading to a stabilization of the lifetime of the charge separated state by more than 3 orders of magnitude.

Supramolecular complexes based on $\text{Zn}(\text{II})\text{Pc}$ and diIm-substituted PDI (Im₂PDI) have recently been described.⁸⁵ ¹H NMR spectroscopy, absorption, and fluorescence titrations reveal the formation of 1:1 $\text{Zn}(\text{II})\text{Pc}\text{-Im}_2\text{PDI}$ and 2:1 $\text{Zn}(\text{II})\text{Pc}\text{-Im}_2\text{PDI-Zn}(\text{II})\text{Pc}$ complexes with binding constants in the order of 10^5 M^{-1} . Time resolved measurements provided insights into efficient photoinduced electron transfer events taking place in these supramolecular systems, which show longer lifetimes of the charge separated states, namely 3 ± 1 ns for the $\text{Zn}(\text{II})\text{Pc}\text{-Im}_2\text{PDI-Zn}(\text{II})\text{Pc}$ complex, than in related covalently linked conjugates.

Supramolecular interaction between a PDI unit bearing two 4-pyridyl substituents at the imido positions (Py₂PDI) and $\text{Ru}(\text{II})\text{Pc}$ monocoordinated with a CO ligand affords triad 30 in Fig. 6 in good yields.⁸⁷ Transient absorption measurements attest the rapid formation of a $[\text{Ru}(\text{II})(\text{CO})\text{Pc}\text{•}^+\text{-Py}_2\text{PDI}\text{•}^- \text{-Ru}(\text{II})(\text{CO})\text{Pc}]$ charge separated state that lives for 115 ± 5 ns upon photoexcitation of either chromophore. As a matter of fact, the unique orthogonal geometry strongly favors exothermic CR dynamics that are placed into the inverted region of the Marcus parabola. Orthogonal geometry has also been achieved in $\text{Ru}(\text{II})\text{Pc}_2\text{-C}_{60}$ triad 32 in Fig. 6, in which the components are assembled through metal coordination of a bispyridyl-fullerene, with a linear arrangement of the pyridyl ligands, to two $\text{Ru}(\text{II})(\text{CO})\text{Pcs}$.⁸⁹ As evidenced by absorption and electrochemical assays, the electroactive components show electronic coupling in the ground state. With respect to the excited state, triad 32 reveals shorter lifetimes than related monopyridyl- C_{60} -based dyads due to the fact that the $\text{Ru}(\text{II})\text{Pc}$ triplet excited state is energetically low enough to offer a rapid deactivation pathway for the charge separated state.

Panchromatic optical absorption behavior has been achieved in the supramolecular $\text{Zn}(\text{II})\text{Pc}_2\text{-squaraine}$ ensemble 31 in Fig. 6, which absorbs light in a wide range of the solar spectrum, namely from 250 to 850 nm.⁸⁸ Fluorescence spectroscopy experiments demonstrate quenching of the squaraine fluorescence, with quantum yields as low as 0.003. Responsible for this trend is an efficient and ultrafast electron transfer from the $\text{Zn}(\text{II})\text{Pc}$ components to the squaraine unit, leading to a charge separated state that lives for 24 ± 2 μs .

In addition to metal-ligand interactions, other supramolecular motifs, such as D-A contacts between appropriately substituted Pcs featuring electron-donating or electron-withdrawing groups, have been utilized to construct binuclear Pc systems linked to other electroactive units. Heteroassociation of a $\text{Zn}(\text{II})\text{Pc-C}_{60}$ conjugate 35 with an electron-deficient $\text{Pd}(\text{II})\text{Pc}$ 34 has been used to construct supramolecular hybrid 33 in Fig. 7,⁹⁰ which features a stability constant of about 10^5 M^{-1} in CHCl_3 . Compared with covalently linked $\text{Zn}(\text{II})\text{Pc-C}_{60}$ dyads, femtosecond flash photolysis evidenced that this heteroassociation leads to substantial stabilization of the charge separated state up to 475 ns. The latter is formed by an exothermic electron transfer from $\text{Zn}(\text{II})\text{Pc}$ to C_{60} upon photoexcitation. The results document the benefits from the supramolecular electronic coupling between the donor and the acceptor Pcs , which assists in the delocalization of the radical cation over the two Pc moieties.

Supramolecular photosynthetic reaction center **36** in Fig. 7 resulting from the coordination of pyridyl-functionalized C₆₀ as an electron acceptor with a cofacially self-assembled Zn(II)Pc dimer as an electron donor has been prepared.⁹³ Model system **36** exhibits superior electron transfer properties, that is, the formation of a longer lived charge separated state (6.7 μ s) than that formed by a related mononuclear Zn(II)Pc–C₆₀ hybrid (4.8 μ s). This observation is rationalized as a slower CR process in **36** as a consequence of the smaller reorganization energy of the cofacial arrangement.

Hydrogen-bonding interactions have also been used to create ensembles of two Pcs with other electroactive subunits. To this end, a supramolecular D–A hybrid **37** in Fig. 8 has been constructed by means of triple hydrogen bonding between two Zn(II)Pc units featuring a melamine moiety and PDI.⁹⁴ By means of absorption and fluorescence titrations, K_{ass} of $2 \times 10^5 \text{ M}^{-1}$ and $7 \times 10^4 \text{ M}^{-1}$ have been determined in THF and benzonitrile, respectively. As predicted from the K_{ass} , quenching of the Zn(II)Pc fluorescence is rather efficient. Transient absorption measurements further corroborated that the photoexcitation of PDI results in the transduction of singlet excited state energy to the energetically lower-lying Zn(II)Pc. CS, on the other hand, could not be confirmed. More recently, a related H₂Pc substituted with six strongly donor thioalkyl chains and one melamine unit was assembled to a complementary PDI through triple hydrogen bonding.⁹⁵ Optical experiments lack evidence for any appreciable ground state electronic interactions, which is explained by the weak electronic coupling through the hydrogen bonds. However, selective photoexcitation of PDI leads to an intramolecular electron transfer, affording a several nanosecond-lived PDI^{•-}/(H₂Pc)₂^{•+} charge separated state, while photoexcitation of H₂Pc is only followed by an intersystem crossing to the triplet excited state of H₂Pc.

5.2 Phthalocyanine–subphthalocyanine systems

As mentioned above, SubPc–Pc systems are perfectly suited for the study of intramolecular energy/electron-transfer processes. Therefore, in a series of covalently linked SubPc–Pc conjugates **40a–c** in Scheme 8, electronic coupling between the two photoactive units is ensured by a rigid and π -conjugated alkynyl spacer.¹⁰¹ In addition, the electronic characteristics of the SubPc moiety were modulated by the introduction of different peripheral substituents. When the charge transfer state lies high in energy, which is the case for **40b**, a quantitative singlet–singlet energy transfer mechanism ($3.0 \times 10^{10} \text{ s}^{-1}$) from the excited SubPc to the Pc takes place. In contrast, stabilization of the radical ion pair state by lowering the redox gap between electron donor and acceptor results in a highly efficient photoinduced electron transfer process ($5.0 \times 10^{10} \text{ s}^{-1}$) with quantum yields as high as 0.9 (as in the case of **40c**).

On the other hand, photoinduced electron transfer in supramolecular ensembles from the electron-donating tetra-*tert*-butyl-Zn(II)Pc to the electron-accepting dodecafluoroSubPc in benzonitrile solutions of both components has been investigated by nanosecond laser photolysis.²⁶⁹ Owing to the particular electronic properties of both entities, such combination

seems to be perfectly suited for the study of intermolecular electron-transfer processes in polar solvents *via* the triplet-excited state of SubPcF₁₂. Upon excitation of SubPcF₁₂ with 570 nm laser light, the electron transfer from Zn(II)Pc to the triplet-excited state of SubPcF₁₂ was confirmed by observing the transient absorption bands of the Zn(II)Pc radical cation and SubPcF₁₂ radical anion in both the visible and near-IR regions.

5.3 Phthalocyanine–porphyrin systems

Pc–Por systems are very interesting from the photophysical point of view for several reasons. The transduction of singlet excited state energy occurs very efficiently from the Por to the Pc owing to the fact that the Q-band absorption of the Pc almost overlaps with the fluorescence of Pors. Importantly, the close separation between the donor Pors and the acceptor Pcs leads in several cases to strong electronic coupling or a partial electronic orbital overlap.

Another interesting objective is the possibility of driving intramolecular energy transfer from higher lying excited states such as the second singlet excited state. Usually, such excited states are too short lived to be involved in energy or electron transfer reactions although such an energy transfer has already been demonstrated in photosynthesis by ultrafast laser spectroscopy. In the context of the latter, the length of the conjugation in carotenoids determines the extent of spectral and electronic overlap with the acceptor bacteriochlorophyll.^{270,271}

Pc–Por conjugates **52–54** in Scheme 11 presenting a direct linkage through the β -pyrrolic position of the Por unit, and having different substituents on the Pc core (H₂, *tert*-butyl or butoxy) and different metal centers in the Por (H₂, Zn(II), and Pd(II)) were studied photophysically by steady-state absorption and emission spectroscopy as well as time-resolved fluorescence, fluorescence up-conversion, and transient absorption measurements.¹⁰⁸ The close location of the two chromophores is the inception to strong excitonic coupling between them due to hindered free rotation through the direct linking bond. Fluorescence spectroscopy shows quenching of the Por emission with quantum yields as low as 0.0005 – when compared to Por references – with the simultaneous appearance of Pc emission upon exclusive excitation of the Por at 420 nm. Responsible for that is an efficient and ultrafast intramolecular energy transfer ($\sim 10^{12} \text{ s}^{-1}$) from the photoexcited Por to the covalently linked Pc, which is not expected to change notably with solvent polarity. Proof for this comes from complementary excitation spectra and transient absorption measurements. From fluorescence up-conversion experiments, an intramolecular energy transfer is observed from the second singlet excited state S₂ as well as from the first singlet excited state S₁ of the Por. Hereafter, the long-lived triplet excited state of the Pc (70 μ s) is populated *via* intersystem crossing ($3.2 \times 10^8 \text{ s}^{-1}$). In contrast, the Por triplet excited state is not formed due to its unfavorable energetic positioning in the Pc–Por arrays.^{108,125}

Later, *N*-bridged, Pc–Por heterodimers directly connected through an amino group, located either at the β -pyrrolic position (**48a,b** in Scheme 10) or at the *p*-position of the *meso* phenyl moiety (**49** in Fig. 10) of the Por, thus allowing a close proximity

of the two units, were studied.²⁹ The nitrogen atom located between the two macrocycles could play the role of an “active” spacer, since it typically behaves as a pH- and redox-sensitive group. The characteristic absorptions of the individual components are noticed in the absorption spectra, but the Pc Q-band is red-shifted by about 20 nm with regard to the mononuclear Pcs references, thus suggesting a reduction of its HOMO–LUMO gap as a consequence of the electron donor character of the Por–NH-substituent. This red-shift is also observed in the fluorescence maxima, with much lower quantum yields than the corresponding references. Upon exclusive excitation of the Por unit at 425 nm, detecting the Pcs fluorescence implies a transduction of singlet excited state energy from the Por to the Pcs ($\sim 10^{11} \text{ s}^{-1}$). Overall, higher energy transfer efficiencies were noted for the β -pyrrolic conjugates **48a,b** in Scheme 10. Fluorescence up-conversion experiments corroborate that an intramolecular energy transfer occurs from the second singlet excited state S_2 as well as from the first singlet excited state S_1 of the Por. The S_2 deactivation efficiencies ($\sim 1.1 \times 10^{12} \text{ s}^{-1}$) were determined to be around 25% for both dyads, while for the S_1 deactivation, values of around 90% were derived. This work underlines the transduction efficiency in β -pyrrolic linked conjugates, while an impact exerted by the NH-connection cannot be ruled out.¹⁰⁷

Alkynyl-bridged Pcs–Por systems are intriguing examples for the design of systems with strong electronic coupling. A conjugate consisting of a Zn(II)Pc and a Sn(IV)Por (**72** in Fig. 13) has also been prepared and photophysically studied.¹¹⁴ The presence of a phenyl-ethynyl bridge reduces the symmetry of the two moieties and leads to a conjugated π -system involving the bridge, which results in red-shifted and broadened absorption bands and a split of the Pcs Q-bands. From the fluorescence spectrum, strong quenching of the fluorescence is deduced. Transient absorption measurements indicate a rapid formation of the radical ion pair state upon photoexcitation, which includes the signatures of the one-electron oxidized form of Zn(II)Pc and the one-electron reduced form of Sn(IV)Por. Excitation at 680 nm results in an electron transfer from the singlet excited state of the Zn(II)Pc (13 ps), which proceeds through the direct super-exchange mechanism, as the bridge is too difficult to be reduced for electron hopping to occur. Starting from the singlet excited state of the Sn(IV)Por upon 440 nm excitation, a hole-hopping mechanism *via* a transiently oxidized bridge is energetically feasible (4 ps). The photolytically observed spectrum is ascribed to the radical ion pair state and agrees well with that derived from spectroelectrochemical measurements. CR *via* a long-range, super-exchange mechanism takes place within 85 ps. Energy transfer from the Sn(IV)Por to the Zn(II)Pc is energetically possible, but is excluded. In this regard, the subsequent CS from the excited Zn(II)Pc would be slower than the observed decay of the photoexcited Sn(IV)Por.

On the other hand, fused Pcs–Por conjugates **85a,b** in Fig. 20 show, as mentioned above, a remarkable bathochromic-shift ($\sim 20 \text{ nm}$) in the Por Soret-band and a broadening, splitting, and red-shift of the Pcs Q-band as a consequence of the desymmetrization of the Pcs, the enlargement of the π -conjugated system,

and the intramolecular electronic coupling between the individual components.¹²⁶ The fluorescence maxima also show the underlying red-shift matching the red-shifted absorption maxima, with, however, much lower quantum yields than in the corresponding references. This infers appreciable electronic interactions. Despite the nearly exclusive excitation of the Por at 434 nm, Pcs fluorescence was seen to develop, while no significant fluorescence is observed for the Por. Here, an efficient intramolecular transduction of singlet excited state energy from the Por to the fused Pcs is implicit ($\sim 30 \text{ ps}$). Support for this notion was lent from excitation spectra as well as transient absorption measurements. Hereafter, the long-lived triplet excited state of the Pcs is populated *via* intersystem crossing (1.5 ns).

Very similar to the aforementioned, singlet–singlet energy transfer prevails in self-assembled H₂Por/Zn(II)Pcs and H₂Por/Zn(II)Ncs in *o*-DCB and toluene. The time constants of ultrafast singlet–singlet energy transfer are on the order of 2–25 ps.¹¹⁶

Besides the already well-known energy transfer reactions, photoinduced electron transfer reactions were investigated in slipped-cofacial supramolecular dimer systems (**64**)₂–**s** (Fig. 11) of a directly linked Zn(II)Por–Zn(II)Pcs heterodiyad **64** by means of picosecond and femtosecond transient absorption spectroscopies.²⁷² In this dimer, two heterodiyads **64** are connected through metal–ligand interactions between two Im-substituted Zn(II)Por, which is advantageous for the effective production of the radical ion pair states due to a decrease in the reorganization energy. The absorption spectrum is composed of the characteristic bands of the individual components, namely Zn(II)Por and Zn(II)Pcs. However, a remarkable broadening and splitting of the Por Soret-band indicates the self-assembled dimerization, and it is explained by the exciton splitting theory proposed by Kasha *et al.*²⁷³ The fluorescence properties suggest a rapid energy transfer (<1 ps) from the photoexcited Por to the Pcs. Despite the nearly exclusive excitation of the Por, Pcs fluorescence is seen, while no significant response is observed in the range of the Por fluorescence. In addition, the Pcs fluorescence quantum yields decrease with an increasing solvent dielectric constant, which suggests an electron transfer reaction. Thus, the rapid energy transfer reaction from the Por to the Pcs is followed by photoinduced electron transfer (47 ps) with a 93% efficiency to create a radical ion pair state. The radical ion pair state reveals features that include the signatures of the one-electron oxidized form of Zn(II)Pcs and the one-electron reduced form of Zn(II)Por. In this particular case, CR takes place in 510 ps. Electrochemical measurements revealed that the radical cation is delocalized over the whole π -system of the dimer.

Using the metal–ligand binding approach, stable molecular dyads **76** in Fig. 15 and pentad featuring Im-substituted H₂Pors and Ru(II)(CO)Pcs were synthesized and spectrally characterized.¹¹⁸ The molecular structure and electronic states are deduced from computational, spectral, and electrochemical studies. Using steady-state and time-resolved transient absorption techniques, photochemical events taking place in these molecular polyads upon excitation of the H₂Por are systematically investigated. To this end, steady-state emission predicted excitation

transfer, in which the linkage on the H₂Por entity and the number of Pcs influence the efficiency of excitation transfer. The kinetics of energy transfer ($3.71 \times 10^{10} \text{ s}^{-1}$), monitored by performing transient absorption measurements using both up-conversion and pump probe techniques and modeled using the Förster-type energy transfer mechanism give rise to a good match between the theoretically estimated and the experimentally measured kinetic results. Interestingly, in the dyads subsequent charge transfer (10^{10} s^{-1}) evolves in polar benzonitrile. Such charge transfer interactions are absent in the case of the pentad in benzonitrile, which could be due to different orientation factors promoting the competing photochemical process.

Stable host-guest complexes were formed in aqueous media between tetrasulfonated Zn(II)TPP **79** in Fig. 17 and several Si(IV)Pcs axially-substituted with two permethylated β-CD units (such as **80** in Fig. 17).¹²² As shown by steady-state measurements, 1:1 complexes are formed with large binding constants in the range from 1.1×10^7 to $3.5 \times 10^8 \text{ M}^{-1}$. In dependence of the length of the spacers between the β-CD units and the silicon center of the Pc, transient absorption measurements reveal two major photoinduced processes, namely fluorescence resonance energy transfer and charge transfer. This behavior is explained by the control of the length and flexibility of the linker on the overall efficiency of the processes. Being in close proximity, lifetimes of the resulting charge separated states are in the picosecond range.

5.4 Phthalocyanine-porphyrin systems connected to other electroactive moieties

Tri-*tert*-butyl Zn(II)Pc-M(II)Por (M = Zn(II) (**54a**), Pd (II) (**54b**) and H₂ (**54c**)) dyads, and their analogs having *tert*-butyloxy (**53a-c**) or no (**52a-c**) substituents on the Pc macrocycle (Scheme 11) were studied in the presence of variable concentrations of two pyridyl-substituted C₆₀ (**83** and **84** in Fig. 19), which axially-coordinated to the Pc Zn(II) center.¹²³ Fluorescence titration experiments show significant quenching of the Pc fluorescence. In fact, the quantum yields of the Pc fluorescence converge towards the end of the titration, which correlates with the successful formation of Por-Pc-fullerene supramolecular hybrids through coordination of the pyridyl moiety of the fullerene species to the zinc metal center of the Pc macrocycle in the dyad. This trend is rationalized on the basis of the larger cavity of Pcs. The calculated K_{ass} for Zn(II)Pc and C₆₀ are very high, with values of around 10^5 to 10^6 M^{-1} . Transient absorption measurements confirm that, after an intramolecular energy transfer from the Por to the Pc component (~15 ps), an intramolecular charge transfer occurs (~14 ps). Radical ion pair state features, which include the signatures of the one-electron oxidized form of the Zn(II)Pc and the one-electron reduced form of C₆₀, appeared. CR takes place (~1.4 ns) without giving rise to any charge shift reaction to yield the one-electron oxidized form of the Por.¹²⁵

Interestingly, a different coordination behaviour is observed in the case of Pc-Por conjugates **85a,b** (Fig. 20) and C₆₀ derivative **83**.¹²⁶ Fluorescence titration experiments show significant quenching of the Pc fluorescence, with values less than 10% of

the initial intensity when fullerenes were absent. Overall, the calculated K_{ass} of around 10^6 M^{-1} are very high. In contrast to the H₂Por-containing dyad **85b**, a red-shift of 7 nm in the absorption spectra of conjugate **85a-83** was observed. This result testifies that **83** coordinates to the Zn(II)Por, leading to an isosbestic point at 433 nm and a K_{ass} of around 10^5 M^{-1} . Transient absorption measurements corroborated that, after an intramolecular energy transfer from the Por to the Pc (~20 ps) occurs, an intramolecular charge transfer takes place in the supramolecular ensemble (~40 ps). This radical ion pair reveals features that include the signatures of the one-electron oxidized form of Zn(II)Pc and the one-electron reduced form of C₆₀. Interestingly, CR takes place (~1.2 ns) without giving rise to any charge shift reaction to yield the one-electron oxidized form of the Por. The latter would be, however, endergonic and would require a significant activation barrier.

Electron acceptors can also be covalently linked to a Pc-Por system. In fact, some Pc-C₆₀-Por triads (**82a-c** in Fig. 18) presenting the three photoactive moieties covalently connected by means of a pyrrolidine spacer have been described and photophysically studied by steady-state absorption and emission spectroscopy as well as time-resolved fluorescence and transient absorption measurements.¹²⁴ Zn(II)Por-C₆₀-Zn(II)Pc **82c**, give rise upon excitation of the Por to a sequence of energy and charge transfer reactions with fundamentally different outcomes. Relative to the component spectra of the single moieties, all individual features are present except those from C₆₀, which are overshadowed by notable blue-shifted and broadened transitions of Zn(II)Por and Zn(II)Pc with lower extinction coefficients. Exclusive photoexcitation of the Por at either 428 or 425 nm leads to a fluorescence pattern that is reminiscent of that of the Pc, while a significant quenching of the Por centered fluorescence is seen. Such an observation lends support for an efficient transduction of singlet excited state energy from the Por to the Pc. The quantum yields of the Pc fluorescence are much lower than in the corresponding reference system. As such, it was concluded that intramolecular interactions play decisive roles in deactivating the photoexcited systems. Support for this notion was lent from excitation spectra as well as transient absorption measurements. In Zn(II)Por-C₆₀-Zn(II)Pc **82c**, an initial energy transfer ($8.3 \times 10^{11} \text{ s}^{-1}$) is followed by a charge transfer ($1.5 \times 10^{11} \text{ s}^{-1}$) to power the formation of Zn(II)Por-(C₆₀^{•-})-Zn(II)Pc^{•+}. No appreciable evidence could be gathered that would prompt to the involvement of the one-electron oxidized Zn(II)Por radical cation, due to the strong coupling between Zn(II)Por and Zn(II)Pc. It is likely that the short methylene linker weakens the interactions between Zn(II)Por and C₆₀. The lifetime of the radical ion pair state is much longer in non-polar solvents like toluene (>3000 ps) than in polar solvents like THF (168 ps).

The combination of Pc-Por ensembles, with electron-accepting SWCNTs is a powerful approach to construct panchromatic electron D-A systems, with reactive cross sections in the visible, infrared, and near-infrared. Such a system was studied photophysically by using highly concentrated SWCNT suspensions, in a mixture of 25% THF and 75% DMF, which were titrated

with variable concentrations of H₂-Zn(II)Por-Zn(II)Pc conjugates **48b** and **48c** in Scheme 10.¹⁰⁶ On one hand, absorption titrations show small red-shifts of ~9 nm of the Por Soret bands and stronger red-shifts of ~34 nm of the Zn(II)Pc bands, which indicate strong interactions between the components. On the other hand, fluorescence titration experiments show significant quenching of the Zn(II)Pc fluorescence. Transient absorption measurements confirm that, after an intramolecular energy transfer from the Por to the Pcs ($\sim 2.0 \times 10^{12} \text{ s}^{-1}$) takes place, an intramolecular charge transfer occurs. Radical ion pair state features, including the signatures of the one-electron oxidized form of the Zn(II)Pc and the one-electron reduced form of SWCNT, evolved. Here, CR occurs within *ca.* 10^9 s^{-1} .¹⁰⁶

5.5 Porphyrin–subphthalocyanine systems

A newly synthesized multimodular system (**86** in Fig. 21) composed of three TPA entities covalently substituted at the *meso* positions of a Zn(II)Por ring, which is linked to a dodecafluoroSubPc by its axial position, reveals appreciable electronic interactions between the subcomponents.¹²⁷ The occurrence of fast and efficient CS processes (10^{12} s^{-1}) *via* the singlet excited state of Zn(II)Por was confirmed by femtosecond transient absorption spectral measurements in polar and nonpolar solvents. On one hand, the lifetimes of the singlet radical ion pair state (20–170 ps) decrease substantially in more polar media, whereas the rate of CS is much less solvent-dependent. On the other hand, the delocalization of the one-electron oxidized π-cation radical over the TPA-Por donor, the lower energy of the radical ion pair state, the particular characteristics of the axial B–O bond, and the triplet radical ion pair character rationalize the charge stabilization of the one-electron oxidized form of the Zn(II)Por and the one-electron reduced form of the SubPc with an extremely long lifetime (370 μs) compared to the reported Pcs-based compounds. Coordination of an Im-containing fullerene **88** coordinating ligand to the Zn(II)Por component of a related Por-SubPc dyad **87** in Scheme 14 affords a moderately stable ensemble ($K_{\text{ass}} = 10^4 \text{ M}^{-1}$).¹²⁸ Redox measurements indicate that the energy level of the radical-ion pair in toluene is located lower than that of the singlet and triplet states of the Zn(II)Por and fullerene. Femtosecond transient absorption measurements revealed fast CS from the singlet Zn(II)Por to the coordinated fullerene is the inception to a long-lived radical ion pair state in toluene ($1.6 \times 10^5 \text{ s}^{-1}$).

A supramolecular complex composed of β-CD-conjugated SubPc and a tetrasulfonated Por has been formed as a stable 2:1 host-guest complex with a K_{ass} of $(1.2 \pm 0.5) \times 10^{12} \text{ M}^{-2}$.¹²² In the resulting hybrid, no significant electronic interactions are evidenced in the ground state, as the absorption spectra are a simple superposition of the absorption spectra of the individual components. Calculations by the Rehm–Weller equation and CV measurements indicate that efficient energy transfer takes place from the excited SubPc to H₂Por. In a competitive way, electron transfer is also favorable as a deactivation pathway of the SubPc singlet excited state.

5.6 Porphyrin–porphyrin binuclear systems

Particular attention has been focused on the construction of artificial light-harvesting complexes to investigate the fundamental

mechanism of the excitation energy hopping processes as mimics of the natural photosynthetic antenna LH1 and LH2. Thus, investigations have been directed towards the construction of various multidimensional Por arrays for the fabrication of artificial, light-harvesting complexes.

In non-coordinating solvents, Osuka *et al.* demonstrated the spontaneous assembly of *meso*-*meso* linked diPors (**130**)₂,(**131**)₂ in Fig. 28b to form tetrameric arrays.²⁰³ By using both steady-state and time resolved spectroscopic methods, excitation-energy migration processes in such assemblies are clearly shown. Assuming that the number of energy-hopping sites is 2 in the tetrameric assembly, respectively, excitation-energy hopping rates of 1.5 ps^{-1} are derived, which are in good agreement with the calculated Förster-type energy transfer rates. The results are explained on the grounds of the competition between H- and J-type coupling of the transition dipole moments along the *meso*-*meso*-linkages in the tetrameric array and the parallel arrangement of transition dipole moments. The latter decreases energy transfer rates.

Self assembled Por boxes constructed by conjugated Por dimers were investigated by Kim *et al.*²¹⁹ Here, *meso*-pyridyl appended, alkynylene-bridged Zn(II)Por dimers **145** in Fig. 33 assemble spontaneously into tetrameric Por boxes in noncoordinating solvents. Interestingly, owing to the free rotation of the di- and tetraalkynylene Por dimers, two kinds of self assembled Por boxes with planar and orthogonal conformers are noted, respectively. The excitation energy migration process within the Por boxes, where the exciton–exciton annihilation time has been described in terms of the Förster-type incoherent energy hopping model, is directly associated with the pump-power dependency on the femtosecond transient absorption decay profiles. In doing so, the excitation energy hopping rates in Por boxes constructed by planar and orthogonal conformers are established as $< 1.2 \text{ ps}^{-1}$ and $< 1 \text{ ps}^{-1}$, respectively. Moreover, the Por boxes constructed by orthogonal conformers give rise to slow excitation energy hopping rates of $< 12 \text{ ps}^{-1}$. Thus, the dihedral angle between the Pors is an important factor to control the energy transfer efficiency using conjugated Por dimer systems.

The next work has also been an example of structural control over photophysical processes. Butadiyne-linked Por dimers were forced by metal coordinating ligands to self assemble into prismatic structures, in which the dimers comprise the faces of the prisms.²⁷⁴ Significant spectral enhancements are shown for the dimers. For example, after photoexcitation of the prismatic assemblies an efficient, through-space energy transfer is observed between the macrocyclic dimers. Interestingly Por and chlorophyll dimer prisms with the same size trigonal ligand show similar exciton migration lifetimes. The independence of the chromophores indicates that energy transfer occurs from the low energy transition situated along the long axis of the dimers and that these transitions for both chlorophylls and Por have similar energies.

Photoexcited state dynamics of triply-fused, Zn(II) and Pd(II)Por dimers **120e** in Fig. 27 were investigated by Schmidt *et al.*²⁷⁵ Both compounds show short excited-state lifetimes.

For the Zn(II)Por dimer, for instance, an average singlet excited state lifetime of 14 ps is noted, proposing a crossing of the singlet excited state and singlet ground state potential energy surfaces as a reason for the fast non-radiative deactivation to the ground state. However, the Pd(II)Por dimer displays longer average singlet excited state lifetimes of 18 ps before inter-system crossing at 1.7 ns sets in. Compared to other diPors that also show intramolecular heavy atom effects, the short triplet lifetime of the palladium diPors is rationalized on the basis of the position of the heavy atom within the diPor framework and the resulting strength of the spin-orbit coupling.

5.7 Binuclear porphyrin systems connected to electroactive moieties

The charge transfer behavior and the CR features of different covalently- and noncovalently linked Por conjugates connected to electroactive moieties were analyzed, to study the influence of both the nature of the bridges between the electron donors and the electron acceptors and the number of Pors and acceptors in multicomponent ensembles.

Photoinduced CS and CR processes in $\text{Por}_2\text{-C}_{60}$ systems were first examined by Imahori, Fukuzumi and coworkers.²⁷⁶ More recently, $\text{Por}_2\text{-C}_{60}$ system **153b** in Fig. 38, in which the Por units are linked by a butadiyne spacer, have been studied to demonstrate how the driving force for electron transfer can be tuned by selective excitation of the different conformations.²²⁹ The butadiyne spacer allows a broad distribution of conformations and, thus, at room temperature, all Por-Por dihedral angles in **153b** are populated. It has been shown that the planar and perpendicular conformations of such Por dimers are spectroscopically distinct and that it is possible to selectively excite either conformer. The fundamental 0–0 transitions of the two conformers are spaced in energy by approximately 0.2 eV and, in turn, two different initial states are formed that feature different driving forces for electron transfer from the Por dimer to the fullerene. The electron transfer rate is significantly faster in the conformationally distorted singlet excited donor ($2.5 \times 10^{11} \text{ s}^{-1}$) than in the planar conformer ($5.8 \times 10^{10} \text{ s}^{-1}$). The larger driving force and the larger electronic coupling of the perpendicular conformer to the appended fullerene rationalize the significantly different rates. It was suggested that in the excited state of the perpendicular conformation of the dimer it is likely that the excitation is localized on one of the Pors, the one that is closest to the C_{60} acceptor. The latter renders the average electron D–A distance shorter. Coordination of **154** to dimer **153b** fixes its conformation giving rise to a larger inter-Por conjugation. Interestingly, the CR rate increases by an order of magnitude when comparing the planar conformer ($1.4 \times 10^9 \text{ s}^{-1}$) with the unconstrained conformer ($1.4 \times 10^8 \text{ s}^{-1}$). The faster recombination in the planar conformer was explained by the higher degree of conjugation. Thus, charges are mediated more efficiently through the delocalized system as evidenced by larger electronic couplings obtained for the planar system when the CR process is treated within the simple Marcus approach. In this context, electronic coupling for the planar system is estimated to be $2.5\text{--}3.9 \text{ cm}^{-1}$, which is significantly higher

than the coupling of 0.92 cm^{-1} in the conformationally heterogeneous system.

Related covalent Por dimer conjugates connected to two distinct electroactive units have also been prepared such as covalent D–A system **153a** in Fig. 38, in which the two Pors are bridging a Fc and a fullerene. By extending the system with a secondary Fc-donor, a long-range charge-separated state can be formed.²²⁹

While the aforementioned system was covalently linked in a linear fashion ($\text{Por}_2\text{-C}_{60}$), in triad **150** in Fig. 36 the two Pors are linked to the fullerene component in a symmetrical manner ($\text{Zn(II)Por-C}_{60}\text{-Zn(II)Por}$)²²⁶ and are held in a conformationally constrained geometry. Transient absorption measurements revealed that in the case of **150**, formation of the singlet excited state of Zn(II)Por is followed by photoinduced electron transfer to the fullerene with a time constant of 20 ps. The resulting radical ion pair state is formed with a quantum yield of 98% and has a lifetime of 820 ps. The first excited singlet state of a H₂Por analog of **150** leads to the radical ion pair state with a time constant of 200 ps and a quantum yield of 98%. The radical ion pair state decays with a lifetime of 2.8 ns. Despite the fact that the rate constant for photoinduced electron transfer is slower in the metal-free D–A derivative ($4.9 \times 10^9 \text{ s}^{-1}$ vs. $4.9 \times 10^{10} \text{ s}^{-1}$), the longer lifetime for its singlet excited state allows a high quantum yield for electron transfer. CR was also shown to be faster for the zinc derivative ($1.2 \times 10^9 \text{ s}^{-1}$) than for the free-base one ($3.6 \times 10^8 \text{ s}^{-1}$). The results are in qualitative accord with the Marcus relationship: the driving force for CR of the Zn(II)Por-based conjugate is lower than for the free-base analog. Reactions, having driving forces for electron transfer that are much larger than those for photoinduced electron transfer, evidently occur in the inverted region of the Marcus relationship, where a decrease in driving force leads to an increase in rate constant.

Diederich *et al.*²²³ showed that changing the linkage between the Pors to a triply-fused, diPor linked to C_{60} (**149** in Fig. 35) results in a weaker electronic interchromophoric interaction than in conjugates, where a face-to-face alignment of Pors and fullerene prevails. Despite the fact that triply-fused Por dimers show much better electron donor properties than simple Pors, their low-lying and very short-lived (4.5 ps) singlet level leads to a competitive deactivation pathway as the radical ion pair state energy was determined to be nearly isoenergetic. In conclusion, in both publications clear differences in the photoinduced process between the triply-fused, Por dimers connected to C_{60} (**149**) and the biaryl-type, Por dimers connected to the C_{60} conjugate **153a** discussed above were evidenced.

Besides $\text{Por}_2\text{-C}_{60}$ conjugates, Por-functionalized SWCNTs have attracted extensive attention as excellent candidates for nanoscale photovoltaic devices. For example, *meso-meso*-linked diPors have successfully been covalently linked to functionalized SWCNTs.²³³ Steady state fluorescence assays as a function of solvent polarity reveal that fluorescence quenching is mainly dominated by excited state electron transfer. Transient absorption measurements confirmed the existence of electron transfer

with a charge separated lifetime of 145 ns and CR kinetics of $6.9 \times 10^6 \text{ s}^{-1}$. Compared to the monoPor-modified SWCNTs showing a CS of 57 ns and $1.8 \times 10^7 \text{ s}^{-1}$, the *meso-meso*-linked diPor system prolonged the CS state lifetime by a factor of 2.5.

Another interesting electron D-A system was shown by Tagmatarchis *et al.*, in which a Por dimer is linked to CNH through a rigid ester bond.²³⁴ The CNH hybrid material gives rise to efficient quenching of the dimeric Por fluorescence, suggesting photoinduced CS evolving from the singlet excited state. Additionally, transient absorption measurements indicate the fingerprints of the one-electron oxidized form of the Por dimer and the one-electron reduced form of CNH with absorption maxima at around 600–650 and 1400 nm, respectively. CS rate constants and quantum yields are $2.1 \times 10^9 \text{ s}^{-1}$ and 0.95, respectively. The rate constant for the CR process is $1.4 \times 10^7 \text{ s}^{-1}$, which corresponds to a lifetime of the radical ion pair of 72 ns in CH_2Cl_2 . In addition, photoactive electrodes were constructed based on nanostructured SnO_2 electrodes, which reveal photocurrent and photovoltage responses with an incident photon-to-current conversion efficiency value as large as 9.6%, without the application of any bias voltage. The mechanism for the photocurrent generation includes electron transfer, followed by electron mediation from the reduced nanohorns to the conduction band of the SnO_2 electrode. Interestingly, CNHs covalently functionalized with mononuclear Pors show an IPCE value of only 2.7%.²⁷⁷

meso-meso-linked Por dimers and larger oligomers have also been immobilized onto ITO electrodes to enhance light-harvesting and generate higher photocurrents as compared to the corresponding monomer system.²⁷⁸ The work showed that because of the exciton coupling of the Pors, visible light is absorbed more widely than in a linear combination of the corresponding Por monomers. By increasing the number of Pors, the photocurrent conversion efficiency per mol cm^{-2} and the quantum yield of photocurrent generation – Φ_{420} (ITO/ $\text{H}_2\text{Por}/\text{TEA}/\text{Pt}$) = 1.7% and Φ_{420} (ITO/(H_2Por)₄/TEA/Pt) = 3.2% (TEA = triethanolamine) – improve. Another approach to achieve improved efficient anodic photocurrent generation by a photoexcited Por on ITO electrodes involves the use of a special-pair mimic Por assembly.²⁷⁹ Accordingly, slipped-cofacial Por dimers related to 128 in Fig. 28, organized through Im-to-zinc complementary coordination of Im-substituted Zn(II)Por units, were covalently fixed by ring closing olefin metathesis of allyl side chains and immobilized on ITO through different linkers. Comparing the results with a Por monomer, the special pair-mimic dimer formation increases the anodic photocurrent by means of improving Φ_{410} values from 8.2 to 10%. The enhanced photocurrent generation documents the advantage of the slipped-cofacial Por dimer in providing photoinduced CS (IPCE₄₁₀ = 0.55%). Furthermore, higher quantum yields for the anodic photocurrent from the second singlet excited state S₂ compared with that from the first singlet excited state S₁ (Φ_{550} = 4.3%) suggests that a sufficiently fast charge injection occurs due to higher driving forces prior to any internal conversion. Further fine-tuning of a photoelectrochemical cell was established one year later with an Fc/slipped cofacial Por dimer/ITO redox assembly.²⁸⁰

The photocurrent properties of a series of covalently linked, slipped-cofacial Zn(II)Por dimers presenting a Fc or nonamethyl Fc moiety attached to one Por macrocycle *via* single bond, phenylene–ethenylene or phenylene–ethylene spacers and a phosphonate group to the other were also investigated.²⁸⁰ In such covalent ensembles, prepared by ring closing metathesis reaction of supramolecular Zn(II)Por heterodimers, the presence of the phosphonate group allows the grafting of the Fc-functionalized Por dimers to the ITO surface forming a monolayer.

Photoactive supramolecular systems, in which the donor Por dimer and the acceptor moieties are noncovalently linked, are also discussed in the following part. One example is a supramolecular $\text{Por}_2\text{C}_{60}$ featured by a ‘two-point’ coordinate bonding between a dipyridyl-substituted C_{60} and a Zn(II)Por dimer.²³⁷ The rather large K_{ass} of $1.8 \times 10^5 \text{ M}^{-2}$ for the coordination of a bidentate C_{60} ligand to the Zn(II)Por dimer is explained by the “two-point” coordinate binding strategy. As predicted from the K_{ass} , quenching of the Por dimer fluorescence is quite efficient. Transient absorption measurements confirm the formation of a radical ion pair state, by means of the 1020 and 480 nm spectral features of the one-electron oxidized form of the dimeric Por and the one-electron reduced form of the fullerene. The rate of CS is $3.3 \times 10^9 \text{ s}^{-1}$ and the CS quantum yield is 0.86. Moreover, the rate of CR is 2×10^8 and $1.8 \times 10^8 \text{ s}^{-1}$ at room temperature and -10°C , respectively, indicating fairly rapid CR.

Self-assembled Im-Zn(II)Por dimers have been functionalized with Fc and C_{60} electroactive units and then chemically fixed by a metathesis reaction to give a covalently linked version of 157 (Fig. 39).²³⁰ While no significant electronic interactions are evidenced in the ground state, steady-state as well as time resolved measurements provided data on the formation of a long lived radical ion pair state with a lifetime longer than 100 μs . The mechanism involves CS between photoexcited Zn(II)Por dimers and the fullerene followed by oxidative charge shift to the Fc unit.

To mimic the photosynthetic reaction center a “special pair”, that is, a supramolecular ensemble resulting from the complexation of two fullerene derivatives functionalized with both a pyridine and a terminal ammonium moiety to two self-assembled, crown ether-containing Zn(II)Pors (158 in Fig. 40) was prepared.²³⁸ Steady state and time-resolved fluorescence assays speak for a CS with rate constants and quantum yields of $5.3 \times 10^9 \text{ s}^{-1}$ and 0.91, respectively. Decisive for the formation of the radical ion pair state upon photoexcitation of the Zn(II)Por dimer are nanosecond transient absorption measurements. Here, the CR takes place with $1.0 \times 10^7 \text{ s}^{-1}$. Additionally, the importance of the cofacial Por dimer as a donor *vs.* a Zn(II)Por monomer is demonstrated by a slower CS with $2.9 \times 10^9 \text{ s}^{-1}$ and a lower quantum yield of 0.85. As a complement to the aforementioned, enhanced electron transfer properties of cofacial Por dimers compared with the reference monomer were studied in another publication.²⁸¹ By using laser flash photolysis, the dynamics of photoinduced electron transfer from the triplet excited states covalently-fixed cofacial Por dimers to a series of electron acceptors (*e.g.* nitrobenzene derivatives and a series of benzoquinone compounds) were followed and

compared with Por monomers. In doing so, the results show that photoinduced electron transfer from cofacial Por dimers to electron acceptors is accelerated, whereas CR is decelerated relative to that observed for the corresponding Por monomer. Due to $\pi-\pi$ interactions among Por components, the Por dimer radical cation is stabilized more efficiently and results in larger driving forces for the CS as indicated by the $\pi-\pi^*$ transition in the near-infrared region and also by the negative shifts of the first oxidation potential with decreasing distances between the Por rings.

Another interesting supramolecular approach is the inclusion of fullerenes in a self assembled Por nanotube.^{257,258} Cyclic Ni(II)Por dimer **171** in Fig. 46 linked by butadiyne moieties, and bearing 4-pyridyl groups at two opposite *meso* positions of the Pors is able to form supramolecular nanotubes, which host fullerenes inside their cavity in solution to form a 1:1 inclusion complex ($2.0 \times 10^5 \text{ M}^{-1}$). By steady-state absorption measurements and electrochemistry, a charge transfer band from the Por to the fullerene was confirmed. In additional experiments, an anisotropic electron mobility of $0.72 \text{ cm}^2 \text{ V}^{-1} \text{ s}^{-1}$ along the linearly arranged fullerenes is established. However, femtosecond transient absorption measurements leading in the solid state to the population of the Por second singlet excited state provides the only proof for the formation of a triplet exciplex, which decays with a lifetime of 34 ps to the ground state. Using H₂Por dimer **170** (Fig. 46), the desired CS is favored.²⁵⁹ Electrochemical studies corroborate the lower oxidation potential of the Por dimer, which results in lower energy levels of the radical ion pair state. Anisotropic charge mobility of the Por nanotube-C₆₀ complex shows a value of $0.16 \text{ cm}^2 \text{ V}^{-1} \text{ s}^{-1}$, likely due to the zig-zag arrangement of the fullerenes. Finally, CS with a lifetime of 470 ps comes from transient absorption measurements in the solid state.

Steady-state measurements on supramolecular complexes with Por dimer tweezers **161** (Fig. 41) and different fullerenes (C₆₀ and C₇₀) demonstrate ground state interactions and fluorescence quenching of the cyclopentene linked Zn(II)Por dimeric tweezers by the fullerenes.²⁴³ Moreover, the value of the K_{ass} implies that the Por tweezers may be used as selective hosts for different fullerenes in benzonitrile. In addition, transient absorption measurements attest the sequence of energy transfer from the singlet excited state of the Por to the fullerene and electron transfer to the fullerenes in benzonitrile with a rate constant of 10^9 s^{-1} . One year later, a newly designed dithiophene-containing Por dimer **162** (Fig. 41) was investigated in an analogous way and the electron transfer properties in combination with fullerenes were probed.²⁴⁴

6. Conclusions and outlook

During the last decade, a large number of reports have appeared on the preparation and study of covalent and supramolecular, homo- and heterobinuclear systems based on Por and Pc chromophores. The most relevant synthetic strategies, molecular topologies and ground- and excited-state features of these systems have been collected in this review.

Covalently and noncovalently linked Por- and Pc-based binuclear systems may find numerous applications, ranging from molecular electronic and NLO devices to sensors and medical applications such as photodynamic therapy, to mention a few. Moreover, porphyrinoid-based binuclear systems hold particular relevance as artificial photosynthetic models in molecular photovoltaics, due to their improved light-harvesting capabilities and the occurrence of photoinduced energy and/or electron transfer events, particularly in the case of heterobinuclear systems.

Electronic coupling between these chromophores is an important parameter that determines the electronic properties of Pc and/or Por dimers. In this regard, the covalent strategy is suitable for fine-tuning this electronic coupling, since it allows to "bridge" the two macrocycles by a variety of spacers of different sizes, shapes and electronic nature.

While non-conjugated dimeric systems are usually weakly coupled *via* through-space and through-bond interactions, strong electronic coupling occurs in binuclear systems linked either directly or through conjugated spacers. The preparation of most of these systems is usually carried out by means of transition metal-catalysed, cross-coupling reactions.

An effective enlargement of π -conjugation can be attained by fusing two Pc and/or Por rings. This strategy is highly useful for constructing rigid and planar structures in which conjugation is fully extended over the whole covalent ensemble, leading to absorptions that reach into the near-mid-IR region. These systems are attractive because of their large nonlinear absorption properties, and can find applications in two-photon fluorescence microscopy and optical power limiting.

Inspired by the noncovalent nature of natural photosynthetic systems, the self-assembly approach has been increasingly pursued in the search for light-harvesting and charge-separation systems. In this context, metal-ligand interactions are widely-used molecular recognition tools for the construction of well-defined supramolecular architectures. Thus, it is not surprising to find, over the last few years, an increasing number of reports devoted to the construction of supramolecular Pc and/or Por dimers by means of the metal coordination approach. In this regard, coordination of pyridyl or imidazolyl ligands, appended to the periphery of Ru(II) or Zn(II) macrocycles is, by far, the most frequently used method to create such supramolecular ensembles. Other types of motifs such as D-A, host-guest, and electrostatic interactions have also been used for the construction of such supramolecular homo- and heterobinuclear systems. The self-assembly of covalent Por and/or Pc homo- and heterodimers into multiporphyrinoid arrays, such as cofacial tetrameric stacks, cyclic ensembles, and boxes deserves special mention.

The enormous interest in porphyrinoid-based binuclear conjugates for the construction of artificial photosynthetic systems has fostered the implementation of these conjugates into a wide range of D-A systems through their connection with different electroactive acceptor units, such as fullerene, PDI and AQ. This approach has proved efficient for the generation of photoinduced intramolecular charge separated states in covalent ensembles. On the other hand, there are many

reported examples in which appropriately functionalized electroactive units interact through supramolecular interactions with covalent or supramolecular Pcs and/or Pors binuclear systems. As mentioned above, coordination between Zn(II) or Ru(II) metal centers and nitrogenated ligands is the most frequently used supramolecular motif to create such ensembles. Nevertheless, remarkable examples have also been reported in which other supramolecular interactions such as highly-directional, hydrogen bonding and host-guest interactions have been employed as tools to construct biomimetic ensembles. Particularly relevant is the use of Pors binuclear systems as receptors for fullerene derivatives. In this case, the formation of supramolecular complexes relies on π - π stacking and charge transfer interactions between fullerene derivatives and the largely aromatic, electron-donor Pors dimers. "Tweezers-like" architectures or cyclic Pors dimers have also been described, which are able to host C₆₀, or even larger fullerene derivatives. Moving one step further, some of these cyclic dimers were found to be able to self-aggregate, giving rise to the formation of supramolecular nanotubes in which several C₆₀ molecules can be hosted in a one-dimensional, "peapod" arrangement. Similar to fullerenes, SWCNTs have also been complexed *via* supramolecular interactions using Pors dimer nanotweezers.

In-depth photophysical characterization of many of the above-mentioned ensembles has also been performed. Regarding porphyrinoid-based binuclear systems, particular attention has been focused on the understanding of the fundamental dynamics of the excitation energy transduction and CS of these systems as model compounds towards the preparation of artificial, light-harvesting complexes.

In this context, some investigations have been focused on the determination of energy transfer rates in supramolecular ensembles of Pors dimers. On the other hand, covalently linked, fused, and supramolecular Pcs-Por heterodimers have been the target of choice to study photoinduced electron/energy transfer processes. It is well known that the long-wavelength absorption of Pcs overlaps quite well with the short-wavelength fluorescence of Pors, which results, upon photoexcitation, in an efficient transduction of singlet excited state energy from the Por to the Pc. Besides energy transfer, photoinduced electron transfer has also been found in some metal-ligand bound Pcs-Por dimers. Additionally, the incorporation of one or more electroactive units into Pcs and/or Pors binuclear systems has also been exploited as a tool to obtain long-lived, charge-separated states. The charge transfer behaviour and the CR features of such D-A, covalent and noncovalent ensembles have been rationalized in terms of the topology of the arrangements and the electronic nature of the subunits.

To conclude, Pcs and Pors have clearly demonstrated to be more than simple dyes, they are highly versatile building blocks for the construction of multifunctional complex architectures. In this regard, organic synthesis holds a prominent role providing the tools to create sophisticated ensembles with improved ground- and excited-state features.

Although important advances have been made in this sense, a lot of understanding is still needed in order to accurately

predict and modulate the physicochemical properties of such conjugates. Moreover, a further step includes the implementation of these Pcs- and Pors-based ensembles into architectures showing long-range order which would provide efficient, solid-state devices.

Acknowledgements

Financial support from the MICINN and MEC, Spain (CTQ-2011-24187/BQU, PIB2010US-00652, CONSOLIDER-INGENIO 2010 CDS 2007-00010, Nanociencia Molecular), CAM (MADRISOLAR-2, S2009/PPQ/1533), the Deutsche Forschungsgemeinschaft (SFB 583 and FCI), "Solar Technologies Go Hybrid" initiative by the state of Bavaria, and Cluster of Excellence "Engineering of Advanced Materials (EAM)" is acknowledged.

References

- 1 D. M. Guldi, *Chem. Soc. Rev.*, 2002, **31**, 22–36.
- 2 H. Imahori, Y. Mori and Y. Matano, *J. Photochem. Photobiol., C*, 2003, **4**, 51–83.
- 3 M. E. El-Khouly, O. Ito, P. M. Smith and F. D'Souza, *J. Photochem. Photobiol., C*, 2004, **5**, 79–104.
- 4 G. de la Torre, C. G. Claessens and T. Torres, *Chem. Commun.*, 2007, 2000–2015.
- 5 S. Fukuzumi, *Phys. Chem. Chem. Phys.*, 2008, **10**, 2283–2297.
- 6 M. R. Wasielewski, *Acc. Chem. Res.*, 2009, **42**, 1910–1921.
- 7 Special issue on "Renewable Energy", D. Nocera and D. M. Guldi, *Chem. Soc. Rev.*, 2009, **38**, 1–293.
- 8 D. Gust, T. A. Moore and A. L. Moore, *Acc. Chem. Res.*, 2009, **42**, 1890–1898.
- 9 G. Bottari, G. de la Torre, D. M. Guldi and T. Torres, *Chem. Rev.*, 2010, **110**, 6768–6816.
- 10 Y. Rio, M. S. Rodríguez-Morgade and T. Torres, *Org. Biomol. Chem.*, 2008, **6**, 1877–1894, and references therein.
- 11 *The Porphyrin Handbook – Multiporphyrins, Multiphthalocyanines and Arrays*, ed. K. M. Kadish, K. M. Smith and R. Guilard, Academic Press, San Diego, 2000, vol. 18.
- 12 *Multiporphyrin Arrays Fundamentals and Applications*, ed. D. Kim, Pan Stanford Publishing, 2012.
- 13 N. Aratani and A. Osuka, in *Handbook of Porphyrin Science*, ed. K. M. Kadish, K. M. Smith and R. Guilard, World Scientific, 2010, vol. 1, pp. 1–129.
- 14 A. Ryan, A. Gehrold, R. Perusitti, M. Pintea, M. Fazekas, O. B. Locos, F. Blaikie and M. O. Senge, *Eur. J. Org. Chem.*, 2011, 5817–5844, and references cited therein.
- 15 G. de la Torre, M. Nicolau and T. Torres, Phthalocyanines Synthesis, Supramolecular Organization and Physical Properties, in *Supramolecular Photosensitive and Electroactive Materials*, ed. H. S. Nalwa, Academic Press, 2001, pp. 1–111.
- 16 M. S. Rodríguez-Morgade, G. de la Torre and T. Torres, in *The Porphyrin Handbook*, ed. K. M. Kadish, K. M. Smith and R. Guilard, Elsevier Science, 2003, vol. 15, pp. 125–159.
- 17 A. Yu Tolbin, L. G. Tomilova and N. S. Zefirov, *Russ. Chem. Rev.*, 2008, **77**, 435–449.

- 18 A. M. V. M. Pereira, A. R. M. Soares, M. J. F. Calvete and G. de la Torre, *J. Porphyrins Phthalocyanines*, 2009, **13**, 419–428, and references therein.
- 19 G. de la Torre, G. Bottari, U. Hahn and T. Torres, *Struct. Bonding*, 2010, **135**, 1–44.
- 20 For seminal work in this area, see: S. Vigh, H. Lam, P. Janda, A. B. P. Lever, C. C. Leznoff and R. L. Cerny, *Can. J. Chem.*, 1991, **69**, 1457–1461.
- 21 G. Bottari, D. D. Díaz and T. Torres, *J. Porphyrins Phthalocyanines*, 2006, **10**, 1083–1100, and references therein.
- 22 P.-C. Lo, X. Leng and D. K. P. Ng, *Coord. Chem. Rev.*, 2007, **251**, 2334–2353.
- 23 J.-Y. Liu, P.-C. Lo and D. K. P. Ng, *Struct. Bonding*, 2010, **135**, 169–210.
- 24 G. Bottari, G. de la Torre, D. M. Guldi and T. Torres, in *Multiporphyrin Arrays: Fundamentals and Applications*, ed. D. Kim, Pan Stanford Publishing, 2012, pp. 149–216.
- 25 H. Imahori, D. M. Guldi, K. Tamaki, Y. Yoshida, C. Luo, Y. Sakata and S. Fukuzumi, *J. Am. Chem. Soc.*, 2001, **123**, 6617–6628.
- 26 B. Grimm, A. Hausmann, A. Kahnt, W. Seitz, F. Spänig and D. M. Guldi, in *Handbook of Porphyrin Science*, ed. K. M. Kadish, K. M. Smith and R. Guilard, World Scientific, 2010, vol. 1, pp. 133–219.
- 27 J. E. Norton and J.-L. Bredas, *J. Chem. Phys.*, 2008, **128**, 034701.
- 28 M. Morisue and Y. Kobuke, *Chem.-Eur. J.*, 2008, **14**, 4993–5000.
- 29 R. M. Soares, M. V. Martínez-Díaz, A. Bruckner, A. M. V. M. Pereira, J. P. C. Tomé, M. C. A. Alonso, M. A. F. Faustino, M. G. P. M. S. Neves, A. C. Tomé, A. M. S. Silva, J. A. S. Cavaleiro, T. Torres and D. M. Guldi, *Org. Lett.*, 2007, **9**, 1557–1560.
- 30 G. Bottari, O. Trukhina, M. Ince and T. Torres, *Coord. Chem. Rev.*, 2012, **256**, 2453–2477.
- 31 J. Jiang, M. Bao, L. Rintoul and D. P. Arnold, *Coord. Chem. Rev.*, 2006, **250**, 424–448.
- 32 H. Isago, D. Terekhov and C. C. Leznoff, *J. Porphyrins Phthalocyanines*, 1997, **1**, 135–140.
- 33 S. O'Malley, B. Schatzmann, D. Diamond and K. Nolan, *Tetrahedron Lett.*, 2007, **48**, 9003–9007.
- 34 V. N. Nemykin, A. Y. Koposov, R. I. Subbotin and S. Sharm, *Tetrahedron Lett.*, 2007, **48**, 5425–5428.
- 35 A. Y. Tolbin, V. E. Pushkareva, E. V. Shulishov and L. G. Tomilova, *J. Porphyrins Phthalocyanines*, 2012, **16**, 341–350.
- 36 H. Yoshiyama, N. Shibata, T. Sato, S. Nakamura and T. Toru, *Org. Biomol. Chem.*, 2008, **6**, 4498–4501.
- 37 H. Yoshiyama, N. Shibata, T. Sato, S. Nakamura and T. Toru, *Org. Biomol. Chem.*, 2009, **7**, 2265–2269.
- 38 A. Y. Tolbin, A. V. Ivanov, L. G. Tomilova and N. S. Zefirov, *J. Porphyrins Phthalocyanines*, 2003, **7**, 162–166.
- 39 T. Ceyhan, A. Altindal, A. R. Özkaya, M. K. Erbil, B. Salih and Ö. Bekaroglu, *Chem. Commun.*, 2006, 320–322.
- 40 T. Ceyhan, A. Altindal, A. R. Özkaya, B. Salih, M. K. Erbil and Ö. Bekaroglu, *J. Porphyrins Phthalocyanines*, 2007, **11**, 625–634.
- 41 T. Ceyhan, A. Altindal, A. R. Özkaya, Ö. Çelikbic, B. Salih, M. Kemal Erbil and Ö. Bekaroglu, *Polyhedron*, 2007, **26**, 4239–4249.
- 42 M. Canlica, A. Altindal, A. R. Özkaya, B. Salih and Ö. Bekaroglu, *Polyhedron*, 2008, **27**, 1883–1890.
- 43 M. Özer, A. Altindal, A. R. Özkaya, B. Salih, M. Bulut and Ö. Bekaroglu, *Eur. J. Inorg. Chem.*, 2007, 3519–3526.
- 44 M. Özer, A. Altindal, B. Salih, M. Bulut and Ö. Bekaroglu, *Tetrahedron Lett.*, 2008, **49**, 896–900.
- 45 Z. Odabas, A. Altindal, A. R. Özkaya, M. Bulut, B. Salih and Ö. Bekaroglu, *Polyhedron*, 2007, **26**, 3505–3512.
- 46 S. Altun, A. Altindal, A. R. Özkaya, M. Bulut and Ö. Bekaroglu, *Tetrahedron Lett.*, 2008, **49**, 4483–4486.
- 47 Z. Odabas, F. Dumludag, A. R. Özkaya, S. Yamauchi, N. Kobayashi and Ö. Bekaroglu, *Dalton Trans.*, 2010, **39**, 8143–8152.
- 48 T. Ceyhan, A. Altindal, A. R. Özkaya, B. Salih and Ö. Bekaroglu, *Dalton Trans.*, 2010, **39**, 9801–9814.
- 49 M. Özer, A. Altindal, A. R. Özkaya and Ö. Bekaroglu, *Dalton Trans.*, 2009, 3175–3181.
- 50 I. Koç, M. Özer, A. R. Özkaya and Ö. Bekaroglu, *Dalton Trans.*, 2009, 6368–6376.
- 51 T. Ceyhan, A. Altindal, A. R. Özkaya, B. Salih and Ö. Bekaroglu, *Dalton Trans.*, 2009, 10318–10329.
- 52 S. M. Gorun, J. W. Rathke and M. J. Chen, *Dalton Trans.*, 2009, 1095–1097.
- 53 H. M. Neu, V. V. Zhdankin and V. N. Nemykin, *Tetrahedron Lett.*, 2010, **51**, 6545–6548.
- 54 A. B. Sorokin, E. V. Kudrik and D. Bouchub, *Chem. Commun.*, 2008, 2562–2564.
- 55 E. V. Kudrik and A. B. Sorokin, *Chem.-Eur. J.*, 2008, **14**, 7123–7126.
- 56 B. Floris, M. P. Donzello and C. Ercolani, in *Porphyrin Handbook*, ed. K. M. Kadish, K. M. Smith and R. Guilard, Elsevier Science, San Diego, 2003, vol. 18, pp. 1–2.
- 57 Y. Chen, D. Dini, M. Hanack, M. Fujitsuka and O. Ito, *Chem. Commun.*, 2004, 340–341.
- 58 Y. Chen, Y. Araki, M. Hanack, M. Fujitsuka and O. Ito, *Eur. J. Inorg. Chem.*, 2005, 4655–4658.
- 59 G. de la Torre, P. Vázquez, F. Agulló-López and T. Torres, *J. Mater. Chem.*, 1998, **8**, 1671–1683.
- 60 G. de la Torre, P. Vázquez, F. Agulló-López and T. Torres, *Chem. Rev.*, 2004, **104**, 3723–3750.
- 61 M. J. F. Calvete, D. Dini, S. R. Flom, M. Hanack, R. G. S. Pong and J. S. Shirk, *Eur. J. Org. Chem.*, 2005, 3499–3509.
- 62 S. Makarov, C. Litwinski, E. A. Ermilov, O. Suvorova, B. Röder and D. Wöhrle, *Chem.-Eur. J.*, 2006, **12**, 1468–1474.
- 63 T. V. Dubinina, A. V. Ivanov, N. E. Borisova, S. A. Trashin, S. I. Gurskiy, L. G. Tomilova and N. S. Zefirov, *Inorg. Chim. Acta*, 2010, **363**, 1869–1878.
- 64 M. Calvete and M. Hanack, *Eur. J. Org. Chem.*, 2003, 2080–2083.
- 65 T. V. Dubinina, S. A. Trashin, N. E. Borisova, I. A. Boginskaya, L. G. Tomilova and N. S. Zefirov, *Dyes Pigm.*, 2012, **93**, 1471–1480.

- 66 G. de la Torre, M. V. Martinez-Diaz, P. R. Ashton and T. Torres, *J. Org. Chem.*, 1998, **63**, 8888–8893.
- 67 G. de la Torre, M. V. Martinez-Diaz and T. Torres, *J. Porphyrins Phthalocyanines*, 1999, **3**, 560–568.
- 68 K. Ishii, N. Kobayashi, Y. Higashi, T. Osa, D. Lelièvre, J. Simon and S. Yamauchi, *Chem. Commun.*, 1999, 969–970.
- 69 D. Fix, S. Makarov, O. Suvorova, L. González, D. Wöhrle and B. Röder, *J. Phys. Chem. B*, 2008, **112**, 8466–8476.
- 70 G. Bottari and T. Torres, *Chem. Commun.*, 2004, 2668–2669.
- 71 H. Yoshiyama, N. Shibata, T. Sato, S. Nakamura and T. Toru, *Chem. Commun.*, 2008, 1977–1979.
- 72 A. J. Jiménez, M. L. Marcos, A. Hausmann, M. S. Rodríguez-Morgade, D. M. Guldi and T. Torres, *Chem.-Eur. J.*, 2011, **17**, 14139–14146.
- 73 A. de la Escosura, M. V. Martínez-Díaz, P. Thordarson, A. E. Rowan, R. J. M. Nolte and T. Torres, *J. Am. Chem. Soc.*, 2003, **125**, 12300–12308.
- 74 B. H. Northrop, Y.-R. Zheng, K.-W. Chi and P. J. Stang, *Acc. Chem. Res.*, 2009, **42**, 1554–1563.
- 75 C. G. Claessens, M. V. Martínez-Díaz and T. Torres, in *Supramolecular Chemistry From Molecules to Nanomaterials*, ed. P. A. Gale and J. W. Steed, John Wiley & Sons, 2012, pp. 1075–1100.
- 76 M. J. Cook and A. Jafari-Fini, *J. Mater. Chem.*, 1997, **7**, 2327–2329.
- 77 K. Ishii, S. Abiko, M. Fujitsuka, O. Ito and N. Kobayashi, *J. Chem. Soc., Dalton Trans.*, 2002, 1735–1739.
- 78 K. Ishii, M. Iwasaki and N. Kobayashi, *Chem. Phys. Lett.*, 2007, **436**, 94–98.
- 79 V. Novakova, P. Zimcik, K. Kopecky, M. Miletin, J. Kunes and K. Lang, *Eur. J. Org. Chem.*, 2008, 3260–3263.
- 80 K. Kameyama, M. Morisue, A. Satake and Y. Kobuke, *Angew. Chem., Int. Ed.*, 2005, **44**, 4763–4766.
- 81 S. Fukuzumi, K. Ohkubo, J. Ortiz, A. M. Gutierrez, F. Fernandez-Lazaro and A. Sastre-Santos, *J. Phys. Chem. A*, 2008, **112**, 10744–10752.
- 82 A. J. Jimenez, F. Spänig, M. S. Rodriguez-Morgade, K. Ohkubo, S. Fukuzumi, D. M. Guldi and T. Torres, *Org. Lett.*, 2007, **9**, 2481–2484.
- 83 A. Kahnt, M. Quintiliani, P. Vázquez, D. M. Guldi and T. Torres, *ChemSusChem*, 2008, **1**, 97–102.
- 84 A. Gouloumis, D. Gonzalez-Rodríguez, P. Vázquez, T. Torres, S. Liu, L. Echegoyen, J. Ramey, G. L. Hug and D. M. Guldi, *J. Am. Chem. Soc.*, 2006, **128**, 12674–12684.
- 85 F. J. Céspedes-Guirao, K. Ohkubo, S. Fukuzumi, F. Fernández-Lázaro and A. Sastre-Santos, *Chem.-Asian J.*, 2011, **6**, 3110–3121.
- 86 A. N. Cammidge, G. Berger, I. Chambrier, P. W. Hough and M. Cook, *Tetrahedron*, 2005, **61**, 4067–4074.
- 87 M. S. Rodríguez-Morgade, T. Torres, C. Atienza-Castellanos and D. M. Guldi, *J. Am. Chem. Soc.*, 2006, **128**, 15145–15154.
- 88 F. Silvestri, I. López-Duarte, W. Seitz, L. Beverina, M. V. Martínez-Díaz, T. J. Marks, D. M. Guldi, G. A. Pagani and T. Torres, *Chem. Commun.*, 2009, 4500–4502.
- 89 M. S. Rodríguez-Morgade, M. E. Plonska-Brzezinska, A. J. Athans, E. Carbonell, G. de Miguel, D. M. Guldi, L. Echegoyen and T. Torres, *J. Am. Chem. Soc.*, 2009, **131**, 10484–10496.
- 90 A. de la Escosura, M. V. Martínez-Díaz, D. M. Guldi and T. Torres, *J. Am. Chem. Soc.*, 2006, **128**, 4112–4118.
- 91 N. Kobayashi and A. B. P. Lever, *J. Am. Chem. Soc.*, 1987, **109**, 7433–7441.
- 92 O. E. Sielcken, M. M. Van Tilborg, M. F. M. Roks, R. Hendriks, W. Drenth and R. J. M. Nolte, *J. Am. Chem. Soc.*, 1987, **109**, 4261–4265.
- 93 F. D'Souza, E. Maligaspe, K. Ohkubo, M. E. Zandler, N. K. Subbaiyan and S. Fukuzumi, *J. Am. Chem. Soc.*, 2009, **131**, 8787–8797.
- 94 W. Seitz, A. J. Jiménez, E. Carbonell, B. Grimm, M. S. Rodríguez-Morgade, D. M. Guldi and T. Torres, *Chem. Commun.*, 2010, **46**, 127–129.
- 95 A. J. Jiménez, R. M. K. Calderón, M. S. Rodríguez-Morgade, D. M. Guldi and T. Torres, *Chem. Sci.*, 2013, **4**, 1064–1074.
- 96 C. G. Claessens, D. Gonzalez-Rodriguez and T. Torres, *Chem. Rev.*, 2002, **102**, 835–853.
- 97 R. S. Iglesias, C. G. Claessens, T. Torres, G. M. A. Rahman and D. M. Guldi, *Chem. Commun.*, 2005, 2113–2115.
- 98 D. González-Rodríguez, T. Torres, M. A. Herranz, L. Echegoyen, E. Carbonell and D. M. Guldi, *Chem.-Eur. J.*, 2008, **14**, 7670–7679.
- 99 D. González-Rodríguez, T. Torres, D. M. Guldi, J. Rivera, M. A. Herranz and L. Echegoyen, *J. Am. Chem. Soc.*, 2004, **126**, 6301–6313.
- 100 D. González-Rodríguez, E. Carbonell, D. M. Guldi and T. Torres, *Angew. Chem., Int. Ed.*, 2009, **48**, 8032–8036.
- 101 D. Gonzalez-Rodriguez, C. G. Claessens, T. Torres, S. G. Liu, L. Echegoyen, N. Vila and S. Nonell, *Chem.-Eur. J.*, 2005, **11**, 3881–3893.
- 102 Z. Zhao, A. N. Cammidge and M. J. Cook, *Chem. Commun.*, 2009, 7530–7532.
- 103 N. Shibata, B. Das, E. Tokunaga, M. Shiro and N. Kobayashi, *Chem.-Eur. J.*, 2010, **16**, 7554–7562.
- 104 H. Xu and D. K. P. Ng, *Inorg. Chem.*, 2008, **47**, 7921–7927.
- 105 S. Gaspard, C. Giannotti, P. Maillard, C. Schaeffer and T.-H. Tran-Thi, *J. Chem. Soc., Chem. Commun.*, 1986, 1239–1241.
- 106 J. Bartelmess, A. R. M. Soares, M. V. Martinez-Diaz, M. G. P. M. S. Neves, A. C. Tome, J. A. S. Cavaleiro, T. Torres and D. M. Guldi, *Chem. Commun.*, 2011, **47**, 3490–3492.
- 107 A. Hausmann, A. R. M. Soares, M. V. Martinez-Diaz, M. G. P. M. S. Neves, A. C. Tomé, J. A. S. Cavaleiro, T. Torres and D. M. Guldi, *Photochem. Photobiol. Sci.*, 2010, **9**, 1027–1032.
- 108 J. P. C. Tomé, A. M. V. M. Pereira, C. M. A. Alonso, M. G. P. M. S. Neves, A. C. Tomé, A. M. S. Silva, J. A. S. Cavaleiro, M. V. Martinez-Diaz, T. Torres, G. M. A. Rahman, J. Ramey and D. M. Guldi, *Eur. J. Org. Chem.*, 2006, 257–267.
- 109 H. Ali and J. E. van Lier, *Tetrahedron Lett.*, 2009, **50**, 1113–1116.
- 110 K. Kameyama, A. Satake and Y. Kobuke, *Tetrahedron Lett.*, 2004, **45**, 7617–7620.
- 111 A. Satake, T. Sugimura and Y. Kobuke, *J. Porphyrins Phthalocyanines*, 2009, **13**, 326–335.

- 112 M. Morisue, K. Ogawa, K. Kamada, K. Ohta and Y. Kobuke, *Chem. Commun.*, 2010, **46**, 2121–2123.
- 113 C. B. Kc, K. Stranius, P. D’Souza, N. K. Subbaiyan, H. Lemmetyinen, N. V. Tkachenko and F. D’Souza, *J. Phys. Chem. C*, 2013, **117**, 763–773.
- 114 J. Fortage, E. Göransson, E. Blart, H.-C. Becker, L. Hammarström and F. Odobel, *Chem. Commun.*, 2007, 4629–4631.
- 115 T. H. Tran-Thi, *Coord. Chem. Rev.*, 1997, **160**, 53–91.
- 116 E. Maligaspe, T. Kumpulainen, H. Lemmetyinen, N. V. Tkachenko, N. K. Subbaiyan, M. E. Zandler and F. D’Souza, *J. Phys. Chem. A*, 2010, **114**, 268–277.
- 117 K. Stranius, R. Jacobs, E. Maligaspe, H. Lemmetyinen, N. V. Tkachenko, M. E. Zandler and F. D’Souza, *J. Porphyrins Phthalocyanines*, 2010, **14**, 948–961.
- 118 R. Jacobs, K. Stranius, E. Maligaspe, H. Lemmetyinen, N. V. Tkachenko, M. E. Zandler and F. D’Souza, *Inorg. Chem.*, 2012, **51**, 3656–3665.
- 119 A. V. Gusev, E. O. Danilov and M. A. J. Rodgers, *J. Phys. Chem. A*, 2002, **106**, 1993–2001.
- 120 A. V. Gusev and M. A. J. Rodgers, *J. Phys. Chem. A*, 2002, **106**, 1985–1992.
- 121 M. R. Pereira, J. A. Ferreira and G. Hungerford, *Chem. Phys. Lett.*, 2005, **406**, 360–365.
- 122 E. A. Ermilov, R. Menting, J. T. F. Lau, X. Leng, B. Roder and D. K. P. Ng, *Phys. Chem. Chem. Phys.*, 2011, **13**, 17633–17641.
- 123 A. Ambroise, R. W. Wagner, P. D. Rao, J. A. Riggs, P. Hascoat, J. R. Diers, J. Seth, R. K. Lammi, D. F. Bocian, D. Holten and J. S. Lindsey, *Chem. Mater.*, 2001, **13**, 1023–1034.
- 124 R. F. Enes, J.-J. Cid, A. Hausmann, O. Trukhina, A. Gouloumis, P. Vázquez, J. A. S. Cavaleiro, A. C. Tomé, D. M. Guldi and T. Torres, *Chem.-Eur. J.*, 2012, **18**, 1727–1736.
- 125 A. M. V. M. Pereira, A. Hausmann, J. P. C. Tomé, O. Trukhina, M. Urbani, M. G. P. M. S. Neves, J. A. S. Cavaleiro, D. M. Guldi and T. Torres, *Chem.-Eur. J.*, 2012, **18**, 3210–3219.
- 126 A. M. V. M. Pereira, A. R. M. Soares, A. Hausmann, M. G. P. M. S. Neves, A. C. Tomé, A. M. S. Silva, J. A. S. Cavaleiro, D. M. Guldi and T. Torres, *Phys. Chem. Chem. Phys.*, 2011, **13**, 11858–11863.
- 127 M. E. El-Khouly, J. B. Ryu, K.-Y. Kay, O. Ito and S. Fukuzumi, *J. Phys. Chem. C*, 2009, **113**, 15444–15453.
- 128 M. E. El-Khouly, D. K. Ju, K.-Y. Kay, F. D’Souza and S. Fukuzumi, *Chem.-Eur. J.*, 2010, **16**, 6193–6202.
- 129 H. Xu, E. A. Ermilov, B. Roder and D. K. P. Ng, *Phys. Chem. Chem. Phys.*, 2010, **12**, 7366–7370.
- 130 R. Menting, J. T. F. Lau, H. Xu, D. K. P. Ng, B. Roder and E. A. Ermilov, *Chem. Commun.*, 2012, **48**, 4597–4599.
- 131 H. Shinmori, T. K. Ahn, H. S. Cho, D. Kim, N. Yoshida and A. Osuka, *Angew. Chem., Int. Ed.*, 2003, **42**, 2754–2758.
- 132 N. Yoshida, T. Ishizuka, A. Osuka, D. H. Jeong, H. S. Cho, D. Kim, Y. Matsuzaki, A. Nogami and K. Tanaka, *Chem.-Eur. J.*, 2003, **9**, 58–75.
- 133 M. U. Winters, J. Kärnbratt, M. Eng, C. J. Wilson, H. L. Anderson and B. Albinsson, *J. Phys. Chem. C*, 2007, **111**, 7192–7199.
- 134 J. Kärnbratt, M. Hammarson, S. Li, H. L. Anderson, B. Albinsson and J. Andréasson, *Angew. Chem., Int. Ed.*, 2010, **49**, 1854–1857.
- 135 T. Muraoka, K. Kinbara and T. Aida, *J. Am. Chem. Soc.*, 2006, **128**, 11600–11605.
- 136 T. Muraoka, K. Kinbara and T. Aida, *Nature*, 2006, **440**, 512–515.
- 137 M. Drobizhev, Y. Stepanenko, Y. Dzenis, A. Karotki, A. Rebane, P. N. Taylor and H. L. Anderson, *J. Am. Chem. Soc.*, 2004, **126**, 15352–15353.
- 138 M. Balaz, H. A. Collins, E. Dahlstedt and H. L. Anderson, *Org. Biomol. Chem.*, 2009, **7**, 874–888.
- 139 M. K. Kuimova, H. A. Collins, M. Balaz, E. Dahlstedt, J. A. Levitt, N. Sergent, K. Suhling, M. Drobizhev, N. S. Makarov, A. Rebane, H. L. Anderson and D. Phillips, *Org. Biomol. Chem.*, 2009, **7**, 889–896.
- 140 E. Dahlstedt, H. A. Collins, M. Balaz, M. K. Kuimova, M. Khurana, B. C. Wilson, D. Phillips and H. L. Anderson, *Org. Biomol. Chem.*, 2009, **7**, 897–904.
- 141 M. K. Kuimova, M. Balaz, H. L. Anderson and P. R. Ogilby, *J. Am. Chem. Soc.*, 2009, **131**, 7948–7949.
- 142 M. K. Kuimova, S. W. Botchway, A. W. Parker, M. Balaz, H. A. Collins, H. L. Anderson, K. Suhling and P. R. Ogilby, *Nat. Chem.*, 2009, **1**, 69–73.
- 143 K. J. Thorley, J. M. Hales, H. L. Anderson and J. W. Perry, *Angew. Chem., Int. Ed.*, 2008, **47**, 7095–7098.
- 144 S. Ohira, J. M. Hales, K. J. Thorley, H. L. Anderson, J. W. Perry and J.-L. Bredas, *J. Am. Chem. Soc.*, 2009, **131**, 6099–6101.
- 145 K. J. Thorley and H. L. Anderson, *Org. Biomol. Chem.*, 2010, **8**, 3472–3479.
- 146 Y.-J. Chen, S.-S. Chen, S.-S. Lo, T.-H. Huang, C.-C. Wu, G.-H. Lee, S.-M. Peng and C.-Y. Yeh, *Chem. Commun.*, 2006, 1015–1017.
- 147 O. Locos, B. Bašić, J. C. McMurtrie, P. Jensen and D. P. Arnold, *Chem.-Eur. J.*, 2012, **18**, 5574–5588.
- 148 L. J. Esdaile, P. Jensen, J. C. McMurtrie and D. P. Arnold, *Angew. Chem., Int. Ed.*, 2007, **46**, 2090–2093.
- 149 A. Ryan, B. Tuffy, S. Horn, W. J. Blau and M. O. Senge, *Tetrahedron*, 2011, **67**, 8248–8254.
- 150 C. Maeda, H. Shinokubo and A. Osuka, *Org. Lett.*, 2010, **12**, 1820–1823.
- 151 K. Osawa, N. Aratani and A. Osuka, *Tetrahedron Lett.*, 2009, **50**, 3333–3337.
- 152 N. N. Sergeeva, A. Scala, M. A. Bakar, G. O’Riordan, J. O’Brien, G. Grassi and M. O. Senge, *J. Org. Chem.*, 2009, **74**, 7140–7147.
- 153 R. Rein, M. Gross and N. Solladié, *Chem. Commun.*, 1994, 1992–1993.
- 154 S. Faure, C. Stern, R. Guillard and P. D. Harvey, *J. Am. Chem. Soc.*, 2004, **126**, 1253–1261.
- 155 G. Pognon, C. Boudon, K. J. Schenk, M. Bonin, B. Bach and J. Weiss, *J. Am. Chem. Soc.*, 2006, **128**, 3488–3489.

- 156 F. Tani, M. Matsu-ura, S. Nakayama and Y. Naruta, *Coord. Chem. Rev.*, 2002, **226**, 219–226.
- 157 G. Simonneaux and P. Le Maux, *Coord. Chem. Rev.*, 2002, **228**, 43–60.
- 158 G.-Y. Gao, J. V. Ruppel, K. B. Fields, X. Xu, Y. Chen and X. P. Zhang, *J. Org. Chem.*, 2008, **73**, 4855–4858.
- 159 T. Ema, N. Ura, K. Eguchi, Y. Ise and T. Sakai, *Chem. Commun.*, 2011, **47**, 6090–6092.
- 160 Q. Ouyang, Y.-Z. Zhu, Y.-C. Li, H.-B. Wei and J.-Y. Zheng, *J. Org. Chem.*, 2009, **74**, 3164–3167.
- 161 M. V. Martinez-Diaz, G. de la Torre and T. Torres, *Chem. Commun.*, 2010, **46**, 7090–7108.
- 162 J. K. Park, J. Chen, H. R. Lee, S. W. Park, H. Shinokubo, A. Osuka and D. Kim, *J. Phys. Chem. C*, 2009, **113**, 21956–21963.
- 163 A. J. Mozer, M. J. Griffith, G. Tsekouras, P. Wagner, G. G. Wallace, S. Mori, K. Sunahara, M. Miyashita, J. C. Earles, K. C. Gordon, L. Du, R. Katoh, A. Furube and D. L. Officer, *J. Am. Chem. Soc.*, 2009, **131**, 15621–15623.
- 164 C.-L. Mai, W.-K. Huang, H.-P. Lu, C.-W. Lee, C.-L. Chiu, Y.-R. Liang, E. W.-G. Diau and C.-Y. Yeh, *Chem. Commun.*, 2010, **46**, 809–811.
- 165 H. Hata, H. Shinokubo and A. Osuka, *J. Am. Chem. Soc.*, 2005, **127**, 8264–8265.
- 166 G. Bringmann, S. Rüdenauer, D. C. G. Götz, T. A. M. Gulder and M. Reichert, *Org. Lett.*, 2006, **8**, 4743–4746.
- 167 G. Bringmann, D. C. G. Götz, T. A. M. Gulder, T. H. Gehrke, T. Bruhn, T. Kupfer, K. Radacki, H. Braunschweig, A. Heckmann and C. Lambert, *J. Am. Chem. Soc.*, 2008, **130**, 17812–17825.
- 168 I. Hisaki, S. Hiroto, K. S. Kim, S. B. Noh, D. Kim, H. Shinokubo and A. Osuka, *Angew. Chem., Int. Ed.*, 2007, **46**, 5125–5128.
- 169 J. Song, S. Y. Jang, S. Yamaguchi, J. Sankar, S. Hiroto, N. Aratani, J.-Y. Shin, S. Easwaramoorthi, K. S. Kim, D. Kim, H. Shinokubo and A. Osuka, *Angew. Chem., Int. Ed.*, 2008, **47**, 6004–6007.
- 170 Y. Matano, K. Matsumoto, Y. Nakao, H. Uno, S. Sakaki and H. Imahori, *J. Am. Chem. Soc.*, 2008, **130**, 4588–4589.
- 171 Y. Matano, K. Matsumoto, H. Hayashi, Y. Nakao, T. Kumpulainen, V. Chukharev, N. V. Tkachenko, H. Lemmetyinen, S. Shimizu, N. Kobayashi, D. Sakamaki, A. Ito, K. Tanaka and H. Imahori, *J. Am. Chem. Soc.*, 2012, **134**, 1825–1839.
- 172 S. Yamaguchi, T. Katoh, H. Shinokubo and A. Osuka, *J. Am. Chem. Soc.*, 2008, **130**, 14440–14441.
- 173 J. Song, N. Aratani, J. H. Heo, D. Kim, H. Shinokubo and A. Osuka, *J. Am. Chem. Soc.*, 2010, **132**, 11868–11869.
- 174 S. Richeter, A. Hadj-Aïssa, C. Taffin, A. van der Lee and D. Leclercq, *Chem. Commun.*, 2007, 2148–2150.
- 175 S. Tokuji, T. Yurino, N. Aratani, H. Shinokubo and A. Osuka, *Chem.-Eur. J.*, 2009, **15**, 12208–12211.
- 176 M. O. Senge, B. Rößler, J. von Gersdorff, A. Schäferb and H. Kurreck, *Tetrahedron Lett.*, 2004, **45**, 3363–3367.
- 177 Y. Tanaka, H. Mori, T. Koide, H. Yorimitsu, N. Aratani and A. Osuka, *Angew. Chem., Int. Ed.*, 2011, **50**, 11460–11464.
- 178 P. S. S. Lacerda, A. M. G. Silva, A. C. Tomé, M. G. P. M. S. Neves, A. M. S. Silva, J. A. S. Cavaleiro and A. L. Llamas-Saiz, *Angew. Chem., Int. Ed.*, 2006, **45**, 5487–5491.
- 179 A. M. G. Silva, P. S. S. Lacerda, A. C. Tomé, M. G. P. M. S. Neves, A. M. S. Silva, J. A. S. Cavaleiro, E. A. Makarova and E. A. Lukyanets, *J. Org. Chem.*, 2006, **71**, 8352–8356.
- 180 S. Tokuji, C. Maeda, H. Yorimitsu and A. Osuka, *Chem.-Eur. J.*, 2011, **17**, 7154–7157.
- 181 M.-C. Yoon, S. Lee, S. Tokuji, H. Yorimitsu, A. Osuka and D. Kim, *Chem. Sci.*, 2013, **4**, 1756–1764.
- 182 H. Uno, K. Nakamoto, K. Kuroki, A. Fujimoto and N. Ono, *Chem.-Eur. J.*, 2007, **13**, 5773–5784.
- 183 M. Akita, S. Hiroto and H. Shinokubo, *Angew. Chem., Int. Ed.*, 2012, **51**, 2894–2897.
- 184 H. Uno, A. Masumoto and N. Ono, *J. Am. Chem. Soc.*, 2003, **125**, 12082–12083.
- 185 H. Mori, T. Tanaka and A. Osuka, *J. Mater. Chem. C*, 2013, **1**, 2500–2519.
- 186 A. Tsuda, H. Furuta and A. Osuka, *Angew. Chem., Int. Ed.*, 2000, **39**, 2549–2552.
- 187 A. Tsuda, H. Furuta and A. Osuka, *J. Am. Chem. Soc.*, 2001, **123**, 10304–10321.
- 188 Q. Ouyang, Y.-Z. Zhu, C.-H. Zhang, K.-Q. Yan, Y.-C. Li and J.-Y. Zheng, *Org. Lett.*, 2009, **11**, 5266–5269.
- 189 S. Hiroto and A. Osuka, *J. Org. Chem.*, 2005, **70**, 4054–4058.
- 190 T. Tanaka, B. Sun Lee, N. Aratani, M.-C. Yoon, D. Kim and A. Osuka, *Chem.-Eur. J.*, 2011, **17**, 14400–14412.
- 191 D. Y. Kim, T. K. Ahn, J. H. Kwon, D. Kim, T. Ikeue, N. Aratani, A. Osuka, M. Shigeiwa and S. Maeda, *J. Phys. Chem. A*, 2005, **109**, 2996–2999.
- 192 H. Mori, T. Tanaka, N. Aratani, B. S. Lee, P. Kim, D. Kim and A. Osuka, *Chem.-Asian J.*, 2012, **7**, 1811–1816.
- 193 L.-A. Fendt, H. Fang, M. E. Plonska-Brzezinska, S. Zhang, F. Cheng, C. Braun, L. Echegoyen and F. Diederich, *Eur. J. Org. Chem.*, 2007, 4659–4673.
- 194 T. Ikeda, N. Aratani, S. Easwaramoorthi, D. Kim and A. Osuka, *Org. Lett.*, 2009, **11**, 3080–3083.
- 195 T. Sakurai, K. Shi, H. Sato, K. Tashiro, A. Osuka, A. Saeki, S. Seki, S. Tagawa, S. Sasaki, H. Masunaga, K. Osaka, M. Takata and T. Aida, *J. Am. Chem. Soc.*, 2008, **130**, 13812–13813.
- 196 T. Sakurai, K. Tashiro, Y. Honsho, A. Saeki, S. Seki, A. Osuka, A. Muranaka, M. Uchiyama, J. Kim, S. Ha, X. K. Kato, M. Takata and T. Aida, *J. Am. Chem. Soc.*, 2011, **133**, 6537–6540.
- 197 K. J. McEwan, P. A. Fleitz, J. E. Rogers, J. E. Slagle, D. G. McLean, H. Akdas, M. Katterle, I. M. Blake and H. L. Anderson, *Adv. Mater.*, 2004, **16**, 1933–1935.
- 198 Y. Inokuma, N. Ono, H. Uno, D. Y. Kim, S. B. Noh, D. Kim and A. Osuka, *Chem. Commun.*, 2005, 3782–3784.
- 199 N. K. S. Davis, A. L. Thompson and H. L. Anderson, *Org. Lett.*, 2010, **12**, 2124–2127.
- 200 V. V. Diev, K. Hanson, J. D. Zimmerman, S. R. Forrest and M. E. Thompson, *Angew. Chem., Int. Ed.*, 2010, **49**, 5523–5526.
- 201 T. S. Balaban, *Acc. Chem. Res.*, 2005, **38**, 612–623 and references therein.

- 202 C. Maeda, S. Yamaguchi, C. Ikeda, H. Shinokubo and A. Osuka, *Org. Lett.*, 2008, **10**, 549–552.
- 203 C. Maeda, P. Kim, S. Cho, J. K. Park, J. M. Lim, D. Kim, J. Vura-Weis, M. R. Wasielewski, H. Shinokubo and A. Osuka, *Chem.-Eur. J.*, 2010, **16**, 5052–5061.
- 204 K. Ogawa, A. Ohashi, Y. Kobuke, K. Kamada and K. Ohta, *J. Phys. Chem. B*, 2005, **109**, 22003–22012.
- 205 A. Satake, J. Tanihara and Y. Kobuke, *Inorg. Chem.*, 2007, **46**, 9700–9707.
- 206 J. Tanihara, K. Ogawa and Y. Kobuke, *J. Photochem. Photobiol., A*, 2006, **178**, 140–149.
- 207 J. T. Dy, K. Ogawa, A. Satake, A. Ishizumi and Y. Kobuke, *Chem.-Eur. J.*, 2007, **13**, 3491–3500.
- 208 J. Dy, K. Ogawa, K. Kamada, K. Ohta and Y. Kobuke, *Chem. Commun.*, 2008, 3411–3413.
- 209 K. Ogawa and Y. Kobuke, *Angew. Chem., Int. Ed.*, 2000, **39**, 4070–4073.
- 210 R. Takahashi and Y. Kobuke, *J. Am. Chem. Soc.*, 2003, **125**, 2372–2373.
- 211 R. Takahashi and Y. Kobuke, *J. Org. Chem.*, 2005, **70**, 2745–2753.
- 212 J. E. Raymond, A. Bhaskar, T. Goodson, N. Makiuchi, K. Ogawa and Y. Kobuke, *J. Am. Chem. Soc.*, 2008, **130**, 17212–17213.
- 213 E. Iengo, E. Zangrando, E. Alessio, J.-C. Chambron, V. Heitz, L. Flamigni and J.-P. Sauvage, *Chem.-Eur. J.*, 2003, **9**, 5879–5887.
- 214 C. Maeda, T. Kamada, N. Aratani and A. Osuka, *Coord. Chem. Rev.*, 2007, **251**, 2743–2752.
- 215 I.-W. Hwang, T. Kamada, T. K. Ahn, D. M. Ko, T. Nakamura, A. Tsuda, A. Osuka and D. Kim, *J. Am. Chem. Soc.*, 2004, **126**, 16187–16198.
- 216 C. Maeda, T. Kamada, N. Aratani, T. Sasamori, N. Tokitoh and A. Osuka, *Chem.-Eur. J.*, 2009, **15**, 9681–9684.
- 217 C. Maeda, H. Shinokubo and A. Osuka, *Org. Lett.*, 2009, **11**, 5322–5325.
- 218 T. Kamada, N. Aratani, T. Ikeda, N. Shibata, Y. Higuchi, A. Wakamiya, S. Yamaguchi, K. S. Kim, Z. S. Yoon, D. Kim and A. Osuka, *J. Am. Chem. Soc.*, 2006, **128**, 7670–7678.
- 219 P. Kim, J. M. Lim, M.-C. Yoon, J. Aimi, T. Aida, A. Tsuda and D. Kim, *J. Phys. Chem. B*, 2010, **114**, 9157–9164.
- 220 S. J. Lee, K. L. Mulfort, J. L. O'Donnell, X. Zuo, A. J. Goshe, P. J. Wesson, S. T. Nguyen, J. T. Hupp and D. M. Tiede, *Chem. Commun.*, 2006, 4581–4583.
- 221 Y. Matano, K. Matsumoto, Y. Terasaka, H. Hotta, Y. Araki, O. Ito, M. Shiro, T. Sasamori, N. Tokitoh and H. Imahori, *Chem.-Eur. J.*, 2007, **13**, 891–901.
- 222 Y. Inaba and Y. Kobuke, *Tetrahedron*, 2004, **60**, 3097–3107.
- 223 D. Bonifazi, M. Scholl, F. Song, L. Echegoyen, G. Accorsi, N. Armarnoli and F. Diederich, *Angew. Chem., Int. Ed.*, 2003, **42**, 4966–4970.
- 224 D. Bonifazi, G. Accorsi, N. Armarnoli, F. Song, A. Palkar, L. Echegoyen, M. Scholl, P. Seiler, B. Jaun and F. Diederich, *Helv. Chim. Acta*, 2005, **88**, 1839–1884.
- 225 M. Prato and M. Maggini, *Acc. Chem. Res.*, 1998, **31**, 519–526.
- 226 P. A. Liddell, G. Kodis, D. Kuciauskas, J. Andreasson, A. L. Moore, T. A. Moore and D. Gust, *Phys. Chem. Chem. Phys.*, 2004, **6**, 5509–5515.
- 227 V. Garg, G. Kodis, M. Chachisvilis, M. Hambourger, A. L. Moore, T. A. Moore and D. Gust, *J. Am. Chem. Soc.*, 2011, **133**, 2944–2954.
- 228 S. Banala, R. G. Huber, T. Muller, M. Fechtel, K. R. Liedl and B. Krautler, *Chem. Commun.*, 2012, **48**, 4359–4361.
- 229 M. U. Winters, J. Kärnbratt, H. E. Blades, C. J. Wilson, M. J. Frampton, H. L. Anderson and B. Albinsson, *Chem.-Eur. J.*, 2007, **13**, 7385–7394.
- 230 H. Nakagawa, K. Ogawa, A. Satake and Y. Kobuke, *Chem. Commun.*, 2006, 1560–1562.
- 231 D. Kalita, M. Morisue and Y. Kobuke, *New J. Chem.*, 2006, **30**, 77–92.
- 232 S. Webster, S. A. Odom, L. A. Padilha, O. V. Przhonska, D. Peceli, H. Hu, G. Nootz, A. D. Kachkovski, J. Maticak, S. Barlow, H. L. Anderson, S. R. Marder, D. J. Hagan and E. W. Van Stryland, *J. Phys. Chem. B*, 2009, **113**, 14854–14867.
- 233 L. He, Y.-Z. Zhu, J.-Y. Zheng, Y.-F. Ma and Y.-S. Chen, *J. Photochem. Photobiol., A*, 2010, **216**, 15–23.
- 234 G. Pagona, G. E. Zervaki, A. S. D. Sandanayaka, O. Ito, G. Charalambidis, T. Hasobe, A. G. Coutsolelos and N. Tagmatarchis, *J. Phys. Chem. B*, 2012, **116**, 9439–9449.
- 235 T. Ichiki, Y. Matsuo and E. Nakamura, *Chem. Commun.*, 2013, **49**, 279–281.
- 236 Y. Terazono, G. Kodis, P. A. Liddell, V. Garg, T. A. Moore, A. L. Moore and D. Gust, *J. Phys. Chem. B*, 2009, **113**, 7147–7155.
- 237 F. D'Souza, S. Gadde, M. E. Zandler, M. Itou, Y. Araki and O. Ito, *Chem. Commun.*, 2004, 2276–2277.
- 238 F. D'Souza, R. Chitta, S. Gadde, L. M. Rogers, P. A. Karr, M. E. Zandler, A. S. D. Sandanayaka, Y. Araki and O. Ito, *Chem.-Eur. J.*, 2007, **13**, 916–922.
- 239 A. S. D. Sandanayaka, N. K. Subbaiyan, R. Chitta, Y. Araki, O. Ito and F. D'Souza, *J. Porphyrins Phthalocyanines*, 2008, **12**, 857–865.
- 240 D. Canevet, E. M. Pérez and N. Martín, *Angew. Chem., Int. Ed.*, 2011, **50**, 9248–9259.
- 241 D. Sun, F. S. Tham, C. A. Reed, L. Chaker, M. Burgess and P. D. W. Boyd, *J. Am. Chem. Soc.*, 2000, **122**, 10704–10705.
- 242 T. Yamaguchi, N. Ishii, K. Tashiro and T. Aida, *J. Am. Chem. Soc.*, 2003, **125**, 13934–13935.
- 243 S. Mukherjee, A. K. Bauri and S. Bhattacharya, *Chem. Phys. Lett.*, 2010, **500**, 128–139.
- 244 S. Mukherjee, S. Banerjee, A. K. Bauri and S. Bhattacharya, *J. Mol. Struct.*, 2011, **1004**, 13–25.
- 245 Z.-Q. Wu, X.-B. Shao, C. Li, J.-L. Hou, K. Wang, X.-K. Jiang and Z.-T. Li, *J. Am. Chem. Soc.*, 2005, **127**, 17460–17468.
- 246 A. Hosseini, S. Taylor, G. Accorsi, N. Armarnoli, C. A. Reed and P. D. W. Boyd, *J. Am. Chem. Soc.*, 2006, **128**, 15903–15913.
- 247 J.-S. Marois, K. Cantin, A. Desmarais and J.-F. Morin, *Org. Lett.*, 2007, **10**, 33–36.
- 248 K. Tashiro and T. Aida, *Chem. Soc. Rev.*, 2007, **36**, 189–197.

- 249 M. Yanagisawa, K. Tashiro, M. Yamasaki and T. Aida, *J. Am. Chem. Soc.*, 2007, **129**, 11912–11913.
- 250 P. T. Corbett, J. Leclaire, L. Vial, K. R. West, J. L. Wietor, J. K. M. Sanders and S. Otto, *Chem. Rev.*, 2006, **106**, 3652–3711.
- 251 A. L. Kieran, S. I. Pascu, T. Jarrosson and J. K. M. Sanders, *Chem. Commun.*, 2005, 1276–1278.
- 252 A. R. Mulholland, C. P. Woodward and S. J. Langford, *Chem. Commun.*, 2011, **47**, 1494–1496.
- 253 Y. Shoji, K. Tashiro and T. Aida, *J. Am. Chem. Soc.*, 2006, **128**, 10690–10691.
- 254 Y. Shoji, K. Tashiro and T. Aida, *J. Am. Chem. Soc.*, 2010, **132**, 5928–5929.
- 255 F. Hajjaj, K. Tashiro, H. Nikawa, N. Mizorogi, T. Akasaka, S. Nagase, K. Furukawa, T. Kato and T. Aida, *J. Am. Chem. Soc.*, 2011, **133**, 9290–9292.
- 256 T. Kamimura, K. Ohkubo, Y. Kawashima, H. Nobukuni, Y. Naruta, F. Tani and S. Fukuzumi, *Chem. Sci.*, 2013, **4**, 1451–1461.
- 257 H. Nobukuni, Y. Shimazaki, F. Tani and Y. Naruta, *Angew. Chem., Int. Ed.*, 2007, **46**, 8975–8978.
- 258 H. Nobukuni, F. Tani, Y. Shimazaki, Y. Naruta, K. Ohkubo, T. Nakanishi, T. Kojima, S. Fukuzumi and S. Seki, *J. Phys. Chem. C*, 2009, **113**, 19694–19699.
- 259 H. Nobukuni, Y. Shimazaki, H. Uno, Y. Naruta, K. Ohkubo, T. Kojima, S. Fukuzumi, S. Seki, H. Sakai, T. Hasobe and F. Tani, *Chem.-Eur. J.*, 2010, **16**, 11611–11623.
- 260 H. Nobukuni, T. Kamimura, H. Uno, Y. Shimazaki, Y. Naruta and F. Tani, *Bull. Chem. Soc. Jpn.*, 2012, **85**, 862–868.
- 261 X. Peng, N. Komatsu, S. Bhattacharya, T. Shimawaki, S. Aonuma, T. Kimura and A. Osuka, *Nat. Nanotechnol.*, 2007, **2**, 361–365.
- 262 X. Peng, N. Komatsu, T. Kimura and A. Osuka, *J. Am. Chem. Soc.*, 2007, **129**, 15947–15953.
- 263 G. Liu, T. Yasumitsu, L. Zhao, X. Peng, F. Wang, A. K. Bauri, S. Aonuma, T. Kimura and N. Komatsu, *Org. Biomol. Chem.*, 2012, **10**, 5830–5836.
- 264 F. Wang, K. Matsuda, A. F. M. M. Rahman, X. Peng, T. Kimura and N. Komatsu, *J. Am. Chem. Soc.*, 2010, **132**, 10876–10881.
- 265 X. Peng, N. Komatsu, T. Kimura and A. Osuka, *ACS Nano*, 2008, **2**, 2045–2050.
- 266 (*nm*) index in SWCNTs is designated as roll-up vector according to the Strano's proposal. M. S. Strano, *Nat. Nanotechnol.*, 2007, **2**, 340–341.
- 267 X. Peng, F. Wang, A. K. Bauri, A. F. M. M. Rahman and N. Komatsu, *Chem. Lett.*, 2010, 1022–1027.
- 268 G. Liu, F. Wang, S. Chaunchaiyakul, Y. Saito, A. K. Bauri, T. Kimura, Y. Kuwahara and N. Komatsu, *J. Am. Chem. Soc.*, 2013, **135**, 4805–4814.
- 269 M. E. El-Khouly and S. Fukuzumi, *J. Porphyrins Phthalocyanines*, 2011, **15**, 111–117.
- 270 J. Petersson, M. Eklund, J. Davidsson and L. Hammarstrom, *J. Am. Chem. Soc.*, 2009, **131**, 7940–7941.
- 271 A. C. Benniston, A. Harriman and P.-Y. Li, *J. Am. Chem. Soc.*, 2010, **132**, 26–27.
- 272 F. Ito, Y. Ishibashi, S. R. Khan, H. Miyasaka, K. Kameyama, M. Morisue, A. Satake and Y. Kobuke, *J. Phys. Chem. A*, 2006, **110**, 12734–12742.
- 273 M. Kasha, H. R. Rawls and M. A. El-Bayoumi, *Pure Appl. Chem.*, 1965, **11**, 371–392.
- 274 R. F. Kelley, S. J. Lee, T. M. Wilson, Y. Nakamura, D. M. Tiede, A. Osuka, J. T. Hupp and M. R. Wasielewski, *J. Am. Chem. Soc.*, 2008, **130**, 4277–4284.
- 275 D. A. Roberts, B. Fückel, R. G. C. R. Clady, Y. Y. Cheng, M. J. Crossley and T. W. Schmidt, *J. Phys. Chem. A*, 2012, **116**, 7898–7905.
- 276 H. Imahori, K. Tamaki, D. M. Guldi, C. Luo, M. Fujitsuka, O. Ito, Y. Sakata and S. Fukuzumi, *J. Am. Chem. Soc.*, 2001, **123**, 2607–2617.
- 277 G. Pagona, A. S. D. Sandanayaka, T. Hasobe, G. Charalambidis, A. G. Coutsolelos, M. Yudasaka, S. Iijima and N. Tagmatarchis, *J. Phys. Chem. C*, 2008, **112**, 15735–15741.
- 278 T. Hasobe, H. Imahori, H. Yamada, T. Sato, K. Ohkubo and S. Fukuzumi, *Nano Lett.*, 2003, **3**, 409–412.
- 279 M. Morisue, N. Haruta, D. Kalita and Y. Kobuke, *Chem.-Eur. J.*, 2006, **12**, 8123–8135.
- 280 M. Morisue, D. Kalita, N. Haruta and Y. Kobuke, *Chem. Commun.*, 2007, 2348–2350.
- 281 A. Takai, C. P. Gros, J.-M. Barbe, R. Guilard and S. Fukuzumi, *Chem.-Eur. J.*, 2009, **15**, 3110–3122.